THE HEME-LYSINE CROSS-LINK OF CYTOCHROME P460: EFFECTS ON CATALYSIS AND MECHANISM OF FORMATION

A Dissertation

Presented to the Faculty of the Graduate School

of Cornell University

In Partial Fulfillment of the Requirements for the Degree of

Doctor of Philosophy

by

Rachael Elizabeth Coleman

August 2021

THE HEME-LYSINE CROSS-LINK OF CYTOCHROME P460: EFFECTS ON CATALYSIS AND MECHANISM OF FORMATION

Rachael Elizabeth Coleman, Ph. D.

Cornell University 2021

Nitrification is the process in which ammonia (NH_3) is ultimately converted to nitrate (NO_3^-) by ammonia-oxidizing microorganisms. In NH_3-oxidizing bacteria (AOB), anammox bacteria, and comammox bacteria the enzyme hydroxylamine oxidoreductase (HAO) is able to convert hydroxylamine (NH_2OH) to nitric oxide (NO). What makes HAO unique is the presence of a P460 cofactor, which has been observed in only one other known protein family: cytochrome (cyt) P460. The P460 cofactor is a modified *c*-heme based cofactor that contains a post-translational modification in the form of a cross-link from the peptide backbone onto the porphyrin macrocycle itself. HAO uses a Tyr residue from a neighboring subunit to bind to the porphyrin macrocycle twice, whereas cyt P460 uses a lysine residue to bind to the γ *meso* carbon once. In cyt P460, the cross-link is absolutely essential for catalysis and a portion of this thesis addresses that the cross-link does not alter the electronic structure of this system in a catalytically meaningful way. Instead, the cross-link plays a vital role in positioning the heme relative to a second-sphere glutamate residue that serves the purpose of deprotonating the bound NH_2OH.

Although the cross-link of cyt P460 is absolutely essential for activity, the mechanism of its formation is unknown, but was reported to occur through an autocatalytic mechanism. The second half of this thesis addresses how the cross-link

of cyt P460 forms. We found that by excluding oxygen during protein expression results in a cross-link-deficient, catalytically incompetent protein, but treatment of this this protein with hydrogen peroxide (H_2O_2) results in a fully cross-linked, catalytically competent cyt P460. Additional studies showed that the fold of cyt P460 promotes cross-link formation, and which residues are important for this post-translational modification to form are also addressed.

BIOGRAPHICAL SKETCH

Rachael Elizabeth Coleman was born in Minot, North Dakota on December 17, 1992. As a child, she spent much of her time in ballet lessons, playing video games, spending time with her cats, or learning how to bake. At the age of twelve, she moved with her family to Cheyenne, Wyoming where she would attend junior high and high school. In high school, Rachael was the captain of her school's Science Olympiad team. Despite her clear love of science, she decided to attend the University of Wyoming to major in French and secondary education with a minor in Spanish so that one day she could be a foreign language teacher.

By the end of her first semester of her sophomore year, however, Rachael realized that she wanted to study chemistry with the goal of becoming a forensic scientist. On a whim, she decided to take the freshman biology class during the second semester of her junior year of college and the course of her life changed entirely. Rachael fell in love with biology, and because of biology, grew to truly *love* chemistry. Before that semester's end, she had added a second major in molecular biology and decided she would obtain a PhD in biochemistry.

While taking her inorganic chemistry laboratory course, she decided that metals were pretty cool and this further defined her interest in metalloprotein research. This eventually led her to work for Professor Elliott Hulley, synthesizing complexes that were meant to mimic the reactivity of cytochrome P450. When it was time to apply to graduate school, Professor Hulley told Rachael to apply to Cornell and he recommended working for Professor Kyle Lancaster, which she ultimately did. Her research focused on characterizing the heme-lysine cross-link of cytochrome P460, which is a way cooler protein compared to cytochrome P450 anyway. Next, Rachael is headed to Cambridge, MA to work as a Senior Protein Biochemist at Draper Laboratory.

This dissertation is dedicated to two titans of the video game industry who indirectly shaped the person I am today. First, I dedicate this to Shigeru Miyamoto, the creator of Mario and The Legend of Zelda. He is a creative visionary who I would love to meet someday. Second, I am also dedicating this to the late Satoru Iwata, a programmer who had a hand in so many games that I love—most notably EarthBound—and who became the president of Nintendo, a position in which he remained until he died of cancer in 2015. He inspires me to be a good person every day. Their work has nothing to do with the contents of this dissertation, but I could not have finished graduate school without them. Similarly, I am also dedicating this to my cat Luna, who I worked hard every day to support.

ACKNOWLEDGMENTS

My first acknowledgement must go to my advisor Kyle. Kyle, thanks for letting me strongarm you into joining your lab and thank you for teaching me how to be a scientist and for always eating my lemon desserts. For the record, however, I will never forgive you for beating me at Mario Party at the 2018 lab party. Toadette screwed me over, and that's a hill I will die on.

Justin and Brian, thank you for being supportive and helpful committee members over the years. I appreciate your help in getting me a job that I'm excited about!

Mom and Dale, thank you for being the most supportive parents I could have asked for. You have always supported me following my dreams, no matter how many times I have changed my mind about what I was doing with my life.

Leif and Amanda; Jason and Bria; and Matt and Jaimee, thank you for being the best brothers and sisters-in-law! I appreciated the support through the years. I am finally done with school!

Grandma, thank you so much for always being available to chat and for always helping me out whenever I needed it. I love you forever!

Luke "Ghost Dog" Cole, you are my absolute best friend and you have been there for me since the start of college. I appreciate that you are always a phone call away and can always make me laugh, whether you are sending me funny things from weird Twitter or we are referencing one of our many "local memes." Thank you for giving me a place to go for Christmas during the pandemic and thank you for including me in your small pandemic wedding. I was happy to be your family on your special day.

Tyler Ellis, one of the greatest joys of my free time in graduate school has been using Google hangouts to play Pokémon games together. Also, as you know, I always appreciate your willingness to be my tech support and helping me in my goal to never use an Apple product.

Jen Andrews, one of my oldest friends, thank you for always providing me a summer retreat in the great state of Minnesota. I appreciate that your guest bedroom was always open when I needed to escape Ithaca. And thank you, of course, for giving me your MBA advice on how to nail an interview!

Patricia "P-dawg" Tolbert, although you have moved on from Cornell, I do not feel like our friendship has changed at all! Thank you for being such a good "friend of the nerds." My favorite thing we ever did together was go to the hill where Joseph Smith discovered the magical golden plates and founded the Mormon religion. It is such a shame we did not get to roll down the hill though.

Peter Sun, my weekly movie buddy, thank you so much for always being down to see whatever I wanted to see and for dragging me to movies I would not have considered without you. I fully intend to come back to Ithaca at some point while you still here to catch the next Marvel movie release and you are of course welcome at my place. Come visit!

Alexandra Van Hall-Beauvais, you are my baking best friend forever (BBFF) and that is a bond that will never be broken! I am so glad we kept up our baking tradition, even with the Atlantic Ocean separating us. Cannot wait for you to be back stateside so we can see each and bake together again.

Will Schumacher, I will never forget first meeting you at our visit weekend, the both of us attending Kyle's talk at ACS San Diego where we recognized each other but did not say a word to each other, and then how you became one of my best friends at Cornell. It has not been the same since you left, but it was like nothing had changed when we all met up in New York City. Cannot wait until next we meet! If you come visit me, you can take another "Homeless Will" photo with Luna!

To my wonderful labmates—past and present—in the Lancaster lab:

Sam, I love that we bonded over Nintendo games and I love that at the end of our time here, we both got into the same podcast. Thank you for everything you do for the lab!

Sean, you have always been so supportive and kind, whether you were hyping my baking, chatting with me about life, or teaching me how to do things in lab. I love when you get the sillies because your laugh is infectious!

Ida, thank you for always being down to chat and for hosting several Bake Off/Baking parties! I missed having you around during my final year!

Avery and Meghan, thank you both for teaching me the ropes of working with cytochrome P460 and for setting me up for success with this protein!

Xristina, I think you made me into a great biochemist, and I always appreciate your unwavering support. And of course, thank you for always being down to join me on trips to Target! I have missed that terribly since you returned to Greece!

Melissa, I will die on the hill that your mutant is the most interesting thing that will ever happen with cytochrome P460. Thanks for using my Mössbauer data somewhere, I am glad that will get out.

Alex, thanks for always bringing some new story to lab.

Joe, thank you for putting up with my incessant questions about British culture or expressions and for always being down to chat in the mornings, it is time I will

treasure always.

Perry, you are one of the sweetest people I have met and I appreciate all your support throughout this past year. When I hosted you, I would have never imagined that over a year later, we would be in my car driving to Potsdam, NY to get a vaccine to stop a global pandemic, but honestly, I am glad we had this experience--twice. And never forget Savannah!

Rob, my favorite office mate, where do I begin?! Thank you for always saying yes, whether that was to decorating our office in the most absurd manner, watching the People vs OJ Simpson, listening to Rita Ora, or playing Fire Emblem: Three Houses. One of things I am the most upset by is that we did not overlap for longer, but I am grateful for the time we had. Obviously, this is not the end of our friendship and we have big things coming on the horizon…

Silas, you were the absolute best undergrad and I think so highly of you. Thank you for doing the pilot work that ultimately set up the rest of my thesis. You are incredible and I cannot wait until we can hang out in Boston.

My last section of acknowledgements might seem strange. Nevertheless, there are several people who I have never met, but have helped me during the wild ride of graduate school. Through many late nights in lab, I was never really alone because of several podcasts who provided me with endless entertainment. While this is by no means comprehensive—I listen to *a lot* of podcasts—these ones in particular have been among the most important to me in grad school. Also, I think these provide my thesis with some amusing searchable terms. And to whoever is actually reading this, treat this as a list of podcast recommendations. I have impeccable taste:

First and foremost, Lindsey and Bobby of *Who? Weekly,* you kept me sane, particularly during the stay-at-home portion of the pandemic. Words cannot describe how much I've loved learning about the antics of D-list celebrities or what Rita Ora was up to. In particular, the Patréon content has been incredible—especially the Chromatica listening party and the Contact episode. Crunch crunch, me in Greece, ScarJo Yummy Pop. Good form, Lindsey and Bobby!

To the hosts of *#Millennial*—Andrew, Laura, Pam (and of course former hosts Elysa and Matt), I grew up with all of you from your previous podcast endeavors. Whether you talked through the newest Marvel movie release or important events in our world and democracy, you were always there to help me make sense of the world.

While this might not be "safe for work" but Jamie, James, and Alice of *My Dad Wrote a Porno* have had me physically bent over in laughter more times than I can count. Of course, this can only be attributed to the literary genius of Rocky Flintstone. I still distinctly remember the experiment I was doing during my first global listening party at the start of book three of the *Belinda Blinked* series when Belinda made her debut at

the Millennium Dome Building and distributed *so many* non-stick tin woks.

Helen, Olly, and Martin the Soundman from *Answer Me This!* have also been a staple of my graduate school career. I remember my first summer going through the bulk of their back catalog and distilling dipyrromethane when I was still synthesizing porphyrins. While that has stopped, my love for this trio has not.

Really, there is no one podcast that I can put here because the McElroy family have an armada of podcasts. So, thank you Justin, Dr. Sydnee, Travis, Teresa, Griffin, Teylor, and Rileigh for all the laughs.

Tanner and Josh from *Exp. Share, a Pokémon Podcast* are so funny and have taken my already considerable love for these wonderful creatures to new heights, whether they were talking about Joshy's Sweeties or Tanner's Ew Make Me Barf Pokémon of the week, I was always down to revisit all regions of the Pokémon world with these two.

Play Watch Listen is technically a video game industry podcast from four different perspectives hosted by Alanah, Troy, Mike, and Austin but because of their loveable inability to remain on topic, I've learned so much more about…everything. I hope they never change.

While this is a newer addition to my podcast rotation, I cannot overstate how much I look forward to listening to Frances and Jordan from *The Podcast Diaries* every Wednesday. Throughout my entire final year of graduate school, these two ladies have discussed my favorite book series from my childhood, *The Princess Diaries* by Meg Cabot, and have been so wonderful with their fanbase online. It's been great hearing their perspectives on these books. I also want to personally thank them for asking Queen Meg Cabot one of my questions in an interview!

While this is not a podcast, I want my last acknowledgement to go to Cassey Ho or *blogilates* on YouTube. Cassey has completely changed my life and my perspective on fitness and health, which has increased my confidence tremendously. I cannot overstate how she has changed my life for the better.

Funding

The work presented in this thesis was funded by the Department of Energy Office of Science (DE-AC02-6CH11357) and the National Institute of Health (NIGMS R35 GM124908).

TABLE OF CONTENTS

LIST OF FIGURES

LIST OF TABLES

LIST OF ABBREVIATION

AOB: Ammonia-oxidizing bacteria

AOA: Ammonia-oxidizing archaea

Cyt: Cytochrome

HAO: Hydroxylamine oxidoreductase

Lys: Lysine

Tyr: Tyrosine

Ala: Alanine

Arg: Arginine

His: Histidine

DCPIP: Dichlorophenolindophenol

PMS: Phenazine methosulftate

CL: Cross-linked

CLD: Cross-link deficient

NH_3: Ammonia

NH_2OH: Hydroxylamine

NO: Nitric Oxide

NO_2^-: Nitrite

NO_3^-: Nitrate

HO: Heme oxygenase

CHAPTER 1
INTRODUCTION

Adapted in part from:

"Heme P460: A (Cross) Link to Nitric Oxide"

Rachael E. Coleman and Kyle M. Lancaster

Acc. Chem. Res. 2020, 53, 12, 2925-2935

Introduction

The element nitrogen is necessary for life. Among other roles, nitrogen is a primary component of both nucleic acids and amino acids. The largest source of nitrogen on Earth is dinitrogen (N_2) gas, making up 78% of the planet's atmosphere.[1] This form of nitrogen, however, is largely unusable to most forms of life, except for diazotrophic microorganisms that can render N_2 bioavailable using the enzyme nitrogenase.[2] Nitrogenase achieves one of the most energetically demanding chemical transformations, converting N_2 into more biologically available ammonia (NH_3) through the following chemical reaction:

$$N_2 + 8e^- + 8H^+ + 16\ ATP \rightarrow 2NH_3 + H_2 + 16ADP + 16P_i$$

This reaction comprises the entry of N_2 into the biogeochemical nitrogen cycle (**Figure 1.1**).[3] Until the advent of the Haber-Bosch process at the beginning of the twentieth century, lightning in the atmosphere[4] and diazotrophic microorganisms were the only sources of bioavailable nitrogen for the planet.[5] Because NH_3 is the one of the primary components of fertilizer,[6] the industrial production of NH_3 directly promoted a rapid rise in the population of the planet because of increased availability of food.[6] However, anthropogenic nitrogen fixation has also caused an imbalance of the nitrogen cycle: biological and anthropogenic nitrogen fixation convert 415 Tg of N_2 to NH_3 per year, whereas denitrification and anammox processes convert ca. 350 Tg of various fixed nitrogen species per year back to N_2.[3, 6] This imbalance has led to a variety of negative environmental outcomes. These include an increased atmospheric concentration of the greenhouse gas nitrous oxide (N_2O) as well as biodiversity-depleting eutrophication of aquatic ecosystems.[6]

Following nitrogen fixation, the process of nitrification occurs.[3, 7] Nitrification is the biochemical oxidation of ammonia (NH_3) to nitrate (NO_3^-).[3, 7-8] This process is performed by chemolithotrophic microorganisms: ammonia-oxidizing bacteria (AOB) and ammonia-oxidizing archaea (AOA) oxidize NH_3 to nitrite (NO_2^-), while nitrite-oxidizing bacteria (NOB) produce NO_3^-.[3, 7] Recently, complete ammonia-oxidizing (comammox) bacteria were discovered that can produce NO_3^- from NH_3, using enzymes common to AOB and NOB.[9-10]

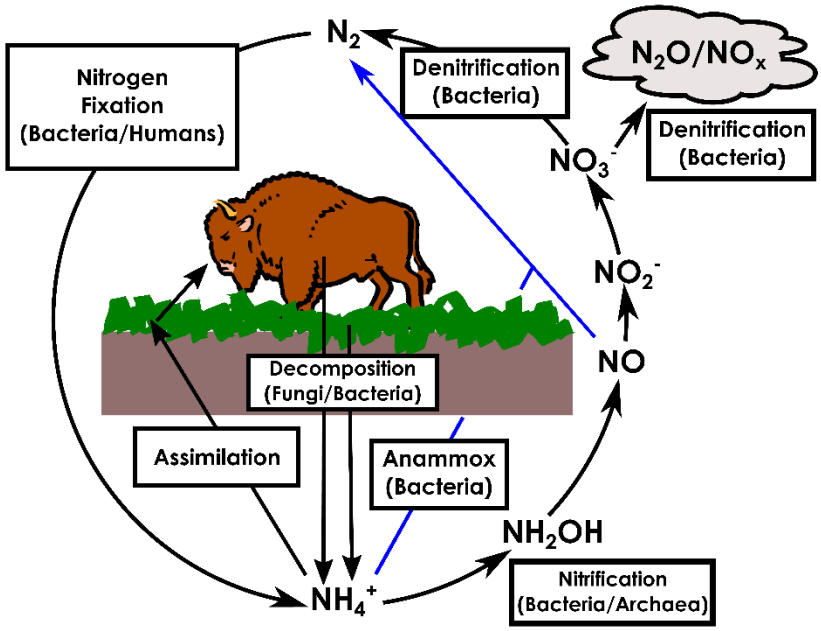

Figure 1.1. The biogeochemical nitrogen cycle with the start of the pathway shown in the boxes.

The first step of nitrification is the hydroxylation of NH_3 to hydroxylamine (NH_2OH) and is carried out by a member of the the copper membrane monooxygenase family of enzymes: ammonia monooxygenase (AMO).[7] This reaction requires dioxygen (O_2) activation,[11] and it has been hypothesized that two electrons are harnessed for this process from the downstream oxidation of NH_2OH,[12] meaning that AMO itself and thus NH_3 hydroxylation yields no net electron flow toward cellular respiration. In AOB and comammox bacteria, the soluble multi-heme enzyme hydroxylamine oxidoreductase (HAO) liberates NH_2OH of reducing equivalents for cellular respiration.[7] The final known reaction is the oxidation of NO_2^- to NO_3^- by the enzyme nitrite oxidoreductase, which is known in NOB, comammox, and anammox bacteria.[3, 7, 9-10]

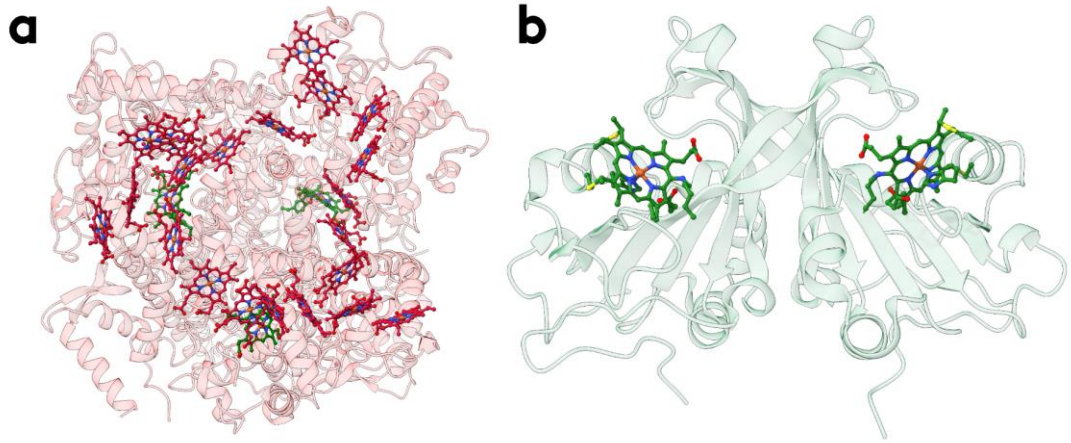

Figure 1.2. Ribbon representation of (a) hydroxylamine oxidoreductase (HAO) (PDB ID: 4N4N) from *Nitrosomonas europaea* and (b) cytochrome (cyt) P460 (PDB ID: 6AMG) from *Nitrosomonas* sp. AL212. Heme moieties are shown as sticks. Standard *c*-type hemes are depicted in red and P460 cofactors are depicted in green.

The oxidation of NH_2OH is the first energy-producing step of the AOB primary metabolism.[7] The metabolic enzyme responsible for this reaction, HAO, is a homotrimer containing eight *c*-type[13] hemes per subunit (**Figure 1.2a**).[14] In one monomer, seven of the hemes are coordinatively saturated; however, the remaining heme—known as the P460 cofactor—is an $S = {}^5/_2$, 5-coordinate (5c) heme with two additional cross-links.[15-16] A single tyrosine (Tyr) residue from a different subunit

binds to the heme twice through the phenolate O and C3 atoms of Tyr467' (**Figure 1.3a**).[14-15, 17-18] Despite the unique heme at the active site, the presence of non-catalytic heme cofactors severely complicates spectroscopy-based mechanistic study. Moreover, to date no recombinant expression system has yielded active, soluble, holo-HAO. This leaves isolation from AOB—which grow slowly and achieve low cell densities[19]—as the sole source of this biogeochemical catalyst.

Nature afforded a convenient proxy for HAO chemistry in the form of the homodimeric cytochrome (cyt) P460 (**Figure 1.2b**),[20] which was reported to oxidize NH_2OH in a manner similar to HAO.[21] Per its name, this enzyme also contains a heme P460 cofactor. Unlike HAO, cyt P460 only bears P460 cofactors, enabling spectroscopic access to the catalytic center. HAO and cyt P460 share little sequence homology.[22] Moreover, a single cross-link between the heme's 13' *meso* carbon through and the N atom of a lysine (Lys) sidechain mark a key difference with HAO (**Figure 1.3b**).[23] Despite this and other differences, elucidating the mechanism of cyt P460 has significantly advanced the understanding of controlled NH_2OH redox biochemistry and ultimately, the primary metabolism used by AOB to make a living off of NH_3.[24-25]

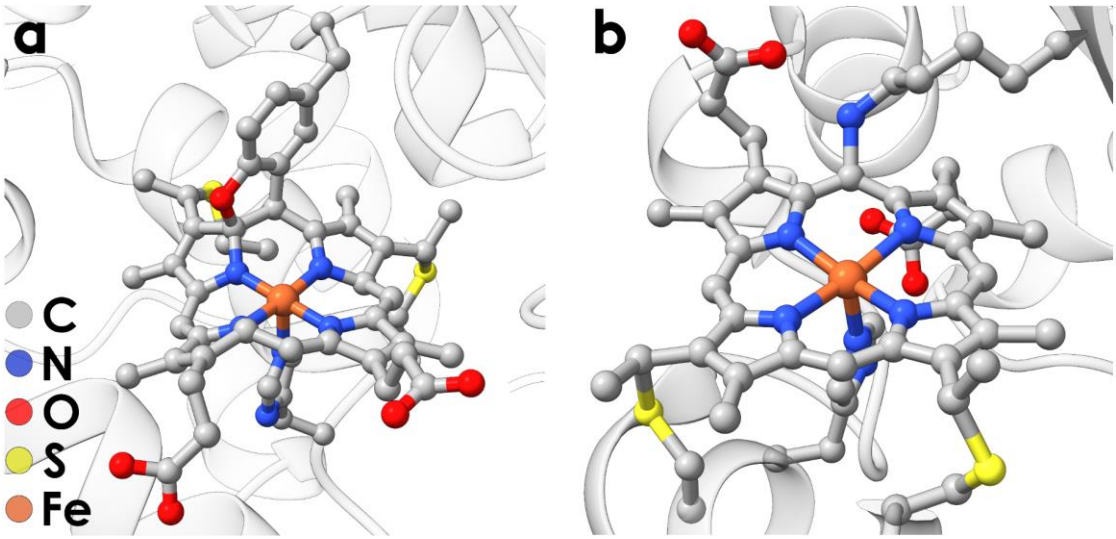

Figure 1.3. Representations of (a) the P460 cofactor of *N. europaea* hydroxylamine oxidoreductase (HAO) (PDB ID: 4N4N) and (b) *N. europaea* cytochrome (cyt) P460 (PDB ID 2JE3).

Establishing the Reactions catalyzed by Cyt P460

Early incarnations of the AOB primary metabolism implicated the Fe protein HAO as the final primary metabolic enzyme, converting NH_2OH to NO_2^- stoichiometrically.[26] This is a remarkable biochemical transformation by virtue of the cytotoxic nature of the metabolite and the precisely controlled product distribution. NH_2OH is a potent nucleophile commonly used in organic synthesis to produce oximes.[27] Moreover, NH_2OH is highly energetic—the enthalpy of the decomposition reaction, which is catalyzed by Fe, is –116.5 kJ mol^{-1} and results in a mixture of products including NH_3, N_2, NO, and N_2O.[28-30] Consequently, studying Nature's controlled release of energy from NH_2OH is fundamentally interesting.

Previously studied cyt P460 variants from *N. europaea*[20] and the methanotroph *Methyloccus capsulatus* (Bath)[21] were reported to oxidize NH_2OH to NO_2^- consistent with observations of HAO's reactivity. These studies linked P460 cofactor-containing enzymes to the production of NO_2^- from NH_2OH and suggested that answers concerning controlled energy release from NH_2OH could be gleaned from cyt P460.

However, there was one known exception: Maalcke and co-workers[16] showed that the HAO homolog from the anammox bacterium *Kuenenia stuttgartiensis* yielded only NO from NH_2OH.

Consistent with the findings of Zahn and co-workers[21], NO_2^- was produced from NH_2OH oxidation by *N. europaea* cyt P460, but only under aerobic conditions.[31] However, NO_2^- production was substoichiometric with NH_2OH. The most NO_2^- produced was 0.7 mole NO_2^- to 1 mole NH_2OH.[31] Gas chromatography (GC) revealed the other major product of the reaction under aerobic conditions to be nitrous oxide (N_2O). When the same experiment was repeated under anaerobic conditions, N_2O was the *only* product in this case. Experiments with a variety of oxidants established that one N_2O is produced for every two NH_2OH.[31]

$$2\ NH_2OH \rightarrow N_2O + H_2O + 4H^+ + 4e^-$$

Up to 20 mM NH_2OH, the steady-state activity plot of cyt P460 is linear with turnover frequencies of 0.3 to 80 μM DCPIP consumed min^{-1}•μM $enzyme^{-1}$.[31] This implied a bimolecular rate-determining step.

N_2O is a potent greenhouse gas, and AOB were thought to account for the majority of N_2O produced from various soil samples through a process known as nitrifier denitrification.[32] N_2O is the product of these reactions, which is the result of the activities of copper nitrite reductase (NirK) and nitric oxide reductase (Nor).[33] A study by Beaumont and co-workers[33] showed that despite knocking out the essential NorB portion of the *norCBQD* gene cluster in *N. europaea*, N_2O was still produced. In a proteomics study of various AOB, including *N. euroapaea*, cyt P460 was found to make up 0.13% of the proteome under NH_3-rich conditions, indicating it is expressed in significant quantities.[34] Thus, cyt P460 likely contributes to global N_2O production.

Towards a Detailed Cyt P460 Mechanism

While these studies identified a new mechanism for biological N_2O formation, the stoichiometry of 2 reducing equivalents withdrawn per equivalent of NH_2OH disconnects cyt P460 from primary metabolism because of the requirement for two electrons for each turnover of AMO. However, further exploration of the cyt P460

mechanism exposed a branching point—an Fe-nitrosyl intermediate—in biological NH_2OH oxidation at heme P460 centers that could establish a net electron flow for cellular respiration.

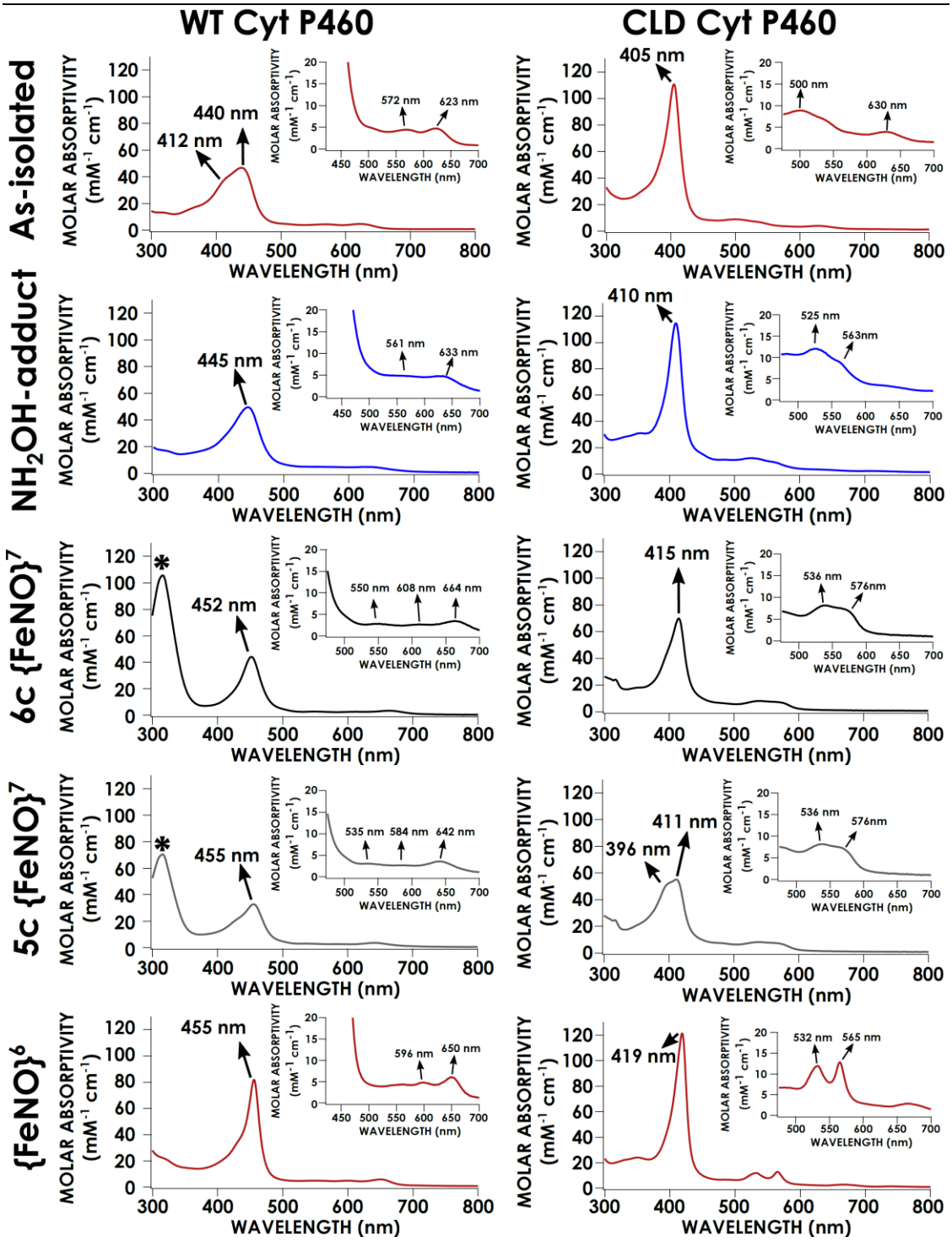

Figure 1.4. Ultraviolet (UV)-visible absorption spectra of (a-e) the species of the WT, cross-link (CL)-containing cyt P460 catalytic cycle and (f-j) the equivalent species in the cross-link deficient (CLD), catalytically incompetent variant, Lys70Tyr. (a, f) The as-isolated species, (b, g) the hydroxylamine (NH_2OH) adduct, (c, h) the six-

coordinate (6c) $\{FeNO\}^7$, (d, i) the five-coordinate (5c) $\{FeNO\}^7$, and (e, j) the $\{FeNO\}^6$ are depicted with Soret maxima shown. The inset shows the Q band region. The * denotes absorption by sodium dithionite used to prepare samples.

This intermediate was detected because the oxidation of the NH_2OH by cyt P460 involves many isolable intermediates. This work was carried out using the *N. europaea* variant, for which spectroscopic data are shown in **Figures 1.4–1.5**. At the beginning of the catalytic cycle, the resting $S = {}^5/_2$ form of the protein binds NH_2OH to form a $S = {}^1/_2$ NH_2OH-adduct. This adduct persists indefinitely in the absence of oxidants. This stability is likely attributable to the negative, ca. – 400 mV (vs NHE) $Fe^{II/III}$ cyt P460 reduction potential.[35] Upon oxidant addition, a new species is observed with a narrow, red-shifted Soret absorption maximum of 455 nm. Both accumulation and decay could be observable under appropriate conditions. Using 12 μM cyt P460, 1 mM NH_2OH, and 70 μM DCPIP, the accumulation was complete within the time of manual-mixing, but the decay phase was slow, implicating the participation of this 455 nm intermediate in the cycle's rate-determining step. In this same setup, the decay hastened upon addition of 10 mM NH_2OH after DCPIP consumption. This evidence supported that NH_2OH also participates in the rate-determining step.

The 455 nm intermediate gave no signal in continuous wave (CW) X-band EPR measurements, whereas the decay product produced EPR signals consistent with the Fe^{III}-NH_2OH adduct or minor 5c $\{FeNO\}^7$ formation. Possible intermediates consistent with an EPR-silent species included a nitrous acid adduct (Fe^{II}-NOOH adduct), an $\{FeNO\}^6$, or an Fe^{III}-$^{\bullet}NH_2OH$. The former two were proposed by Férnandez and co-workers[24] in a theoretical study of HAO catalysis, and the latter was proposed to be involved in the reduction of NO by cyt P450 NO reductase enzymes.[36-37] The Fe^{II}–NOOH adduct would be competent for anaerobic NO_2^- production, which was not observed. In support of the $\{FeNO\}^6$ species, the UV-vis absorption spectrum of the resting enzyme treated with the NO donor 1-(hydroxy-NNO-azoxy)-L-proline (PROLI-NONOate) was identical to the spectrum of the 455 nm intermediate produced under turnover conditions. This "shunted" $\{FeNO\}^6$ was also EPR-silent and was similarly stable to excess oxidant. When the shunted $\{FeNO\}^6$ was treated with 2

mM NH_2OH, it decayed with a dependence on NH_2OH, producing the same second-order rate constant. Finally, the $\{FeNO\}^6$ produced from the shunted experiment also generated N_2O as determined by GC-mass spectrometry (MS). The added [NO] was varied and the protein treated with excess NH_2OH and the N_2O produced had a 1:1 stoichiometry with NO, which was consistent with the established stoichiometry. Using $^{15}NH_2OH$, the GC-MS results showed that the N_2O produced was the mixed isotope species.

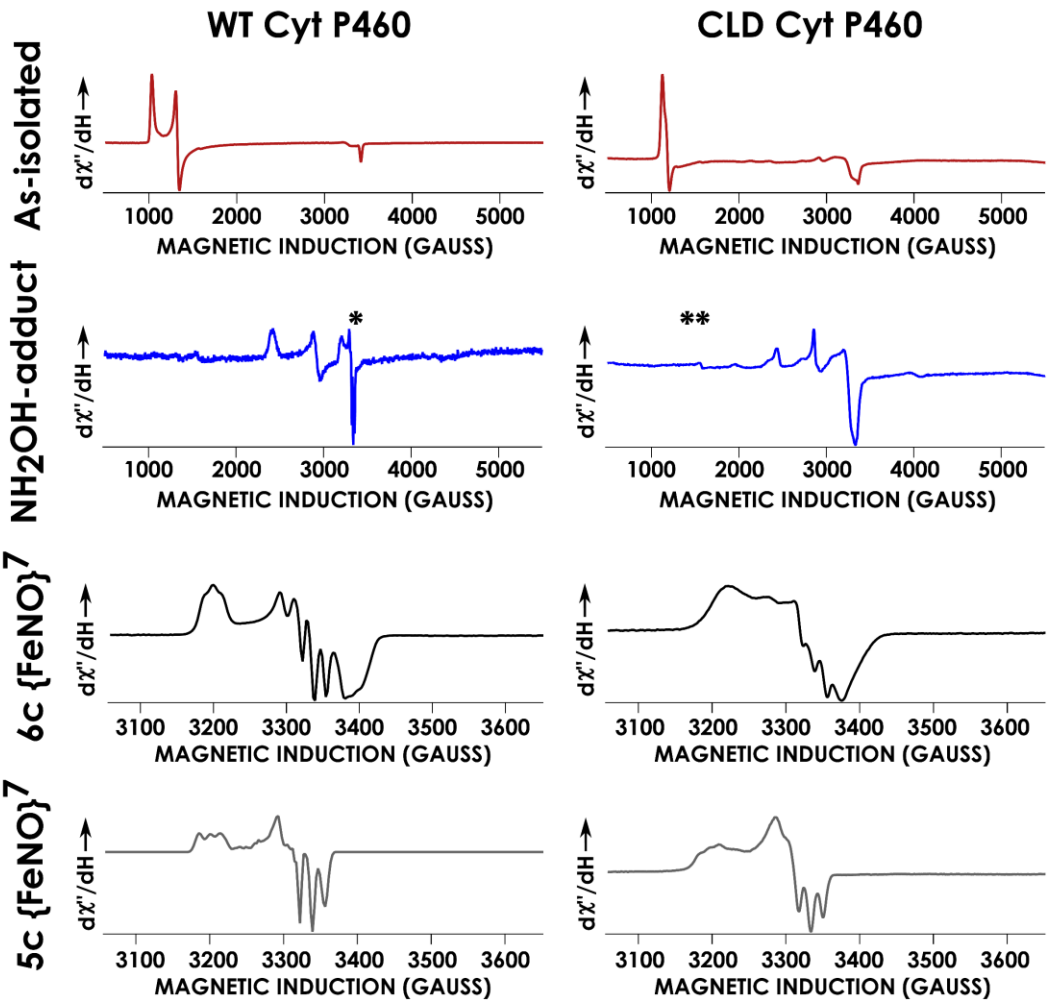

Figure 1.5. Continuous wave X-band electron paramagnetic resonance spectra of (a-d) various species of the WT cyt P460 catalytic cycle and (e-h) the equivalent species in the CLD Lys70Tyr. The * in b denotes the minor presence of the 5c $\{FeNO\}^7$ that is a result of the freezing process. The ** in f is the presence of a HS contaminant.

These results allowed us to propose a mechanism for cyt P460 catalysis. First, the resting enzyme binds NH_2OH to produce the Fe^{III}-NH_2OH adduct. In the presence of oxidant, a two-electron oxidation occurs to produce a six-coordinate (6c) $\{FeNO\}^7$ species (*vide infra*), followed by an additional one electron oxidation to produce the $\{FeNO\}^6$. A second equivalent of NH_2OH reacts with the $\{FeNO\}^6$ by nucleophilic attack to produce N_2O and H_2O in the rate-determining step. Presumably, the final

oxidizing equivalent regenerates the ferric enzyme, but this reaction was too rapid to be observed (**Figure 1.6**). Importantly, the stability of the $\{FeNO\}^6$ to hydrolysis excluded the long-postulated formation of NO_2^- and thus the ability to withdraw 4 electrons from NH_2OH, at least by cyt P460.

The presence of two NH_2OH-oxidizing enzymes in the proteome of *N. europaea* is interesting, especially since cyt P460 catalysis cannot generate energy for the cell. It is possible the role of cyt P460 in *N. europaea* is protective; its K_d for NH_2OH binding is 9 mM, which is high for an enzyme and its substrate. We have speculated that cyt P460 serves to detoxify NH_2OH if HAO is saturated, although this awaits experimental validation. Given that *N. europaea*, which expresses Nor genes,[33] and *Nitrosomonas ureae* Nm10, which lacks Nor genes,[38] both express cyt P460,[34] it seems unlikely that cyt P460's purpose is to remove NO.[34] Regardless, the production of N_2O and not NO_2^- by a P460 cofactor-containing enzyme indicated that there must be some substantial difference in the reaction profiles of HAO and cyt P460 enabling HAO to generate reducing equivalents for cellular respiration.

Bacterial Nitrification: Revised

NH_2OH was long thought to be the only obligate intermediate of nitrification by AOB.[39] Both NO and N_2O had been observed from anaerobic cell extracts of *N. europaea,*[40-41] but the absence of NO_2^- was explained by the presumption that nitroxyl (HNO) was an enzyme-bound intermediate. HNO can react with itself to produce N_2O[42] or be further oxidized to NO. The bound NO would react with O_2 and produce NO_2^-. Given our work with cyt P460[31] and *K. stuttgartiensis*'s NO-producing HAO homolog,[16] we were eager to test *N. europaea*'s HAO.

Upon assaying HAO, oxidant, and various concentrations of NH_2OH in aerobic buffer at pH 8.0, at least 85% of the NH_2OH was converted to NO_2^- or NO_3^-, consistent with previous reports.[26, 43] In the absence of the enzyme and after five hours, only 3.4% of NH_2OH was converted to NO_2^- and NO_3^-. Similarly, in absence of PMS—therefore only using O_2 as an oxidant—and after five hours, only 12% of NH_2OH was converted to NO_2^- or NO_3^-.[44] However, the same experiment conducted

under anaerobic conditions resulted in only 0.9% of NH_2OH being converted to NO_2^- or NO_3^-.[44] The lack of these products under anaerobic conditions still supported the idea that O_2 was necessary to convert NH_2OH to NO_2^-, but no evidence suggested that it was enzymatic.

Under anaerobic conditions, NO produced from HAO was quantified by use of catalase as an NO-scavenger as described by Pacheco and co-workers,[45-46] where any NO produced will bind catalase.[44] Using HAO, catalase, oxidant, and various amounts of NH_2OH in an anaerobic buffer at pH 8.0, we showed quantitative conversion of NH_2OH to NO. In addition, stoichiometry of oxidant consumption was consistent with a three-electron oxidation of NH_2OH. Like the Griess assay, this did not conclusively show that HAO catalysis terminates at NO because the enzyme could still require O_2 to produce NO_2^-. A similar experiment was conducted aerobically, using the reaction of oxyhemoglobin (Fe^{II}-O_2) with NO, thereby producing methemoglobin (Fe^{III}) and NO_3^- to detect NO.[47] By determining the amount of oxyhemoglobin converted to methemoglobin we had a measurement of NO production.[47] The assay only showed that 75% of the provided NH_2OH was converted to NO, likely because some of the NO and oxyhemoglobin did not react. However, the stoichiometry of oxidant consumption was consistent with a full conversion of NH_2OH to NO.

These experiments demonstrate that NO_2^- is not the enzymatic product of HAO catalysis; rather, NO is. In earlier studies, the NO_2^- observed was most likely a result of NO reacting with O_2. Therefore, the first energy producing step of AOB metabolism produces but one electron for cellular respiration, assuming two electrons are furnished to AMO. To maximize the energy AOB obtain from NH_3, another enzyme must exist that is able to react with the NO produced from HAO to liberate the additional electron and produce NO_2^-. The existence of such an enzyme is supported by stable isotope mass spectrometry that has identified the "second" O atom in NO_2^- as originating from H_2O.[11] The identify of this enzyme remains elusive.

Identifying NO as a nitrification intermediate further underscores the importance of NO in the nitrogen cycle. NO is now known to be an intermediate in the denitrification[3, 48-49] and anaerobic ammonium oxidation pathway.[3] Further, anammox

bacteria were recently shown to be capable of using NO as a terminal electron acceptor in continuous cultures that were provided only NO and NH_4^+.[50] Finally, NO has been produced by AOA[51] and is necessary for them to live,[52] emphasizing this molecule's role as a nexus of the nitrogen cycle.

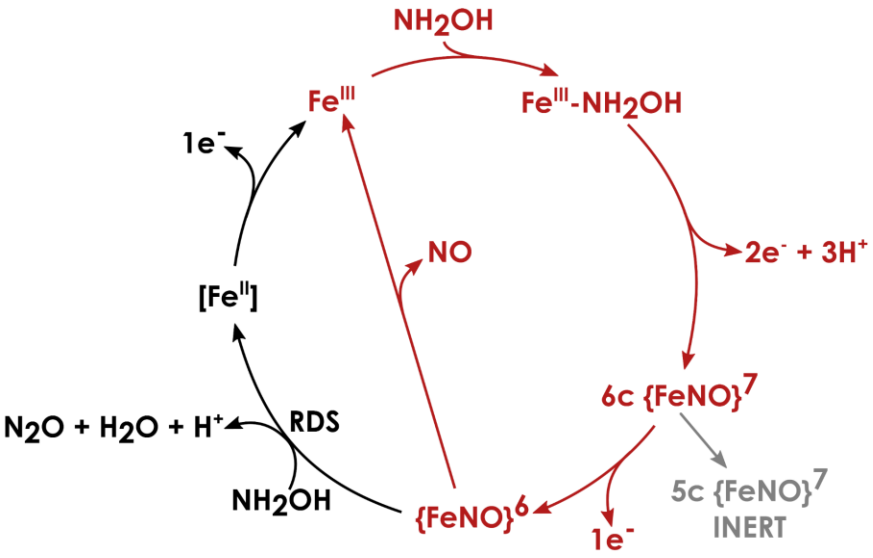

Figure 1.6. Catalytic cycle of P460 cofactors. The red pathway has been observed in HAO, whereas the red and black pathways have been observed in cyt P460. The gray line represents an off-pathway species. Reproduced from reference X.

A proton relay must complement the P460 cofactor for NH_2OH oxidation activity

The P460 cofactor is a source of an obligate nitrification intermediate and is unique among heme cofactors for several reasons. The most apparent is the non-canonical cross-link. Another difference is the direct oxidation of a bound substrate; in contrast, enzymes like cyt P450 oxidize substrates by producing a ferryl center that hydroxylates the substrate.[53-54] However, our study of a cyt P460 from the microorganism *Nitrosomonas* sp. AL212 made it apparent that the presence of a P460 cofactor alone is insufficient for NH_2OH oxidation.[55] This cyt P460 variant is able to bind NH_2OH and NO similar to the active enzyme from *N. europaea*.[55] Moreover, its $Fe^{II/III}$ reduction potentials and spectroscopic features are similar, indicating there are

no major electronic differences between the active and inactive cyt P460 variants.[35] However, the protein is inactive.

A crystal structure of the inactive *N.* sp. AL212 cyt P460 (PDB ID: 6AMG) compared to the active *N. europaea* cyt P460 (PDB ID: 2JE3)[23] showed that the active sites of these proteins were identical except for the presence of a glutamate (Glu) residue at position 96 in the active enzyme and an alanine (Ala) at position 131 in the inactive protein (**Figure 1.7a)**.[35] Site-directed mutagenesis was used to generate the *N.* sp. AL212 Ala131Glu cyt P460 variant that was capable of NH_2OH oxidation.[35] A GC analysis showed N_2O production, with the expected stoichiometry of NH_2OH to N_2O. Finally, mutating Glu96 in *N. europaea* cyt P460 to Ala abolished activity, indicating the Glu residue is important for the catalytic competence of cyt P460 enzymes. A similar strategy is likely employed by HAO—the active site of that enzyme houses an Asp and His couple that was predicted to be involved in proton transfer.[16]

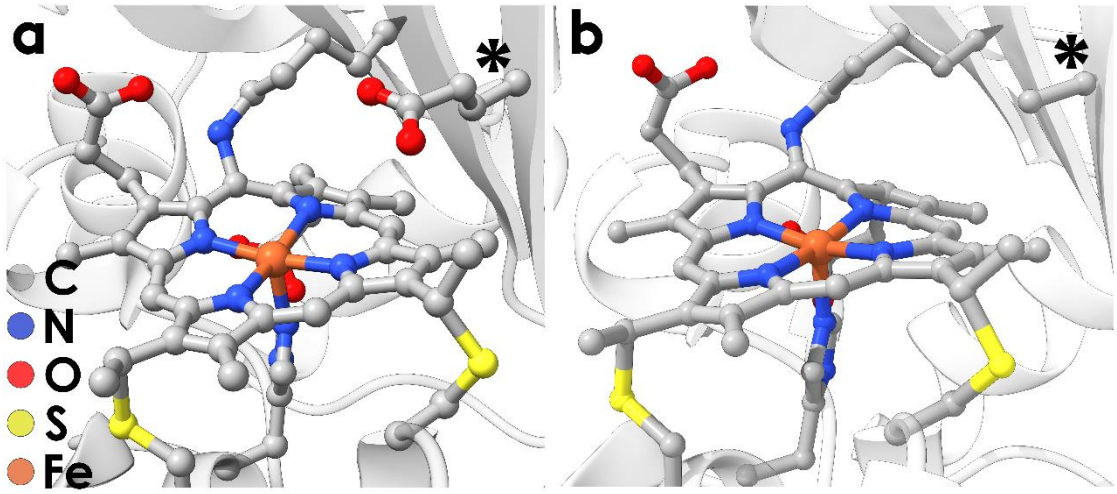

Figure 1.7. (a) The active sites of *N. europaea* cyt P460 (PDB ID 2JE3) and (b) *Nitrosomonas* sp. AL212 (PDB ID 2AMG). The * indicates the presence of a second-sphere glutamate (Glu) residue in *N. europaea* and an alanine (Ala) residue in *N.* sp. AL212.

Other mutants of *N.* sp. AL212 cyt P460 were generated to test the effect of different types of residues on the Glu position: an isostructural glutamine variant

(Ala131Gln), a basic aspartate variant (Ala131Asp), and a nonpolar leucine variant (Ala131Leu). All these mutations failed to restore activity, indicating the importance of the Glu in this position because it can reach the bound NH_2OH and accept protons.[35] Importantly, compared the active enzyme, all of these cyt P460 variants exhibited identical UV-vis absorption spectra, had similar binding affinities for NH_2OH and NO, and had $Fe^{II/III}$ reduction potentials near –400 mV vs NHE.[35]

This emphasizes the importance of the secondary coordination sphere in defining metalloprotein functionality. The effective electronic and structural invariance between functional and inactive cyt P460s aside from the presence of a single carboxylate provides a clear example of the necessity of a polypeptide matrix to imbue function to what would otherwise be a "dead" coordination complex. This phenomenon has, of course, been extensively demonstrated in synthetic inorganic chemistry where second-sphere interactions—typically hydrogen bonds—are gaining popularity as key design elements toward complexes capable of small molecule activation or stabilizing reactive moieties.[56-58]

Influences of the heme-lysine cross-link on cyt P460 reactivity and nitric oxide sensitivity

The second-sphere Glu residue is necessary for oxidation of Fe^{III}-NH_2OH to the reactive intermediate of cyt P460 catalysis. The $\{FeNO\}^6$ can be accessed with either 1- or 2-electron oxidants. A concerted 3-electron oxidation is unlikely in biological systems, meaning that potential intermediates could be the Fe^{III}-$^{\bullet}NH_2OH$, an Fe^{III}-HNO, or an $\{FeNO\}^7$. In our first study of cyt P460,[31] minor 5c $\{FeNO\}^7$ contamination was observed in the EPR of the Fe^{III}-NH_2OH adduct. Treatment of Fe^{III} WT *N. europaea* cyt P460 with the chemical HNO donor, disodium diazen-1-ium-1,2,2-triolate ($Na_2N_2O_3$) produces a new species in the UV-vis spectrum with a Soret maximum at 452 nm that decays to a new species with a Soret maximum at 455 nm over 15 minutes.[59] Both of these species were also generated by treating the Fe^{II} protein with NO from PROLI-NONOate. X-band EPR of the initial product and the decay product were consistent with these two species being a $S = {}^1/_2$, 6-coordinate (6c)

{FeNO}^{7} and a $S = {}^1/_2$, 5c {FeNO}^{7}, respectively. In addition, the extended X-ray absorption fine structure provided Fe-His distances that were consistent with a bound His (~2.1 Å) in the presumed 6c species and a dissociated His (~2.5 Å) in the 5c species.[59]

WT *N. europaea* cyt P460 was treated with HNO from $Na_2N_2O_3$ at pH 8.0 under anaerobic conditions to produce the {FeNO}^{7}. This species was treated with NH_2OH, but no further reaction occurred. However, when the 6c {FeNO}^{7} was treated with either oxidant, {FeNO}^{6} formed. This is in contrast to the unreactive 5c {FeNO}^{7}.[59] These data suggested that the 6c {FeNO}^{7} was an intermediate of the NH_2OH oxidation pathway of cyt P460 catalysis. To allow the 6c {FeNO}^{7} species to accumulate, WT cyt P460 was treated with NH_2OH and a sufficiently low concentration of oxidant to allow for the His dissociation pathway to compete with the oxidation pathway. EPR revealed the presence of 6c {FeNO}^{7}. This experiment confirmed the intermediacy of 6c {FeNO}^{7} in the catalytic cycle. This species has two potential fates: In the presence of sufficient oxidant, it will be oxidized to the {FeNO}^{6}. If there is insufficient oxidant, the 6c {FeNO}^{7} slowly converts to the inactive 5c {FeNO}^{7}.

Axial His dissociation is common for heme proteins bound to NO,[60] and is proposed to be the basis for how signaling proteins like soluble guanylate cyclase (sGC) function.[60] In sGC, there is a rate-dependence on [NO]. However, the 6c-to-5c conversion in WT *N. europaea* cyt P460 shows no dependence on the [NO] or [HNO] and is substantially slower.[59] To test if the lack of [NO]-dependence was an effect of the heme-Lys cross-link, a CLD mutant of *N. europaea* cyt P460 was generated—Lys70Tyr cyt P460—which was unreactive with NH_2OH but otherwise similar to WT *N. europaea* cyt P460. In stark contrast to the cross-link containing protein, this CLD variant displayed a rapid conversion to the 5c {FeNO}^{7} when treated with excess NO and followed both NO-dependent and NO-independent pathways to dissociate the axial His. An Eyring analysis showed that in the CLD variant, there is a large entropic driving force for this reaction that is not seen in the cross-link-containing protein. This indicates that the cross-link protects an on-pathway intermediate.

The cross-link of cyt P460 is important for the reactivity of the enzyme. The presence of the cross-link also substantially alters its spectroscopic properties, but is not functionally relevant. It was unclear if the red-shifted Soret maximum of WT cyt P460 was a result of the *meso* carbon being sp^3 hybridized. When the original crystal structure of cyt P460 was solved in 2007,[23] the 13' *meso* carbon was classified as such a based on similarity of the cofactor to the P460 in HAO.[14, 16, 18, 61] This would indicate that the porphyrin of HAO is not actually a porphyrin, but is instead either an isoporphyrin or a phlorin. However, a 1.45 Å resolution crystal structure from WT *N.* sp. AL212 cyt P460 (PDB ID: 6AMG) showed that this carbon is actually more consistent with sp^2 hybridization and is a true porphyrin.[55] This was tested by restraining the Lys N and the *meso* carbon during refinement to produce an sp^2-sp^3 bond length, but this resulted in negative electron density in the omit map.[55]

Time-dependent density functional theory was used to calculate the UV-vis absorption profiles of cyt P460 assuming a porphyrin, isoporphyrin, or phlorin tetrapyrrole geometry using the coordinates of the heme macrocycle and any inner-sphere ligands. The absorption profile of the *b* hemoprotein horse heart metmyoglobin was also calculated using the coordinates from its structure (PBD ID: 1WLA)[62] as a positive control.[55] This calculation showed that sp^3 hybridization is not necessary to produce a red-shifted absorption spectrum, and it showed that a phlorin configuration is unlikely because it would produce a feature near 700 nm. Additional calculations tested whether a C–N or C–C cross-link would produce a red-shifted Soret. Both calculations showed red-shifts of ca. 35 nm compared to porphyrin with no cross-link or to metmyoglobin. The C–N cross-link had the broadest and least intense Soret band, which was attributed to the nitrogen lone pair interacting with the a_{2u} orbital and an e_g orbital.

The cross-link of cyt P460—and presumably HAO—imparts unique properties onto the P460 cofactor. To our knowledge, no other heme system has a naturally-occurring post-translational modification directly onto the porphyrin ring itself.[63] Even hydrazine synthase, another enzyme involved in the biogeochemical nitrogen cycle,

has a heme with an additional non-canonical cross-link from a cysteine residue to one of the heme-methyl groups.[64]

Outline of Thesis

The focus of this thesis is on understanding both the purpose of the heme-lysine cross-link in cytochrome P460 and the mechanism of its formation. Chapter two addresses the role of the heme-lysine cross-link in NH_2OH oxidation step. We investigated the electronic structure and thermodynamic properties of a CLD cyt P460 species in comparison to the WT, cross-link containing protein to discern any electronic differences that the cross-link imparts. We also used X-ray crystallography to obtain the first CLD cyt P460 crystal structure.

Chapter Three addresses the mechanism of cross-link formation in cyt P460. The mechanism of formation of the Lys cross-link in cyt P460 is unknown but was reported to be an autocatalytic process. AOB are obligate aerobic microorganisms and therefore always have oxygen present in the cell. Further, a previous crystal structure of cyt P460 showed that one of the heme *meso* carbons was hydroxylated, leading us to believe that the heme site might be very prone towards reaction with oxygen. Recombinant expression in *Escherichia coli*, a facultative anaerobic microorganism, has allowed us to isolate a cyt P460 species with the Lys in its primary structure, but without it being bound to the 13′ *meso* carbon.

Chapter Four addresses preliminary work in establishing which residues are essential for cyt P460 cross-link formation. The P460 cofactor is defined by a high-degree of heme-ruffling—an out-of-plane distortion in which two opposing sides of the porphyrin macrocycle are bent above and below the heme plane. This chapter shows preliminary work with mutants the remove key residues in the distal and proximal pockets of the heme site and by crystallography, seem to affect the heme-ruffling. We speculated that ruffling might promote the reactivity of the 13′ *meso* carbon with activated oxygen, enabling further reaction with Lys to form the cross-link.

REFERENCES

1. Fields, S., Global nitrogen: cycling out of control. *Environ Health Perspect* **2004,** *112* (10), A556-A563.

2. Raymond, J.; Siefert Jl Fau - Staples, C. R.; Staples Cr Fau - Blankenship, R. E.; Blankenship, R. E., The natural history of nitrogen fixation. (0737-4038 (Print)).

3. Kuypers, M. M. M.; Marchant, H. K.; Kartal, B., The microbial nitrogen-cycling network. *Nature Reviews Microbiology* **2018,** *16* (5), 263-276.

4. Gruber, N.; Galloway, J. N., An Earth-system perspective of the global nitrogen cycle. *Nature* **2008,** *451* (7176), 293-296.

5. Burk, D.; Lineweaver, H.; Horner, C. K., The Specific Influence of Acidity on the Mechanism of Nitrogen Fixation by Azotobacter. *J Bacteriol* **1934,** *27* (4), 325-340.

6. Erisman, J. W.; Sutton, M. A.; Galloway, J.; Klimont, Z.; Winiwarter, W., How a century of ammonia synthesis changed the world. *Nature Geoscience* **2008,** *1* (10), 636-639.

7. Lancaster, K. M.; Caranto, J. D.; Majer, S. H.; Smith, M. A., Alternative Bioenergy: Updates to and Challenges in Nitrification Metalloenzymology. *Joule* **2018,** *2* (3), 421-441.

8. Lehnert, N.; Dong, H. T.; Harland, J. B.; Hunt, A. P.; White, C. J., Reversing nitrogen fixation. *Nature Reviews Chemistry* **2018,** *2* (10), 278-289.

9. Daims, H.; Lebedeva, E. V.; Pjevac, P.; Han, P.; Herbold, C.; Albertsen, M.; Jehmlich, N.; Palatinszky, M.; Vierheilig, J.; Bulaev, A.; Kirkegaard, R. H.; von Bergen, M.; Rattei, T.; Bendinger, B.; Nielsen, P. H.; Wagner, M., Complete nitrification by Nitrospira bacteria. *Nature* **2015,** *528* (7583), 504-509.

10. van Kessel, M. A. H. J.; Speth, D. R.; Albertsen, M.; Nielsen, P. H.; Op den Camp, H. J. M.; Kartal, B.; Jetten, M. S. M.; Lücker, S., Complete nitrification by a single microorganism. *Nature* **2015,** *528* (7583), 555-559.

11. Andersson, K. K.; Hooper, A. B., O2 and H2O are each the source of one O in NO_2^- produced from NH3 by Nitrosomonas: 15N-NMR evidence. *FEBS Letters* **1983,** *164* (2), 236-240.
12. Arp, D. J.; Sayavedra-Soto, L. A.; Hommes, N. G., Molecular biology and biochemistry of ammonia oxidation by *Nitrosomonas europaea*. *Archivesof Microbiology* **2002,** *178* (4), 250-255.
13. Kranz, R. G.; Richard-Fogal, C.; Taylor, J.-S.; Frawley, E. R., Cytochrome *c* Biogenesis: Mechanisms for Covalent Modifications and Trafficking of Heme and for Heme-Iron Redox Control. *Microbiology and Molecular Biology Reviews* **2009,** *73* (3), 510-528.
14. Igarashi, N.; Moriyama, H.; Fujiwara, T.; Fukumori, Y.; Tanaka, N., The 2.8 Å structure of hydroxylamine oxidoreductase from a nitrifying chemoautotrophic bacterium, Nitrosomonas europaea. *Nature Structural Biology* **1997,** *4* (4), 276-284.
15. Cedervall, P.; Hooper, A. B.; Wilmot, C. M., Structural Studies of Hydroxylamine Oxidoreductase Reveal a Unique Heme Cofactor and a Previously Unidentified Interaction Partner. *Biochemistry* **2013,** *52* (36), 6211-6218.
16. Maalcke, W. J.; Dietl, A.; Marritt, S. J.; Butt, J. N.; Jetten, M. S. M.; Keltjens, J. T.; Barends, T. R. M.; Kartal, B., Structural Basis of Biological NO Generation by Octaheme Oxidoreductases. *Journal of Biological Chemistry* **2014,** *289* (3), 1228-1242.
17. Arciero, D. M.; Hooper, A. B., Evidence for a crosslink between c-heme and a lysine residue in cytochrome P460 of Nitrosomonas europaea. *FEBS Letters* **1997,** *410* (2), 457-460.
18. Cedervall, P. E.; Hooper, A. B.; Wilmot, C. M., Crystallization and preliminary X-ray crystallographic analysis of a new crystal form of hydroxylamine oxidoreductase from Nitrosomonas europaea. *Acta crystallographica. Section F, Structural biology and crystallization communications* **2009,** *65* (Pt 12), 1296-1298.
19. Papp, B.; Török, T.; Sándor, E.; Fekete, E.; Flipphi, M.; Karaffa, L., High cell density cultivation of the chemolithoautotrophic bacterium Nitrosomonas europaea. *Folia Microbiologica* **2016,** *61* (3), 191-198.

20. Numata, M.; Saito, T.; Yamazaki, T.; Fukumori, Y.; Yamanaka, T., Cytochrome P-460 of Nitrosomonas europaea: Further Purification and Further Characterization. *The Journal of Biochemistry* **1990,** *108* (6), 1016-1021.
21. Zahn, J. A.; Duncan, C.; DiSpirito, A. A., Oxidation of hydroxylamine by cytochrome P-460 of the obligate methylotroph Methylococcus capsulatus Bath. *J Bacteriol* **1994,** *176* (19), 5879-5887.
22. Bergmann, D. J.; Hooper, A. B., The primary structure of cytochrome P460 of Nitrosomonas europaea: Presence of a c-heme binding motif. *FEBS Letters* **1994,** *353* (3), 324-326.
23. Pearson, A. R.; Elmore, B. O.; Yang, C.; Ferrara, J. D.; Hooper, A. B.; Wilmot, C. M., The Crystal Structure of Cytochrome P460 of Nitrosomonas europaea Reveals a Novel Cytochrome Fold and Heme−Protein Cross-link. *Biochemistry* **2007,** *46* (28), 8340-8349.
24. Fernández, M. L.; Estrin, D. A.; Bari, S. E., Theoretical insight into the hydroxylamine oxidoreductase mechanism. *Journal of Inorganic Biochemistry* **2008,** *102* (7), 1523-1530.
25. Ferousi, C.; Majer, S. H.; DiMucci, I. M.; Lancaster, K. M., Biological and Bioinspired Inorganic N–N Bond-Forming Reactions. *Chemical Reviews* **2020**.
26. Hooper, A. B.; Terry, K. R., Hydroxylamine oxidoreductase of Nitrosomonas: Production of nitric oxide from hydroxylamine. *Biochimica et Biophysica Acta (BBA) - Enzymology* **1979,** *571* (1), 12-20.
27. Barrett, E.; Lapworth, A., IX.—The influence of acids and alkalis on the velocity of formation of acetoxime. *Journal of the Chemical Society, Transactions* **1908,** *93* (0), 85-93.
28. Bengtsson, G.; Fronæus, S.; Bengtsson-Kloo, L., The kinetics and mechanism of oxidation of hydroxylamine by iron(iii). *Journal of the Chemical Society, Dalton Transactions* **2002,** (12), 2548-2552.
29. Alluisetti, G. E.; Almaraz, A. E.; Amorebieta, V. T.; Doctorovich, F.; Olabe, J. A., Metal-Catalyzed Anaerobic Disproportionation of Hydroxylamine. Role of

Diazene and Nitroxyl Intermediates in the Formation of N2, N2O, NO+, and NH3. *Journal of the American Chemical Society* **2004,** *126* (41), 13432-13442.

30. Cisneros, L. O.; Rogers, W. J.; Mannan, M. S.; Li, X.; Koseki, H., Effect of Iron Ion in the Thermal Decomposition of 50 mass % Hydroxylamine/Water Solutions. *Journal of Chemical & Engineering Data* **2003,** *48* (5), 1164-1169.

31. Caranto, J. D.; Vilbert, A. C.; Lancaster, K. M., *Nitrosomonas europaea* cytochrome P460 is a direct link between nitrification and nitrous oxide emission. *Proceedings of the National Academy of Sciences* **2016,** *113* (51), 14704-14709.

32. Zhu, X.; Burger, M.; Doane, T. A.; Horwath, W. R., Ammonia oxidation pathways and nitrifier denitrification are significant sources of N_2O and NO under low oxygen availability. *Proceedings of the National Academy of Sciences* **2013,** *110*, 6328-6333.

33. Beaumont, H. J. E.; van Schooten, B.; Lens, S. I.; Westerhoff, H. V.; van Spanning, R. J. M., *Nitrosomonas europaea* Expresses a Nitric Oxide Reductase during Nitrification. *J Bacteriol* **2004,** *186*, 4417-4421.

34. Zorz, J. K.; Kozlowski, J. A.; Stein, L. Y.; Strous, M.; Kleiner, M., Comparative Proteomics of Three Species of Ammonia-Oxidizing Bacteria. *Frontiers in Microbiology* **2018,** *9* (938).

35. Smith, M. A.; Majer, S. H.; Vilbert, A. C.; Lancaster, Kyle M., Controlling a burn: outer-sphere gating of hydroxylamine oxidation by a distal base in cytochrome P460. *Chemical Science* **2019,** *10* (13), 3756-3764.

36. Lehnert, N.; Praneeth, V. K. K.; Paulat, F., Electronic structure of iron(II)–porphyrin nitroxyl complexes: Molecular mechanism of fungal nitric oxide reductase (P450nor). *Journal of Computational Chemistry* **2006,** *27* (12), 1338-1351.

37. Daiber, A.; Nauser, T.; Takaya, N.; Kudo, T.; Weber, P.; Hultschig, C.; Shoun, H.; Ullrich, V., Isotope effects and intermediates in the reduction of NO by P450NOR. *Journal of Inorganic Biochemistry* **2002,** *88* (3), 343-352.

38. Kozlowski, J. A.; Kits, K. D.; Stein, L. Y., Complete Genome Sequence of *Nitrosomonas ureae* Strain Nm10, an Oligotrophic Group 6a Nitrosomonad. *Genome Announcements* **2016,** *4* (2), e00094-16.

39. Arp, D. J.; Stein, L. Y., Metabolism of Inorganic N Compounds by Ammonia-Oxidizing Bacteria. *Critical Reviews in Biochemistry and Molecular Biology* **2003,** *38* (6), 471-495.

40. Anderson, J., The metabolism of hydroxylamine to nitrite by Nitrosomonas. *Biochemical Journal* **1964,** *91* (1), 8-17.

41. Ritchie, G. A. F.; Nicholas, D. J. D., Identification of the sources of nitrous oxide produced by oxidative and reductive processes in Nitrosomonas europaea. *Biochemical Journal* **1972,** *126* (5), 1181-1191.

42. Shafirovich, V.; Lymar, S. V., Nitroxyl and its anion in aqueous solutions: Spin states, protic equilibria, and reactivities toward oxygen and nitric oxide. *Proceedings of the National Academy of Sciences* **2002,** *99* (11), 7340-7345.

43. Hooper, A. B.; Nason, A., Characterization of Hydroxylamine-Cytochrome c Reductase from the Chemoautotrophs Nitrosomonas europaea and Nitrosocystis oceanus. *Journal of Biological Chemistry* **1965,** *240* (10), 4044-4057.

44. Caranto, J. D.; Lancaster, K. M., Nitric oxide is an obligate bacterial nitrification intermediate produced by hydroxylamine oxidoreductase. *Proceedings of the National Academy of Sciences* **2017,** *114* (31), 8217-8222.

45. Pacheco, A. A.; McGarry, J.; Kostera, J.; Corona, A., Chapter twenty - Techniques for Investigating Hydroxylamine Disproportionation by Hydroxylamine Oxidoreductases. In *Methods in Enzymology*, Klotz, M. G., Ed. Academic Press: 2011; Vol. 486, pp 447-463.

46. Purwar, N.; McGarry, J. M.; Kostera, J.; Pacheco, A. A.; Schmidt, M., Interaction of Nitric Oxide with Catalase: Structural and Kinetic Analysis. *Biochemistry* **2011,** *50* (21), 4491-4503.

47. Salter, M.; Knowles, R. G., Assay of NOS Activity by the Measurement of Conversion of Oxyhemoglobin to Methemoglobin by NO. In *Nitric Oxide Protocols*, Titheradge, M. A., Ed. Humana Press: Totowa, NJ, 1998; pp 61-65.

48. Braun, C.; Zumft, W. G., Marker exchange of the structural genes for nitric oxide reductase blocks the denitrification pathway of Pseudomonas stutzeri at nitric oxide. *J Biol Chem* **1991,** *266* (34), 22785-8.

49. Ye, R. W.; Averill, B. A.; Tiedje, J. M., Denitrification: production and consumption of nitric oxide. *Applied and environmental microbiology* **1994,** *60* (4), 1053-1058.
50. Hu, Z.; Wessels, H. J. C. T.; van Alen, T.; Jetten, M. S. M.; Kartal, B., Nitric oxide-dependent anaerobic ammonium oxidation. *Nature Communications* **2019,** *10* (1), 1244.
51. Martens-Habbena, W.; Qin, W.; Horak, R. E.; Urakawa, H.; Schauer, A. J.; Moffett, J. W.; Armbrust, E. V.; Ingalls, A. E.; Devol, A. H.; Stahl, D. A., The production of nitric oxide by marine ammonia-oxidizing archaea and inhibition of archaeal ammonia oxidation by a nitric oxide scavenger. *Environ Microbiol* **2015,** *17* (7), 2261-74.
52. Sauder, L. A.; Ross, A. A.; Neufeld, J. D., Nitric oxide scavengers differentially inhibit ammonia oxidation in ammonia-oxidizing archaea and bacteria. *FEMS Microbiology Letters* **2016,** *363* (7).
53. Denisov, I. G.; Makris, T. M.; Sligar, S. G.; Schlichting, I., Structure and Chemistry of Cytochrome P450. *Chemical Reviews* **2005,** *105* (6), 2253-2278.
54. Rittle, J.; Green, M. T., Cytochrome P450 Compound I: Capture, Characterization, and C-H Bond Activation Kinetics. *Science* **2010,** *330* (6006), 933-937.
55. Smith, M. A.; Lancaster, K. M., The Eponymous Cofactors in Cytochrome P460s from Ammonia-Oxidizing Bacteria Are Iron Porphyrinoids Whose Macrocycles Are Dibasic. *Biochemistry* **2018,** *57* (3), 334-343.
56. Cook, S. A.; Borovik, A. S., Molecular Designs for Controlling the Local Environments around Metal Ions. *Accounts of Chemical Research* **2015,** *48* (8), 2407-2414.
57. Ford, C. L.; Park, Y. J.; Matson, E. M.; Gordon, Z.; Fout, A. R., A bioinspired iron catalyst for nitrate and perchlorate reduction. *Science* **2016,** *354* (6313), 741-743.
58. Hale, L. V. A.; Szymczak, N. K., Hydrogen Transfer Catalysis beyond the Primary Coordination Sphere. *ACS Catalysis* **2018,** *8* (7), 6446-6461.

59. Vilbert, A. C.; Caranto, J. D.; Lancaster, Kyle M., Influences of the heme-lysine crosslink in cytochrome P460 over redox catalysis and nitric oxide sensitivity. *Chemical Science* **2018,** *9* (2), 368-379.
60. Zhao, Y.; Brandish, P. E.; Ballou, D. P.; Marletta, M. A., A molecular basis for nitric oxide sensing by soluble guanylate cyclase. *Proceedings of the National Academy of Sciences* **1999,** *96* (26), 14753-14758.
61. Arciero, D. M.; Hooper, A. B., Consideration of a phlorin structure for haem P-460 of hydroxylamine oxidoreductase and its implications regarding reaction mechanism. *Biochemical Society transactions* **1998,** *26* (3), 385-389.
62. Maurus, R.; Overall, C. M.; Bogumil, R.; Luo, Y.; Mauk, A. G.; Smith, M.; Brayer, G. D., A myoglobin variant with a polar substitution in a conserved hydrophobic cluster in the heme binding pocket. *Biochimica et biophysica acta* **1997,** *1341* (1), 1-13.
63. Lin, Y.-W., Structure and function of heme proteins regulated by diverse post-translational modifications. *Archives of Biochemistry and Biophysics* **2018,** *641*, 1-30.
64. Dietl, A.; Ferousi, C.; Maalcke, W. J.; Menzel, A.; de Vries, S.; Keltjens, J. T.; Jetten, M. S. M.; Kartal, B.; Barends, T. R. M., The inner workings of the hydrazine synthase multiprotein complex. *Nature* **2015,** *527* (7578), 394-397.

CHAPTER 2

THE HEME-LYSINE CROSS-LINK IN CYTOCHROME P460 PROMOTES CATALYSIS BY ENFORCING SECONDARY COORDINATION SPHERE ARCHITECTURE

Adapted in part from:

"The Heme-Lysine Cross-link in Cytochrome P460 Promotes Catalysis by Enforcing Secondary Coordination Sphere Architecture"

Rachael E. Coleman, Avery C. Vilbert, and Kyle M. Lancaster

Introduction

Heme P460 cofactors have thus far been found in two protein families—the octaheme hydroxylamine oxidoreductase (HAO) family and the cytochrome (cyt) P460 family.[1] These *c*-type heme enzymes contain a histidine-ligated, five-coordinate (5c), high spin Fe center and each participate in the controlled oxidation of hydroxylamine (NH_2OH), but share little sequence and structural homology otherwise.[2] Their respective active sites each harbor a heme cofactor that is covalently attached to the cysteine (Cys) residues of a highly conserve CXXCH amino acid motif via two thioether bonds, as in canonical *c*-type cytochromes.[3] Both P460 cofactors feature additional covalent cross-links between the porphyrin macrocycle and the polypeptide. These cross-links contribute to red-shifted Soret absorption maxima near 460 nm in their ferrous oxidation state,[4] thus giving the cofactors their name. In HAO, the heme is cross-linked to the sidechain of a tyrosine (Tyr) residue via two covalent attachments. In the well-characterized *N. europaea* HAO, the C3 atom of Tyr467 forms a bond with the C5 atom of a *c*-heme from a neighboring subunit. A second attachment is formed through the phenolate oxygen atom of Tyr467 to the C4 atom (**Figure 2.1a**).[5-6] The cofactor in cyt P460 has only a single non-thioether heme-protein cross-link, which is formed between the N of a Lys and the 13′ *meso* carbon of the heme porphyrin (**Figure 2.1b,c**).[2, 7-8]

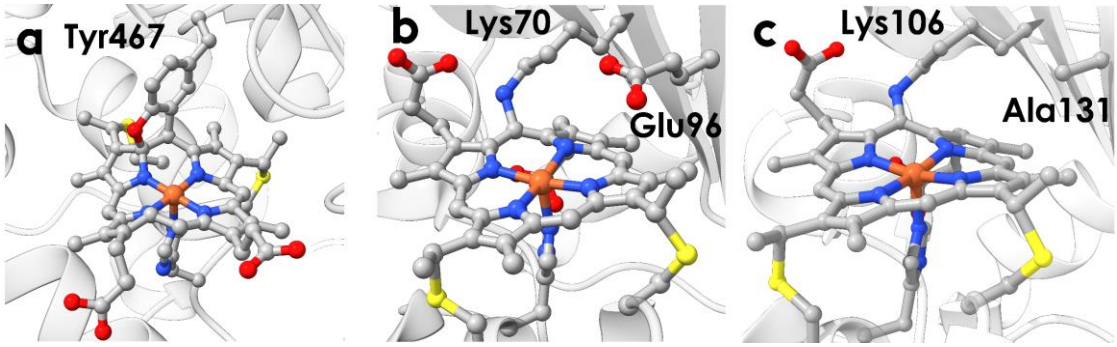

Figure 2.1. The active site of various P460 cofactors with the cross-linking residues and key second-sphere residues labeled. (a) The active site of *Nitrosomonas europaea* hydroxylamine oxidoreductase (HAO), (b) shows the active site of *N. europaea* cytochrome (cyt) P460, and (c) shows the active site of *Nitrosomonas* sp. AL212 cyt P460. A second sphere glutamate (Glu) is necessary for reactivity in cyt P460.

Despite the differences between their cofactors, both HAO and cyt P460 oxidize NH_2OH, albeit to different products: HAO produces nitric oxide (NO), while cyt P460 produces nitrous oxide (N_2O).[9-11] The physiological role of HAO is known—it is the first enzyme to produce reducing equivalents for the cell.[9, 12] The role of cyt P460 is unknown, but we have speculated that it may play a role in abating the cellular burden of NH_2OH and/or NO at high concentrations.[10] Mechanistic studies concerning NH_2OH oxidation by heme P460 cofactors are largely limited to the case of cyt P460. Presumably, this is due to the difficulty associated with amassing HAO and the subsequent complications in deconvoluting spectra because of the sheer number of heme cofactors present. However, the enzymes plausibly share similar mechanistic steps. The cyt P460 catalytic cycle begins with NH_2OH binding to the P460 Fe in its resting ferric oxidation state (**Figure 1.6**).[10] If a suitable oxidant is available, two electrons and three protons will be removed from NH_2OH to generate a six-coordinate (6c) $\{FeNO\}^7$ (written in the Enemark-Feltham notation, where the superscript denotes the sum of electrons in the d manifold and the NO π* orbitals) species.[10, 13-15] The cyt P460 cross-link stabilizes the 6c $\{FeNO\}^7$ against loss of its axial histidine

(His), which produces an off-pathway 5c $\{FeNO\}^7$ under limiting oxidant conditions.[15] Subsequent oxidation of the 6c $\{FeNO\}^7$ produces an $\{FeNO\}^6$ intermediate that reacts with a second equivalent of NH_2OH to generate N_2O in the rate-determining step.[10] Finally, the Fe is rapidly re-oxidized to the resting ferric form to complete the catalytic cycle.[10, 16] Because of the modest ca., 10 μM K_d of ferric cyt P460 for NO, any available O_2 may react with dissociated NO to form nitrite (NO_2^-), driving the equilibrium toward loss of NO from the $\{FeNO\}^6$,and thus return to the ferric resting state. However, in the absence of O_2 or NH_2OH, the $\{FeNO\}^6$ of cyt P460 will persist.[10]

Recently, we showed that the secondary coordination sphere of cyt P460 must include a deprotonated carboxylate residue to serve as a proton-relay in order to effect oxidation of NH_2OH.[14] One of the cyt P460 genes present in the *Nitrosomonas* sp. AL212 genome is inactive but otherwise spectroscopically identical to the active *N. europaea* variant;[4] the most significant difference is structural. This cyt P460 from *Nitrosomonas* sp. AL212 lacks the catalytically relevant glutamate (Glu) residue in the secondary coordination sphere of the P460 cofactor, and harbors an alanine (Ala) residue instead (**Figure 2.1c**).[14] Mutation of Ala131 in *N.* sp. AL212 to Glu restored activity. Meanwhile, mutating Glu96 to Ala in *N. europaea* abolished activity.[14] This study also provided insights into the behavior of the Glu residue during catalysis. Crystal structures of the inactive Ala131Gln mutant with and without NH_2OH bound to the heme Fe (PDB IDs: 6E0Y and 6E0Z, respectively), showed that Gln has two possible sidechain conformations: one where it orients towards the bound substrate and another where it orients away in its absence (resting state).[14] This is supported by the original crystal structure of *N. europaea* cyt P460 (PDB ID: 2JE3) where a phosphate is bound to the heme Fe and the Glu is oriented towards the heme center.[2] Although no additional structural data exist for the outwards conformation of the Glu sidechain in *N. europaea* cyt P460, it plausibly behaves the same way as Gln in the *N.* sp. AL212 Ala131Gln mutant.

Another key finding in the same study was that the presence of a carboxylate group alone is insufficient for NH_2OH oxidation; mutation of *N.* sp. AL212 Ala131 to

an aspartate (Asp) residue could not re-establish activity.[14] Assuming that an Asp exhibits the same behavior as a Glu in that position, this indicates that there is a narrow positional tolerance for the proton-relay site.[14] While the active site of HAO does not have a second-sphere Glu residue, it does have an Asp and His couple which likely serves the same purpose as cyt P460's Glu.[14, 17]

The tight positional tolerance for the proton-relay and the fact that removal of the cross-link has been shown to abolish activity[15, 18] prompted the hypothesis that the Lys cross-link serves to position the heme close to the second-sphere Glu residue. To address the role of the cross-link in dictating cyt P460 function, we now report a 2.2 Å crystal structure of cross-link deficient (CLD) *N. sp.* AL212 Lys106Leu/Ala131Glu cyt P460. Structural and spectroscopic analysis of this variant permitted detailed scrutiny into the relationship between the heme-Lys cross-link and heme P460 out-of-plane (OOP) distortions. Importantly, we establish a structural link between the heme-Lys cross-link and the positioning of the essential proton-relay. This strongly suggests that the cross-link enables NH_2OH oxidation by enforcing an active site architecture suitable for substrate redox chemistry to proceed, likely via an initial concerted proton-electron transfer (CPET) process.

Characterization of the CLD cyt P460: Activity, thermodynamics, and electronic structure

Both the proton-relay deficient (PRD) and the CLD cyt P460 can form all of the observed catalytically relevant intermediates (**Figure 1.5)** when treated with exogenous chemical donors (**Figure 1.3**).[4, 15] However, the Fe^{III}–NH_2OH adducts do not react with the chemical oxidants DCPIP ($E°$ = +224 mV vs normal hydrogen electrode (NHE)[15]) or PMS ($E°$ = +92 mV vs NHE[15]) (**Figure 2.2**).[14-15] Before addition of protein, the background consumption of DCPIP was 7.7 ± 2.4 μM DCPIP•min^{-1} whereas after addition of 10 μM *N.* sp. AL212 Lys106Leu/Ala131Glu the consumption was 8.3 ± 3.9 μM DCPIP•min^{-1} (**Figure 2.2**), indicating no change in the consumption of DCPIP. In the case of the PRD variant, significant variations in substrate binding affinity were excluded as the cause of this behavior,[14] although this

had not been rigorously examined in a CLD variant.[15] Titration of the CLD variant with NH_2OH revealed that removal of the Lys cross-link in *N.* sp. AL212 does not substantially alter the binding affinity, resulting in a twofold decrease in the 25°C K_d for NH_2OH (**Table 2.1, Figure 2.3**).

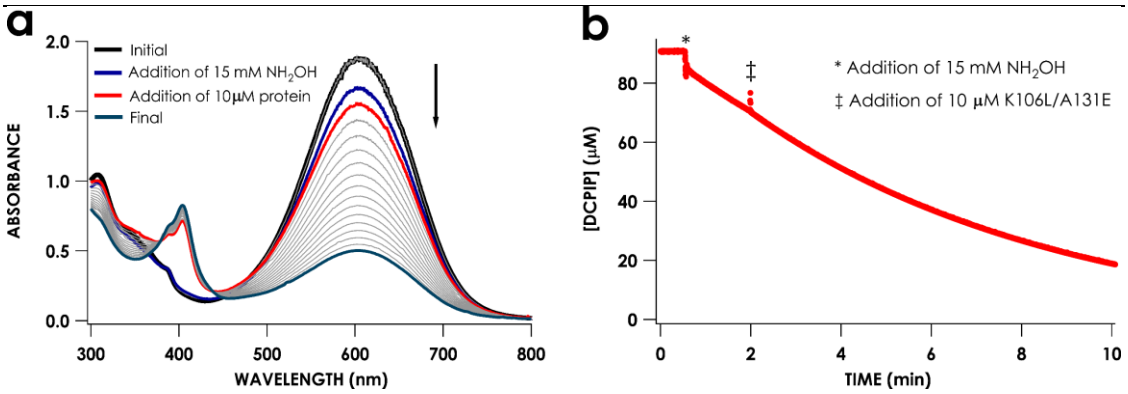

Figure 2.2. Oxidation of NH_2OH by 90 μM dichlorophenolindophenol (DCPIP) and 6 μM phenazine methosulfate (PMS) in 50 mM potassium phosphate pH 8.0 buffer with a spiked addition of 10 μM *N.* sp. AL212 Lys106Leu/Ala131Glu. (a) Full wavelength scans every 30 seconds where the black line represents the initial absorption of DCPIP and PMS, the blue line represents the addition of 15 mM NH_2OH, the red line represents the addition of protein, and the teal line is the final scan. (b) Representative single wavelength decay of DCPIP monitored at 605 nm and converted to [DCPIP] using $\varepsilon_{605\ nm} = 20.6\ mM \bullet cm^{-1}$ using the same conditions as in (a). The * indicates the injection of NH_2OH and the ‡ represents addition of *N.* sp. AL212 Lys106Leu/Ala131Glu. The background consumption of DCPIP across three trials averaged to 7.7 ± 2.4 μM DCPIP•min^{-1} whereas the consumption of DCPIP after addition of protein averaged to 8.3 μM ± 3.9 μM DCPIP•min^{-1}.

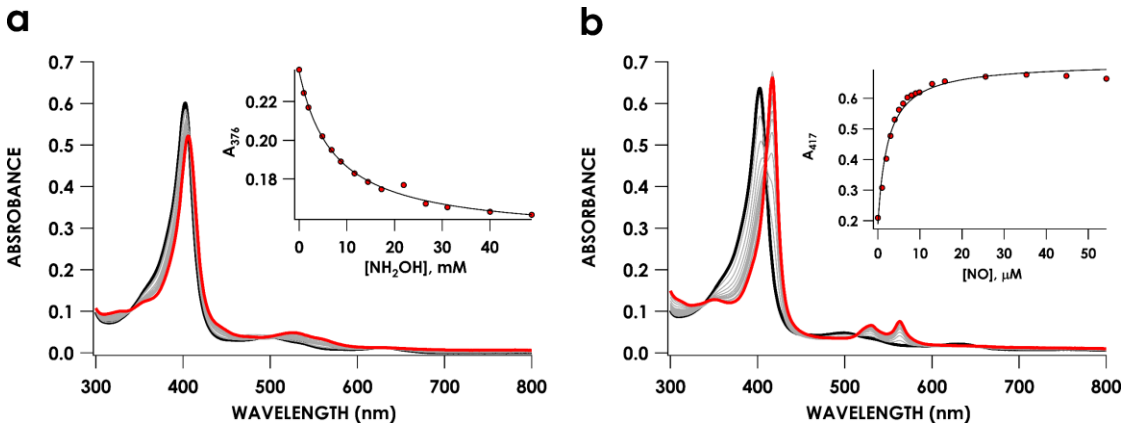

Figure 2.3. Representative titration curves for the determination of the K_d for (a) NH_2OH binding and (b) NO binding. The insets show hyperbolic fit described by equation 2.1.

Table 2.1. Thermodynamic and electronic properties of various cyt P460 species

Variant	K_d NH_2OH (mM)	K_d NO (µM)	Reduction Potential (mV vs NHE, pH = 8)	Reference
WT *N. europaea*	9 ± 1	10 ± 2	–400 ± 5	[10, 14]
WT *N.* sp. AL212 (PRD)*	18 ± 1	8 ± 1	–424 ± 7	[14]
N. sp. AL212 Ala131Glu	16 ± 5	5 ± 1	–428 ± 2	[14]
N. sp. AL212 Lys106Leu/Ala131Glu (CLD)**	7.7 ± 0.3	2.5 ± 0.1	–428 ± 3	This work

**PRD; proton-relay deficient*
***CLD; cross-link deficient*

In their ferric forms, cyt P460 as well as its CLD variants can be treated with NO to form a stable $\{FeNO\}^6$ that persists in the absence of NH_2OH and/or O_2 for at least a week (**Figure 2.4**). For CLD *N.* sp. AL212 Lys106Leu/Ala131Glu cyt P460, the Soret shifts from 402 nm to 417 nm upon binding NO. Similar to the NH_2OH K_d, removal of the cross-link in *N.* sp. AL212 results in a twofold decrease in the 25°C K_d for NO binding (**Table 2.1**), but the change is small, indicating that the lack of a cross-link does not inhibit NO binding; therefore, the cross-link is not essential for the formation of a stable $\{FeNO\}^6$.

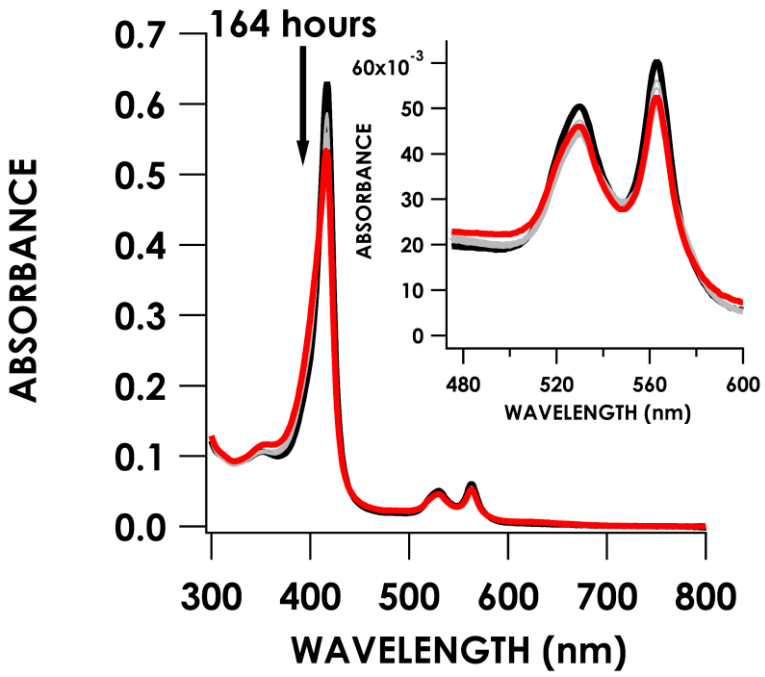

Figure 2.4.. 5 µM *N.* sp. AL212 Lys106Leu/Ala131Glu treated with 56 µM NO generated from the NO donor 1-(hydroxy-NNO-azoxy)-L-proline (PROLI-NONOate) over the course of 164 hours. The black spectrum is the initial time point after the addition of NO and the red spectrum shows the final time point. The inset shows the Q-band region.

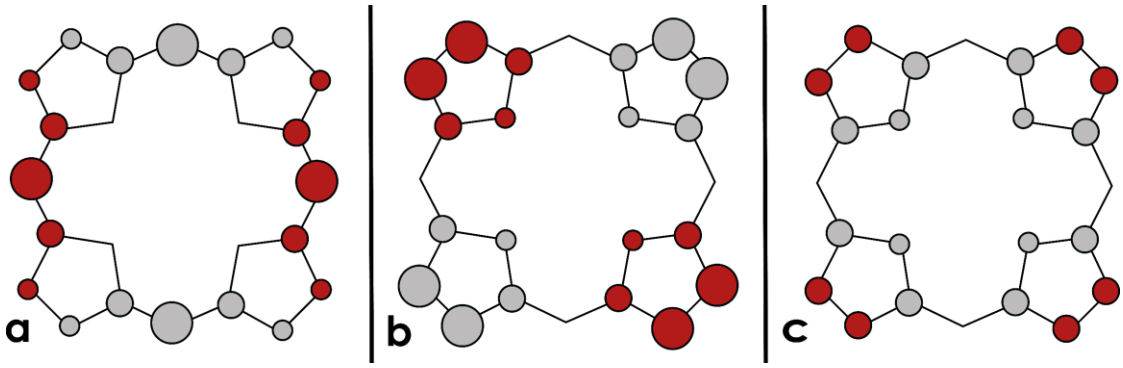

Figure 2.5. Major heme out-of-plane (OOP) distortions where the red circles represent distortions above the heme plane and the gray circle represent distortions below the heme plane. The major distortions are (a) ruffling, (b) saddling, and (c) doming. Adapted from references 41 and 42.

The persistence of a heme {FeNO}^{6} is unusual; typically, ferric hemoproteins, in the presence of NO, will rapidly undergo reductive nitrosylation to produce an {FeNO}^{7} species as well as nitrous acid (HNO_2) as a by-product.[19] For example, it has been reported that metmyoglobin (metMb) at pH > 8 reacts with NO ({FeNO}^{6}) to ultimately produce the Mb^{II}-NO ({FeNO}^{7}) adduct after twenty minutes.[20] This reaction was determined to be rate-limited by the nucleophilic attack of OH^- on the $metMb^{III}$-NO adduct, and a plot of k_{OH}' as a function of [OH^-] produced a slope where $k_{OH} = 3.2 \times 10^2\ M^{-1}\bullet s^{-1}$.[20] Similarly, The Fe^{III}–NO adduct of methemoglobin was reported to react with either H_2O or OH^- to produce the Fe^{II}-nitrosyl species over the course of thirty minutes, yielding $k_{OH}' = 3.2 \times 10^3\ M^{-1}\bullet s^{-1}$ and $k_{H2O} = 1.1 \times 10^{-3}\ M^{-1}\bullet s^{-1}$.[20] The fact that cyt P460's {FeNO}^{6} does not undergo this process is likely attributable to the high degree of heme ruffling, an OOP distortion that is a hallmark of P460 cofactors.[4, 21] Ruffling is one of three major heme OOP distortions, the others being saddling and doming (**Figure 2.5)**. Case in point, the ability of the *b*-hemoprotein nitrophorin, found in *Rhodinius prolixus* (the kissing bug) and *Cimex lectularius* (the bedbug), to form stable {FeNO}^{6} adducts has been attributed to the ruffling OOP distortion.[22] The nitrophorin-1-NO complex was reported to autoreduce on the time scale of hours to days,[23] which is similar to the behavior exhibited by CLD *N.* sp AL212 Lys106Leu/Ala131Glu (**Figure 2.4)** and other cyt P460 variants. All reported cyts P460 can maintain an {FeNO}^{6} for days without showing any indication of {FeNO}^{7} formation.[15] The observation of the long-lived CLD cyt P460 {FeNO}^{6} suggests that CLD cyt P460 species maintain a ruffled heme, similar to the cross-linked (CL) cyt P460. It is worth noting that whether a heme {FeNO}^{6} adduct is long-lived or rapidly autoreduces, the UV-vis spectra of these species are quite similar; specifically, His-ligated {FeNO}^{6} species have Soret maxima near 415 nm and Q-bands near 530 nm and 575nm, indicating that the electronic structures are very similar, at least initially.[20, 23] However, what distinguishes nitrophorin—and likely cyt P460 species—is the degree of heme ruffling. Walker[24] has proposed that in the case of a ruffled heme {FeNO}^{6} species, the π^* molecular orbital (MO) harboring the unpaired electron in NO is unable to mix with any MO containing an unpaired Fe 3d

electron because ruffling promotes an electronic ground state change. In planar heme Fe^{III}–NO adducts, the electronic ground state is $(d_{xy})^2(d_{xz}, d_{yz})^3$, but when a heme is ruffled, the d_{xy} orbital is destabilized to produce a ground state of $(d_{xz}, d_{yz})^4(d_{xy})^1$. This results in an antiferromagnetic interaction between NO and Fe^{III}, which is proposed as key to nitrophorin's function in NO delivery.[24] This is because Fe^{II}–nitrosyls typically bind NO with nano- or picomolar affinities, which would not facilitate NO release from nitrophorin upon dilution into the bloodstream.[25-26] Additionally, Lehnert and co-workers[27-28] have proposed that ferric heme nitrosyls contain an admixture of states—both Fe^{III}-$NO^{\bullet}$ and the Fe^{II}-NO^{+}— that is dependent on elongation of the Fe-NO bond length and therefore allows these centers to release NO more readily than their ferrous counterparts. Regardless, the persistence of the cyt P460 $\{FeNO\}^6$ is a strong indicator of heme ruffling.

Ruffling has not only been implicated in the stabilization of heme NO-adducts, but it has also been associated with a decrease in the $Fe^{II/III}$ reduction potential since the ability of the d-manifold to mix with the porphyrin π system is diminished.[29] Ruffling has been shown to be a common distortion that tunes reduction potentials in heme proteins involved in electron transfer such as cytochrome *c* proteins.[26, 30] In further support of the ruffled conformation, the reduction potential of the CLD *N*. sp. AL212 Lys106Leu/Ala131Glu cyt P460 is –428 ± 3 mV vs NHE (**Figure 2.6**). All measured cyt P460 proteins have reduction potentials around –400 mV vs NHE (**Table 2.1**).[14] This offers further support that the cyt P460 heme can maintain a ruffled conformation without the Lys cross-link.

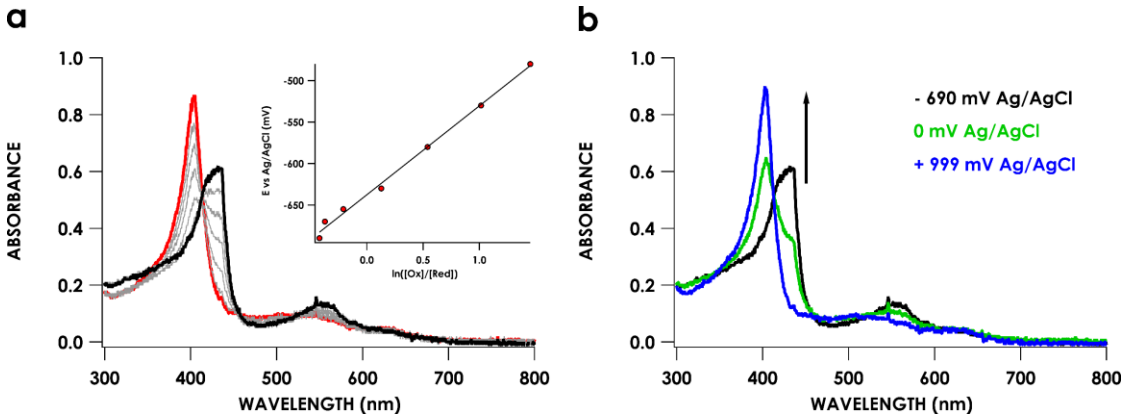

Figure 2.6. UV-vis absorption spectrum of 90 μM *N.* sp. AL212 Lys106Leu/Ala131Glu in 50 mM potassium phosphate pH 8.0, 100 mM NaCl. (a) No potential was applied in the red trace. The gray traces represent applied potentials from -480 to -630 mV in 50 mV increments, as well as applied potentials of –655 and –670 mV vs Ag/AgCl. The black trace shows the fully reduced protein at –690 mV. The inset shows the fit to the linearized Nernst equation. The reduction potential of this species was determined to be –428 ± 3 mV vs NHE. (b) The reduction was shown to be reversible by applying oxidizing potentials of 0 mV and +999 mV vs Ag/AgCl to the electrochemically reduced protein.

As shown previously,[15] the Fe^{III} EPR spectra of the CL and the CLD cyts P460 show significant differences from one another. The as-isolated protein for the CL species exhibits an $S = {}^5/_2$ rhombic spectrum whose parameters are in **Table 2.2**.[10, 14] *N.* sp. AL212 variants typically give multi-component EPR spectra—this was previously speculated to be a result of two conformations of a distal phenylalanine, but was never conclusively shown.[14] Upon removal of the heme-Lys cross-link from *N.* sp. AL212 cyt P460, the $S = {}^5/_2$ EPR spectrum of the resting ferric form exhibits two components, although each is less rhombic than the corresponding CL protein. The two signals observed in this spectrum could be two different heme conformations—a ruffled form and a more planar variant, instead of the previously speculated conformations of the distal phenylalanine. In addition, there is a minor low-spin (LS) species present that is likely a temperature-dependent variant of the protein (**Figure**

2.7a). Binding of NH_2OH, however, drives all variants to exhibit type II LS rhombic spectra with only one observable spin system in each case. A type II LS ferriheme center has a ground state electron configuration of $(d_{xy})^2(d_{xz}, d_{yz})^3$ and all the g values are observable, although g_{min} is broad and g_{max} is less than 3.2.[24, 31] In a type II center, there is a large difference in energy between the d_{xz} and d_{yz} orbitals.[31] Using the method described by Taylor,[32] the relative energetic difference between the t_{2g}-derived orbitals can be determined from the LS g-values.[24, 32-33] The axial term (Δ) describes the relative energetic difference between the d_{xy} and the average energy of the d_{xz} and d_{yz} orbitals and the rhombic term (V) describes the difference between the d_{xz} and d_{yz} orbitals.[24, 32-33] The rhombicity (V/Δ) can be determined from the axial and rhombic ligand field terms.[29, 32-33] Previously, it has been it has been shown for the His/Met ligated hemes cyt c_{552} and cyt c_{551} from *Hydrogenobacter thermophilus* and *Pseudomonas aeruginosa*, respectively, that a decrease in the axial term correlated with an increase in the amount of heme ruffling.[29, 33] The ligand-field parameters for various cyt P460 variants determined from the g-values in **Table 2.2** were used to generate the data in **Table 2.3**. Inspection of the ligand field parameters indicates that within the *N.* sp. AL212 variants, removal of the cross-link serves to increase both the axial and rhombic ligand field terms by 0.35 and 0.37, respectively, relative to WT *N.* sp. AL212. There is no substantial difference in the rhombicity. If the trend observed previously[29, 33] can be extended to His/NH_2OH ligated heme systems, this could suggest that the CLD heme is less ruffled than the CL heme. However, it is worth noting that with both cyt c_{551} and cyt c_{552} the rhombic term did not change substantially when mutations to alter ruffling were introduced,[33] so it is possible this comparison to cyt P460 is invalid. Regardless, we speculate that based on the reduction potential and the ability to form a long-lived $\{FeNO\}^6$ that the heme is still capable of maintaining a ruffled conformation in solution, but this further supports that the heme conformation is more dynamic without the cross-link to stabilize the conformation (*vide infra*).

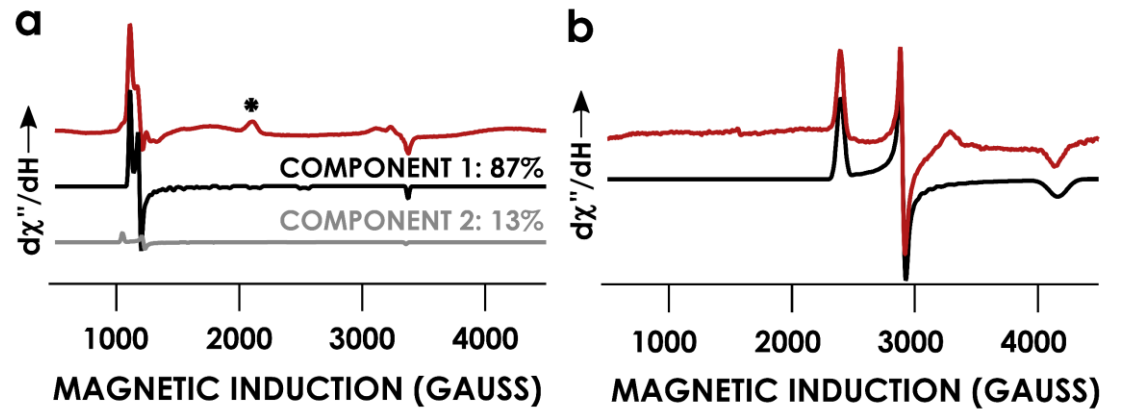

Figure 2.7. X-band EPR spectra obtained at 10 K for 160 μM of *N.* sp. AL212 Lys106Leu/Ala131Glu cyt P460 in (a) the ferric, as-isolated form with simulations of the major component in black and the minor component in gray and (b) its NH_2OH adduct with the simulation in black. The red spectra are experimental data. All protein solutions were in 200 mM 4-(2-hydroxyethyl)-1-piperazineethanesulfonic acid (HEPES) pH 8.0. The * denotes the presence of a temperature-dependent low-spin variant of the protein.

Table 2.2. EPR parameters of select cyt P460 variants.

Cyt P460 Variant	**Resting Fe^{III} Component 1 (S = 5/2)**		**Resting Fe^{III} Component 2 (S = 5/2)**		**Fe^{III}-NH_2OH (S = 1/2)**	**Reference**
	g_{eff} values	***E/D***	***g_{eff} values***	***E/D***	***g_{eff} values***	
N. europaea	6.57, 5.09, 1.97	0.03	N/A	N/A	2.75, 2.28, 1.54	[10, 14]
N. sp. AL212 (PRD)*	6.39, 5.13, 1.97	0.03	6.00, 5.52, 1.99	0.012	2.84, 2.25, 1.44	[14]
N. sp. AL212 Ala131Glu	6.40, 5.14, 1.97	0.03	6.00, 5.51, 1.99	0.012	2.86, 2.27, 1.46	[14]
N. sp. AL212 Lys106Leu/Ala131Glu (CLD)**	6.04, 5.65, 1.99	0.01	6.40, 5.50, 2.00	0.02	2.80, 2.31, 1.61	This work

**PRD; proton-relay deficient*
***CLD; cross-link deficient*

Table 2.3. EPR-derived ligand field parameters of select cyt P460 variants.

Variant	Δ/λ[a] (Axial term)	V/λ[a] (Rhombic term)	V/Δ (Rhombicity)
WT *N. europaea*	2.93	2.19	0.75
WT *N.* sp. AL212 (PRD)*	2.84	1.89	0.66
N. sp. AL212 Ala131Glu	2.86	1.91	0.67
N. sp. AL212 Lys106Leu/Ala131Glu (CLD)**	3.19	2.26	0.71

**PRD; proton-relay deficient*
***CLD; cross-link deficient*
[a]λ; the spin-orbit coupling constant is assumed to be 400 cm^{-1}.

The cross-link structurally constricts the secondary coordination sphere of cyt P460

Since removal of the cross-link does not substantially change the spectroscopic and electrochemical properties of the protein compared to the cross-link containing variant to an extent that would have obvious impact on catalytic activity, we hypothesized that the lack of reactivity could instead be explained by physical differences in the enzyme upon removal of the cross-link. The CL cyt P460 crystal structure exhibits a rare protein fold;[2] cyt c′-beta, a protein class that is thought to be evolutionarily related to cyt P460,[34] is the only other known class of proteins to share this fold.[35] The major feature of the polypeptide is a β-sheet consisting of five antiparallel β-strands.[2] The heme, which is connected to the CXXCH binding domain in a small α-helix, is relatively solvent-exposed. One loop extends from the first two β-strands and caps the open coordination site of the heme. Another loop from the fourth and fifth β-strands of the other subunit also extends over to the heme, covering the side of the heme containing the β *meso* carbon. The Lys cross-link is located on the third β-strand and the Glu residue is located on the fourth β-strand of the sheet.[2, 4] The CLD crystal structure showed that, globally, the protein fold was not affected by the lack of a cross-link, but finer details did change.

The crystal of *N.* sp. AL212 Lys106Leu/Ala131Glu diffracted to a resolution of 2.2 Å. The CLD crystal structure was aligned with the structure of the *N.* sp. AL212 Ala131Glu (PDB ID 6E0X) and gave a global RMSD value of 0.241Å, indicating the aligned proteins are very similar. The Glu residue was disordered in both subunits of

the crystal structure. Specifically, in the crystallographic A subunit, Glu131 has half occupancy in the two known conformations, which had been seen previously with *N*. sp. AL212 Ala131Gln mutants, where crystal structures showed that the residue at the proton-relay position was oriented towards the heme center when NH_2OH was bound and away when no substrate was present.[14] Both hemes of the homodimer are axially coordinated by water molecules, which might explain the presence of both Glu conformations; the Fe^{III}-H_2O adduct has a very transient bond and the solvent ligand is readily displaced by NH_2OH. In the B chain, there was no electron density corresponding to the Glu sidechain and, therefore, the sidechain was removed from the final structure.

When comparing the CLD crystal structure to the *N*. sp. AL212 Ala131Glu structure and pair-fitting the heme nitrogen and *meso* carbon atoms to each other, it becomes apparent that the cross-link constricts the whole β-sheet closer to the heme active site (**Figure 2.8a**). This is exemplified by the third β-strand containing the Lys cross-link. When the Lys is removed, the strand is offset by 1.4 ± 0.3 Å. Similarly, the fourth β-strand containing the catalytic Glu residue is perturbed by 1.1 ± 0.3 Å. Looking at the Glu residue specifically and comparing its location in the CLD structure to its position in the CL structure, we see that the difference between the C_α atoms is 0.8 Å (**Figure 2.8c**). Moreover, the distance between the Glu C_α and the Fe atom elongates by 0.3 Å in the CLD variant (**Figure 2.8c**). The cross-link dictates the positioning of the β-sheet, and the most prominent effect germane to enzyme function is that the Glu can no longer reach the bound substrate. Since proton transfer must be a mechanistic step in the oxidation of NH_2OH, the positional shift of the catalytic Glu residue is the most likely reason that the CLD cyt P460 variants lack NH_2OH oxidase activity; that is, the Glu is unable to reach the bound NH_2OH and therefore cannot extract protons—much in the same way that an Asp residue is insufficient[14]—which shuts down NH_2OH oxidation. In a CPET reaction, the probability that a reaction will occur is dictated by two factors: the electron coupling constant and the overlap of the proton vibrational wavefunctions in their initial and final state.[36] Increasing the distance by which a proton must be transferred over the course of the reaction

substantially slows down the rate during a CPET, where tenths of an angstrom can impede the rate by orders of magnitude.[37] The fact that the increase in the Glu positioning by nearly 1 Å abolishes catalysis accords with the notion that the oxidation of NH_2OH occurs by a CPET. More detailed mechanistic study to solidify this claim is underway in our laboratory. Regardless, the present results indicate that the proton-relay position is influenced by the heme-Lys cross-link.

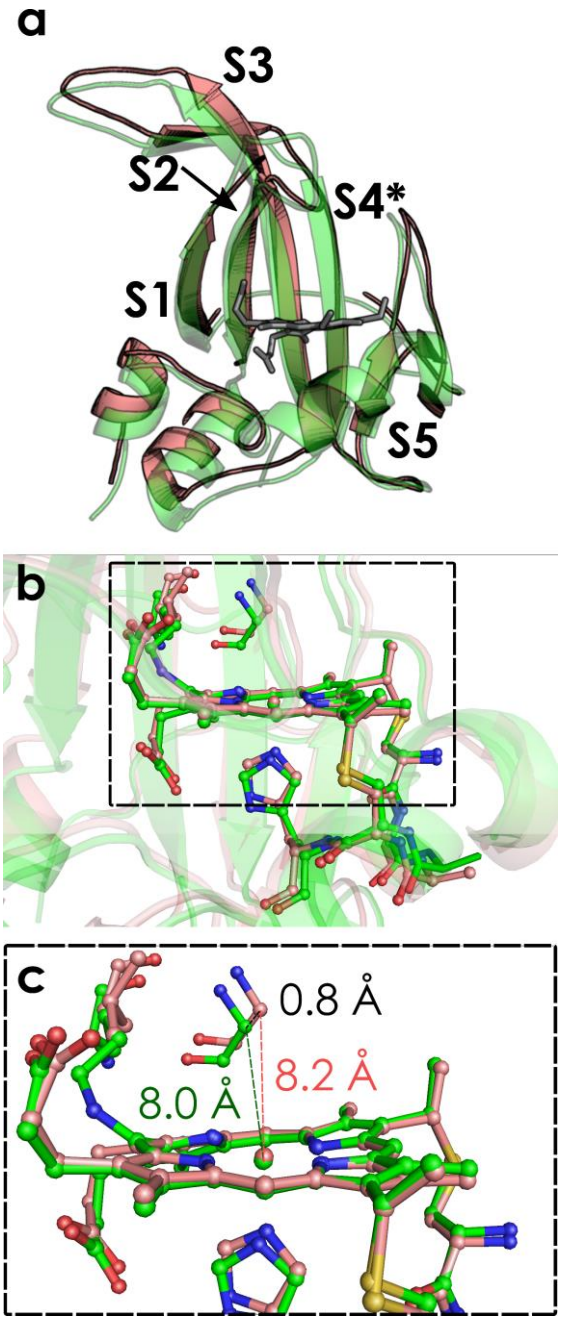

Figure 2.8. (a) Ribbon representation of the B subunit of *N.* sp. AL212 Ala131Glu (green, PDB ID 6E0X) and the A subunit *N.* sp. AL212 Lys106Leu/Ala131Glu (pink, PDB 6W6N) aligned with the alignment function in PyMol and pair-fitted to the pyrrole N atoms and the *meso* C atoms. Only a single monomer is depicted and S1 through S5 correspond to the β-strands of the β-sheet in order from the amino to carboxyl terminus. The * indicates the strand with the catalytic Glu reside. The heme is colored in gray and from the *N.* sp. AL212 Ala131Glu cyt P460 structure. (b) Structural alignment using the A subunits of the structures mentioned in (a).

Following structural alignment, heme planes were normalized to each other by pair fitting the heme *meso* carbons and the pyrrole nitrogen atoms to each other. (c) Close-up view of the compared active sites with the distances denoted. The green dashed line denotes the distance from the Glu C_α to the Fe center for *N.* sp. AL212 Ala131Glu cyt P460. The pink dashed line denotes the same distance for *N.* sp. AL212 Lys106Leu/Ala131Glu. The black dashed line illustrates the distance between the Glu131 C_α atoms from the different protein variants.

Table 2.4. Crystallographic parameters of *N.* sp. AL212 Lys106Leu/Ala131Glu cyt P460.

Wavelength (Å)	0.979
Temperature (K)	100
Space Group	$P2_12_12_1$
a (Å)	47.4
b (Å)	80.1
c (Å)	110.8
α (deg)	90
β (deg)	90
γ (deg)	90
No. of reflections	20467 (1756)
No. of reflections in the R_{work} set	20291 (1754)
No. of reflections in the R_{free} set	1999 (173)
Resolution (Å)	45.57-2.25 (2.33 – 2.25)
R_{merge} (%)	0.1507 (1.824)
$CC_{1/2}$	0.995 (0.518)
Completeness (%)	98.1 (86.45)
Redundancy	6.5 (6.0)
$I/\sigma(I)$	7.66 (0.99)
R_{work}	0.2574 (0.4256)
R_{free}	0.2775 (0.4627)
Root-mean-square deviation from ideality	
Bonds (Å)	0.01
Angles (deg)	0.98
Average *B* factor (Å^2)	63.15
Ramachandran plot (%)	
Favored Regions	96.18
Allowed regions	3.50
Disallowed regions	0.32
PDBID	6W6N

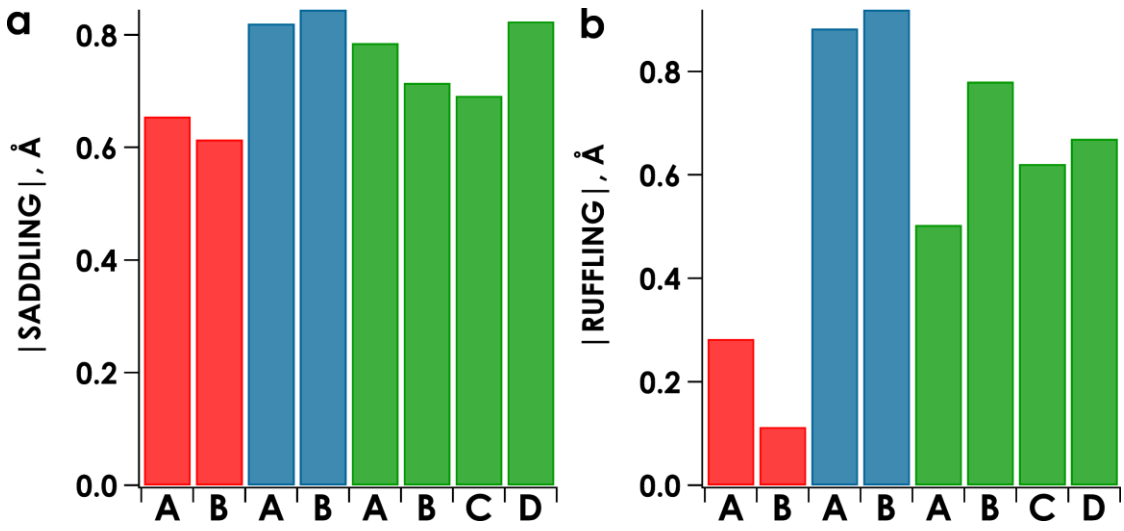

Figure 2.9. (a, b) Absolute value of the saddling and ruffling distortions, respectively, in various *N.* sp. AL212 cyt P460 crystal structures with the crystallographic subunit denoted. The red color represents *N.* sp. AL212 Lys106Leu/Ala131Glu (PDB 6W6N), the blue color represents *N.* sp AL212 WT cyt P460 (PDBG 6AMG), and the green color represents *N.* sp. AL212 Ala131Glu (PDB 6E0X).

Crystal structures of cyt P460s from *N. europaea* and *N.* sp. AL212 show that the heme is both ruffled and saddled.[5,12,14] The saddling distortion is not affected substantially by the lack of a cross-link (**Figure 2.9a**), but the crystal structure of *N.* sp. AL212 Lys106Leu/Ala131Glu shows marked differences in ruffling compared to previous cyt P460 crystal structures (**Figure 2.9b**). Typically, ruffled hemes are a result of a few factors, some of which depend on the hydrogen-bonding interactions present in the conserved CXXCH binding domain in *c*-type cyts and can be tuned by mutating, removing, or adding X residues.[33, 38] Ruffling has also been shown to be influenced by the presence of bulky residues in the heme pocket, which perturb the planarity of the macrocycle.[39]

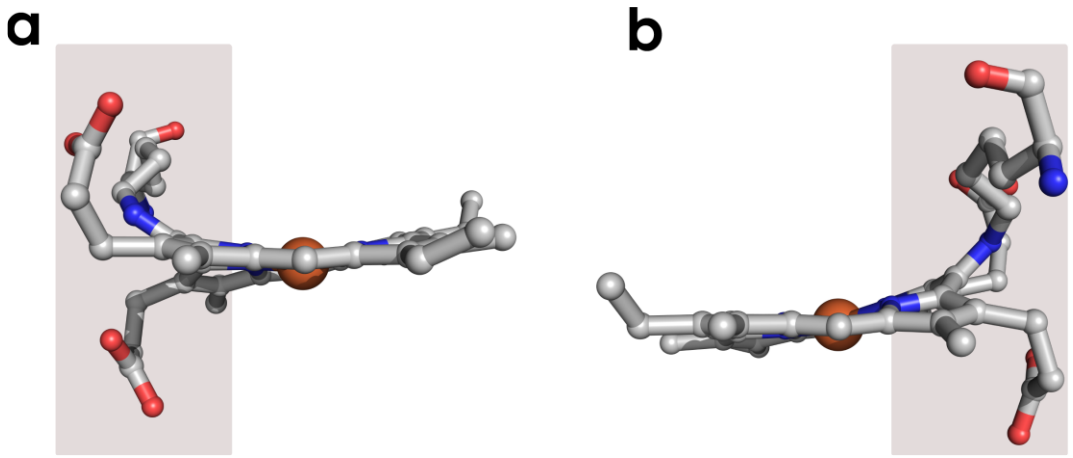

Figure 2.10. (a,b) View of opposing sides of the same cofactor from the WT *N.* sp. AL212 cyt P460 crystal structure (PDB ID: 6AMG**).** The gray box is meant to draw the eye to the most prominent distortion.

Expanding the view of the cyt P460 active site to include the residues surrounding the heme cofactor, the OOP distortions seem to be influenced more by hydrogen-bonding interactions of the heme propionate groups with nearby residues instead of any interactions in the binding domain (**Figure 2.10**). The WT *N.* sp. AL212 and the Ala131Glu crystal structures show that the propionate groups interact with nearby residues—His80 and Ser118 in the distal pocket and Tyr186 in the proximal pocket—as well as the N atom of the Lys cross-link, which is attached to the 13' *meso* carbon in between the two heme propionates. (**Figure 2.11c,d**). Naturally, the CLD species are incapable of this final interaction, but the propionates can still interact with the other amino acids mentioned (**Figure 2.11a,b**).

Ruffling and other heme OOP distortions, such as saddling or doming (**Figure 2.5**)[40-41] can be quantitatively assessed by comparing the crystallographic coordinates of specific atoms of the porphyrin macrocycle to a planar porphyrin in D_{4h} symmetry, in a process known as normal-coordinate structural decomposition (NSD).[42] When subjecting the CLD crystal structure to the NSD procedure to assess all of the OOP distortions,[29, 43] the two subunits give minorly different values: In the A subunit, the ruffling distortion is –0.28 Å and in the B subunit is 0.11 Å (**Figure 2.9**). These results

are substantially less ruffled compared to the structures of CL cyt P460, but crystal structures are inherently static. The heme propionates of the CLD mutants are all oriented towards the same residues as in CL cyt P460 crystal structure, indicating that in solution, they likely still interact with these residues and thus, even without the Lys cross-link, the heme can still maintains a ruffled conformation. This is supported by the negative reduction potential; as mentioned previously, *N.* sp. AL212 Lys106Leu/Ala131Glu has a reduction potential of -428 mV vs NHE, which is unchanged from the previously reported *N.* sp. AL212 Ala131Glu variant.[14] A negative reduction potential has been correlated with increased heme ruffling.[29]

Given these crystallographic results, it seems likely that the cross-link serves the purpose of stabilizing the heme in a more rigid ruffled conformation by providing an additional site for hydrogen bonding, but it is not necessary to maintain a ruffled heme conformation in solution. It is possible that when the cross-link is present, there is a higher probability that the cofactor retains its ruffled conformation. We have previously shown that the cross-link is essential to prevent the 6c $\{FeNO\}^7$ to 5c $\{FeNO\}^7$ conversion and that when the cross-link is absent, there is a significant entropic driving force for this reaction.[15] Perhaps the cross-link serves a similar purpose for the ruffling deformation—it could make the conversion to a planar porphyrin less favorable. Molecular dynamics simulations toward addressing this possibility are underway.

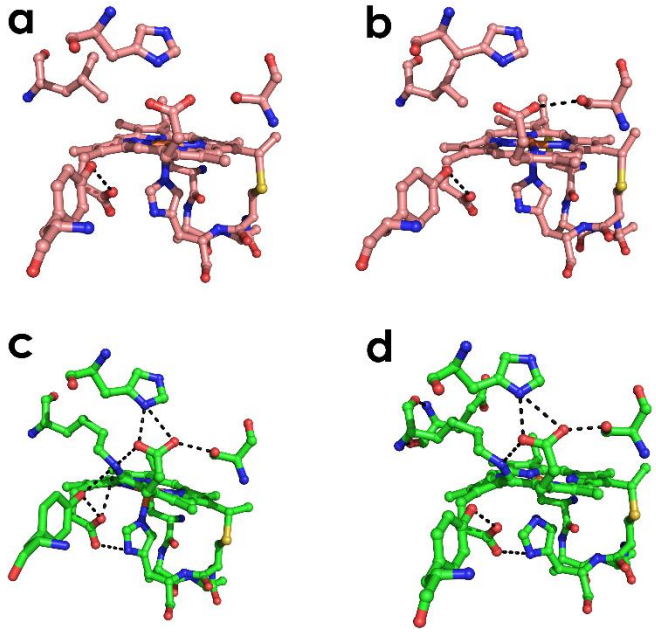

Figure 2.11. Stick representations of P460 cofactors from various cyt P460 variants with hydrogen bonding interactions depicted with black dashed lines. (a,b) Hydrogen bonding interaction in both the crystallographic A and B subunits of *N.* sp. AL212 Lys106Leu/Ala131Glu (PDB 6W6N). (c) Hydrogen bonding interactions in WT *N.* sp. AL212 (PDB 6AMG) and (d) hydrogen bonding interactions in *N.* sp. AL212 Ala131Glu (PDB 6E0X)

Conclusion

The functional role of the cyt P460 heme-Lys cross-link has been scrutinized biophysically and shown to principally dictate the relative positioning of the heme P460 cofactor and an essential second-sphere proton-relay residue. No substantive changes in NH_2OH or NO binding affinities are affected when the cross-link is removed. Similarly, EPR shows no substantial differences in the electronic structures of the first catalytic intermediate, the Fe^{III}–NH_2OH adducts. The reduction potential of the CLD P460 variant is unchanged compared to the *N.* sp. AL212 Ala131Glu reduction potential. The lack of reactivity seems more likely attributable to the difference in positioning of the catalytically essential second-sphere Glu residue, which shifts out of reach of the heme when the cross-link is removed. It is unknown if the Tyr-heme cross-link of HAO serves a similar purpose, but given that homologous proteins with no cross-link perform reductive chemistry, it seems unlikely that the Tyr

is necessary to shift the heme towards the Asp and His—assuming those residues do in fact serve the same purpose as cyt P460's Glu residue. It still remains to be seen if the presence of any cross-link is necessary for the oxidation of NH_2OH, or if it is possible to mutate the heme pocket in some fashion that will reposition the heme in such a manner that a CLD cyt P460 could oxidize NH_2OH. Work by Liptak and co-workers showed that electrophilicity or radical character on the heme *meso* carbons increased with heme ruffling.[43] Previously, Hooper[18] postulated that the heme-Lys cross-link forms by an autocatalytic mechanism because of the ease of recombinant expression by phylogenetically distant hosts. Taken together, this indicates that the cross-link is likely formed through either a nucleophilic attack of the Lys or a radical rebound, facilitated by the fact that the 13′ *meso* carbon is ruffled. Current work in our lab is working on addressing the formation of this fascinating post-translational modification.

Experimental

General Considerations

18.2 MΩ water was used to prepare all buffers and solutions. Protein samples were stored aerobically at 4°C or anaerobically at room temperature in an MBraun N_2-filled glovebox in 50 mM potassium phosphate pH 8.0 buffer unless otherwise noted. All anaerobic protein solutions and solids were allowed to equilibrate with the glovebox atmosphere overnight before use. Anaerobic solutions were prepared by three cycles of degassing and sparging with N_2 for fifteen minutes each, ending with N_2 saturation. A Cary 60 spectrometer (Agilent) outfitted with a Peltier cell maintained at 25°C was used to obtain all UV-visible (UV-vis) absorption spectra. Data were fit in Igor Pro version 6.37 (WaveMetrics). $\{FeNO\}^6$ species were generated by addition of disodium 1-(hydroxyl-NNO-azoxy)-L-proline (PROLI-NONOate) (Cayman Chemicals) after quantification of NO delivery as described previously.[44] The $\{FeNO\}^7$ species was generated by treating *N.* sp. AL212 Lys106Leu/Ala131Glu with the HNO donor disodium diazen-1-ium-1,2,2,-triolate (Angeli's Salt, Caymen

Chemicals). Unless otherwise noted, all other chemicals were purchased from VWR International.

Protein Overexpression and Purification

Lys106 in *N.* sp. AL212 Ala131Glu—in a pET22b(+) vector with the gene located between the NcoI and XhoI restriction sites—was mutated to remove the cross-link with primers synthesized by Integrated DNA Technologies. The expression and purification of *N.* sp. AL212 Lys106Leu/Ala131Glu was carried out with slight modification to what has been described previously.[15] In brief, after growth of transformed *Escherichia coli* cells at 37 °C for 6–8 hours, protein expression was induced by the addition of isopropyl β-D-1-thiogalactopyranoside (IPTG) to a final concentration of 1 mM and the temperature was lowered to 20 °C. Cells were harvested after 24 hours of induction. Cells were resuspended in 30 mL of lysis buffer containing 20 mM Tris pH 8.0, 300 mM NaCl, and 0.1% (v/v) Triton-X and were lysed by four subsequent passages through a French Pressure Cell operating at 103 MPa. Cell debris was removed by centrifugation at 18,000 *x g* for 1 hour. The resulting soluble fraction was applied by gravity to HisPur Ni-NTA resin (Thermo Scientific), washed, and eluted as previously described.[10] Pinkish-red fractions were combined, concentrated and loaded onto a HiLoad Superdex 75 equilibrated with 50 mM morpholinepropanesulfonaic acid (MOPS) pH 7.2 and 150 mM NaCl running at a flow-rate of 1.0 mL/min in an AKTA pure 25 M (GE Healthcare).[10]

Plasmids and mutagenesis

The *N.* sp. AL212 Lys106Leu/Ala131Glu was prepared using constructs that have been described previously. [4, 10, 14] Primers were synthesized by Integrated DNA Technologies. In the 5′→3′ direction, the forward and reverse primer are as follows, with the underlined nucleotides representing Lys106Leu mutation:
FWD: CC GTG ATC GTT <u>CTT</u> GAA CTG CGC GGT GTT
REV: TTC <u>AAC</u> AAC GAT CAC GGT GCC ATC ACG

PCR products were DpnI digested overnight at 37 °C and transformed into DH5α cells. Colonies were picked, grown in LB, and miniprepped per Qiagen instructions. DNA was submitted to the Cornell University Institute for Biotechnology for Sanger sequencing, with the results below.

_N._ sp. AL212 Lys106Leu/Ala131Glu sequencing results

NGAGAAATTCCCTCNGAATATTTTGTTTAACTTTAAGAAGGAGATATACAT
ATGAAATACCTGCTGCCGACCGCTGCTGCTGGTCTGCTGCTCCTCGCTGCC
CAGCCGGCGATGGCCATGGGCCTGCAGTTCAAGAAAACCCTGCTGAGCAG
CATTGCGCCGGTGCTGCTGAGCATTGTTCTGGCGAACCCGGTGATTGCGAG
CGATGCGCACCATGCGCACAAGGGTCTGAACTACGGCAGCTTCACCAAGG
AGCACGTTCTGCTGACCCCGAAAGGTTATCGTGAATGGGTTTTTATTGGCG
CGAGCGTGACCCCGAACGAGCTGAACGACGATAAAGCGGCGTTCCCGGAA
TTTCACAACGTGTACATTGACCCGACCAGCTGGGGTCACTGGAAGAAAAC
CGGCGAGTTCCGTGATGGCACCGTGATCGTTCTTGAACTGGCGGGTGTTGG
CAGCAAAGCGAGCCCGAGCGGTAACGGCTATTTCCCGGGCGAGTTTAACG
GCATCGAAGCGATGGTGAAGGATAGCAAACGTTACCCGGAACGTCCGGGT
AACTGGGCGTTCTTTGGCTTTGAGAGCTATGAAGCGAAGCAGGGTATCATT
CAAACCGACGAGACCTGCGCGGCGTGCCACAAAGAACATGCGGCGCACG
ATATGGTTTTCACCCAATTTTATCCGGTGCTGCGTGCGGGCAAGCCGAGCA
AACTCGAGCACCACCACCACCACCACTGAGATCCGGCTGCTAACAAAGCC
CGAAAGGAAGCTGAGTTGGCTGCTGCCACCGCTGAGCAATAACTAGCATA
ACCCCTTGGGGCCTCTAAACGGGTCTTGAGGGGTTTTTTGCTGAAAGGAGG
AACTATATCCGGATTGGCGAATGGGACGCGCCCTTGTAGCGGCGCATTAA
NCGCGGCANGTGTGGTGGTTACCCGCAGCGTGACCGCTACACTTNGCNAG
CGCCCTANCGCCCGCTCCTTTCNCTTTCTTCCCTTCNTTTCTCGCCCCGTTN
NCCNGGCTTTCCCGTCAAGCTNTTAAATCGGGGGNCTNCCTTTTAGGTTCC
AATTTAGTGCTTTTCGGCACCTCCNACCCNAAAAATTNNATTAGGGTGATG
NTTCNCTANGGGGCCATCCCCCTAANAANGNTTTTNCNCCTTNANGTTGNN
TCNAN

CTT = K106L
GAA = A131E

NH_2OH and NO binding affinities

The K_d for hydroxylamine (NH_2OH) and nitric oxide (NO) were determined by titration by sequential addition of NH_2OH•HCl and PROLI-NONOate, respectively. 5 μM of *N*. sp. AL212 Lys106Leu/Ala131Glu were added to a septum-sealed cuvette equipped with a stir bar maintained at 25 °C with a Peltier-controlled cuvette holder.

The solution was equilibrated for five minutes before injecting either NH_2OH or NO anaerobically via a Hamilton syringe and allowed to equilibrate for five minutes before measuring a full wavelength scan. In the case of the NH_2OH adduct, the absorbance at 376 nm was plotted against the total [NH_2OH], corrected for dilution. The same procedure was used for NO, using the absorbance at 417 nm. Both curves were fit to a hyperbolic of the form:

$$A = A_0 + \frac{\Delta A * [substrate]_0}{K_d + [substrate]_0} \quad (2.1)$$

In this equation, A is the absorbance at either 376 or 417 nm, A_0 is the initial absorbance value before addition of NH_2OH or NO, ΔA is the maximum change in absorbance, $[substrate]_0$ is the concentration of added NH_2OH or NO, and K_d is the dissociation constant. The reported K_d values are the averages of three separate trials.

Steady-State Activity Assays

Approximately 69 mg of NH_2OH•HCl salt was brought into the glovebox and 1 mL of 50 mM potassium phosphate pH 8.0 was used to dissolve the salt. The NH_2OH content was quantified using the method described by Frear *et al*,[45] and a stock solution was prepared and placed inside a crimpable GC vial (Wheaton). Similarly, a stock solution of *N.* sp. AL212 Lys106Leu/Ala131Glu was also prepared in a crimpable GC vial. With a final volume of 2 mL, an anaerobic Spectrosil quartz cuvette (Starna Cells, 10 mm) containing 90 μM dichlorophenolindophenol (DCPIP) (quantified by its absorbance at 605 nm, $\varepsilon = 20.6\ mM^{-1}•cm^{-1}$ [46]), 6 μM phenazine methosulfate (PMS) (quantified by its absorbance at 388 nm, $\varepsilon = 26.3\ mM^{-1}•cm^{-1}$ [47]), and a stir bar were placed in the UV-vis absorption spectrometer and maintained at 25°C. After equilibrating for 5 minutes while stirring, a single-wavelength scan (default settings) at 605 nm was initiated, followed by addition of NH_2OH via a Hamilton syringe to a final concentration of 15 mM. Background DCPIP consumption was allowed to proceed for 90 seconds before addition of *N.* sp. AL212 Lys106Leu/Ala131Glu to a final concentration of 10 μM, also via Hamilton syringe. Background consumption was determined by linear regression, fitting the 30 s prior to addition of protein. Rates after addition of protein were determined by linear

regression, using the first 10% of oxidant consumption. Rates reported are the average of three trials.

N. sp. AL212 Lys106Leu/Ala131Glu {FeNO}^{6} stability

At the end of the NO titration, one cuvette was saved and treated as the initial time point. The cuvette was kept at room temperature and UV-vis spectra were collected at 16.7, 21.2, 53.3, 89.0, 114.9, and 164.1 hours after finishing the titration.

Electron Paramagnetic Resonance Spectroscopy

Continuous-wave EPR spectra were measured at X-band (9.40 GHz) using a Bruker Elexsys-II spectrometer and maintained at 10 K by a liquid He cryostat. Samples contained a final volume of 100 μL of 160 μM protein in 200 mM 4-(2-hydroxyethyl)-1-piperazineethanesulfonic acid (HEPES) pH 8.0. The NH_2OH adducts were prepared in an anaerobic glovebox. To that end, a stock solution of NH_2OH•HCl was prepared and assayed for NH_2OH content.[16] The appropriate amount of this stock solution was added to the protein sample to bring the final concentration of NH_2OH to 50 mM. EPR spectra were simulated using SpinCount.[48]

Spectroelectrochemical Potentiometric Titrations

Spectroelectrochemical titrations of *N.* sp. AL212 Lys106Leu/Ala131Glu cyt P460 were performed as previously described with slight modifications.[14] In brief, a 1 mm pathlength cell (Basi) was brought into an N_2 filled glovebox and 90 μM protein in 50 mM potassium phosphate pH 8.0, 100 mM NaCl was added to the protein to a total volume of 700 μL. 20 μM methyl viologen was added as an electrochemical mediator. A WaveNow Potentiosat (Pine Research) was used to apply potential to the spectroeletrochemical cell using a platinum (Pt) working electrode, a Pt counter electrode, and a Ag/AgCl reference electrode that used 3 M NaCl as an electrolyte. Reducing potentials were applied in 50 mV increments from -480 to -630 mV, followed by potentials of -655, -670, and finishing with -690 mV vs Ag/AgCl. Bulk

electrolysis proceeded for 500 s and then the solution was allowed to equilibrate for 10 to 20 minutes before recording a full wavelength spectrum. The reduction was checked for reversibility by applying oxidizing potentials to the fully reduced species from -605 mV up to 999 mV. To obtain the reduction potential, data were fit to the linearized Nernst equation:

$$E = E° - \frac{RT}{nF} \ln \frac{[Ox]}{[Red]} \quad (2.2)$$

In this equation, E is the applied potential, E° is the standard reduction potential, R is the ideal gas constant, T is the temperature, n is the moles of electrons, and F is Faraday's constant. The absorbance of the oxidized peak at 404 nm was used as the concentration of the oxidized species and the absorbance of the reduced peak at 437 nm was used as the concentration of the reduced species.[14, 23]

Determination of Ligand Field Parameters from the S = ½ EPR spectrum

The axial (Δ/λ) ligand field term and the rhombic (V/λ) ligand field term were determined using the method described by Taylor[32] and used the following equations and under the assumption that $g_{max} = g_{zz}$, $g_{mid} = g_{yy}$, and $g_{min} = g_{xx}$ and with a spin-orbit coupling (λ) of 400 cm^{-1}. These equations assume no covalency:[32-33]

$$\frac{V}{\lambda} = \frac{g_{xx}}{g_{zz}+g_{yy}} + \frac{g_{yy}}{g_{zz}-g_{xx}} \quad (2.3)$$

$$\frac{\Delta}{\lambda} = \frac{g_{xx}}{g_{zz}+g_{yy}} + \frac{g_{zz}}{g_{yy}-g_{xx}} - \frac{V}{2\lambda} \quad (2.4)$$

$$\frac{V}{\Delta} = \frac{V/\lambda}{\Delta/\lambda} \quad (2.5)$$

We also checked the normalization conditions (equations S6 and S7) to use the above equations S3-S5.

$$g_{xx}^2 + g_{yy}^2 + g_{zz}^2 + g_{yy}g_{zz} - g_{xx}g_{zz} - g_{xx}g_{yy} + 4(g_{xx} - g_{yy} - g_{zz}) = 0 \quad (2.6)$$

With equation S6, we allowed a range of 0 ± 0.3 for the cross-linked cyt P460 species.

$$a^2 + b^2 + c^2 = 1 \quad (2.7)$$

With equation S7, we allowed a range of 0 ± 0.02 for the cross-linked cyt P460 species. In these equations, a, b, and c reflect the contributions of d_{xz}, d_{yz}, and d_{xy} to the singly occupied molecular orbital.

$$a = \frac{g_{max}+g_{mid}}{D} \quad (2.8a)$$

$$b = \frac{g_{max}-g_{min}}{D} \quad (2.8b)$$

$$c = \frac{g_{mid}-g_{min}}{D} \quad (2.8c)$$

$$D = \sqrt{8(g_{zz} + g_{yy} - g_{xx})} \quad (2.9)$$

In performing these calculations, we have assumed that the components of the g-tensor are positive for the cross-linked cyt P460 species as well as the cross-link deficient cyt P460 species. A table of the values obtained from the above equations can be found below.

Protein Crystallography

N. sp. AL212 Lys106Leu/Ala131Glu cyt P460 crystals were grown using the sitting drop method. 3 μL of a stock solution of 650 μM protein in 50 mM MOPS pH 8.0 was mixed with 1-4 μL of a crystallization buffer consisting of 0.1 M sodium acetate pH 5.0, 0.2 M NaCl, and 17-22% (w/v) PEG 6000, with the best crystals growing in solutions containing 17% or 18% PEG 6000.[4] The crystals were brownish-red and looked like long plates. Samples were looped using the crystallization buffer that contained an added 30% ethylene glycol as a cryoprotectant. Diffraction data were collected at NE-CAT beamline 24-ID-E with a wavelength of 0.979 Å. The structure was solved by molecular replacement in Phenix using the *N.* sp. AL212 cyt P460 (PDB ID: 6AMG) as a model.[49] Data were refined using PHENIX[49] using restraints

on the S-C and the N-Fe distances of 2.2 ± 0.2 Å and 2.0 ± 0.2 Å, respectively, for the Cys residues and His residue in the CXXCH binding domain. The Fe atoms were refined anisotropically. The structure was built using COOT.[50] Structural figures were generated with PyMol.[51] All measured distances are relative to Cα atoms unless otherwise noted. Root-mean-square deviations (RMSD) values were determined using the align feature in PyMol.[51] Both subunits of the *N.* sp. AL212 Lys106Leu/Ala131Glu structure (PDB ID: 6W6N) were aligned with the default settings in PyMol[51] to the A and D subunits of *N.* sp. AL212 Ala131Glu (PDB ID: 6E0X) to determine the RMSD of the two crystal structures. Then to compare distances from the heme planes, the pyrrole nitrogen and heme *meso* carbon atoms were pair fitted[51] to each other in the A subunits of both structures.

Heme Normal Coordinate Structural Decomposition

Crystallographic coordinates for all hemes present in the crystal structures of *N.* sp. AL212 cyt P460 (PDB ID 6AMG), *N.* sp. AL212 Ala131Glu cyt P460 (PDB ID 6E0X), and *N.* sp. AL212 Lys106Leu/Ala131Glu cyt P460 (PDB ID 6W6N) were uploaded into the Normal-Coordinate Structural Decomposition (NSD) calculator found at http://mliptak.w3.uvm.edu/scripts/hemeDistortion/finalDraft.pl per their instructions[42-43] to assess heme ruffling and saddling.

REFERENCES

1. Andersson, K. K.; Kent, T. A.; Lipscomb, J. D.; Hooper, A. B.; Münck, E., Mössbauer, EPR, and Optical Studies of the P-460 Center of Hydroxylamine Oxidoreductase from *Nitrosomonas* A Ferrous Heme With an Unusually Large Quadrupole Splitting. *The Journal of Biological Chemistry* **1984,** *259* (11), 6833-6840.

2. Pearson, A. R.; Elmore, B. O.; Yang, C.; Ferrara, J. D.; Hooper, A. B.; Wilmot, C. M., The Crystal Structure of Cytochrome P460 of Nitrosomonas europaea Reveals a Novel Cytochrome Fold and Heme−Protein Cross-link,. *Biochemistry* **2007,** *46* (28), 8340-8349.

3. Kranz, R. G.; Richard-Fogal, C.; Taylor, J.-S.; Frawley, E. R., Cytochrome *c* Biogenesis: Mechanisms for Covalent Modifications and Trafficking of Heme and for Heme-Iron Redox Control. *Microbiology and Molecular Biology Reviews* **2009,** *73* (3), 510-528.

4. Smith, M. A.; Lancaster, K. M., The Eponymous Cofactors in Cytochrome P460s from Ammonia-Oxidizing Bacteria Are Iron Porphyrinoids Whose Macrocycles Are Dibasic. *Biochemistry* **2018,** *57* (3), 334-343.

5. Cedervall, P.; Hooper, A. B.; Wilmot, C. M., Structural Studies of Hydroxylamine Oxidoreductase Reveal a Unique Heme Cofactor and a Previously Unidentified Interaction Partner. *Biochemistry* **2013,** *52*, 6211-6218.

6. Maalcke, W. J.; Dietl, A.; Marritt, S. J.; Butt, J. N.; Jetten, M. S. M.; Keltjens, J. T.; Barends, T. R. M.; Kartal, B., Structural Basis of Biological NO Generation by Octaheme Oxidoreductases. *Journal of Biological Chemistry* **2014,** *289* (3), 1228-1242.

7. Arciero, D. M.; Hooper, A. B., Evidence for a crosslink between c-heme and a lysine residue in cytochrome P460 of Nitrosomonas europaea. *FEBS Letters* **1997,** *410* (2), 457-460.

8. Bergmann, D. J.; Hooper, A. B., The primary structure of cytochrome P460 of Nitrosomonas europaea: presence of a c-heme binding motif. *FEBS Letters* **2001,** *353* (3), 324-326.

9. Caranto, J. D.; Lancaster, K. M., Nitric oxide is an obligate bacterial nitrification intermediate produced by hydroxylamine oxidoreductase. *Proceedings of the National Academy of Sciences* **2017,** *114* (31), 8217-8222.

10. Caranto, J. D.; Vilbert, A. C.; Lancaster, K. M., Nitrosomonas europaea cytochrome P460 is a direct link between nitrification and nitrous oxide emission. *Proceedings of the National Academy of Sciences* **2016,** *113* (51), 14704-14709.

11. Fernández, M. L.; Estrin, D. A.; Bari, S. E., Theoretical insight into the hydroxylamine oxidoreductase mechanism. *Journal of Inorganic Biochemistry* **2008,** *102* (7), 1523-1530.

12. Kuypers, M. M. M.; Marchant, H. K.; Kartal, B., The microbial nitrogen-cycling network. *Nature Reviews Microbiology* **2018,** *16* (5), 263-276.

13. Enemark, J. H.; Feltham, R. D., Principles of structure, bonding, and reactivity for metal nitrosyl complexes. *Coordination Chemistry Reviews* **1974,** *13* (4), 339-406.

14. Smith, M. A.; Majer, S. H.; Vilbert, A. C.; Lancaster, K. M., Controlling a burn: outer-sphere gating of hydroxylamine oxidation by a distal base in cytochrome P460. *Chemical Science* **2019**, 10, 3756-3764.

15. Vilbert, A. C.; Caranto, J. D.; Lancaster, K. M., Influences of the heme-lysine crosslink in cytochrome P460 over redox catalysis and nitric oxide sensitivity. *Chemical Science* **2018,** *9* (2), 368-379.

16. Ferousi, C.; Majer, S. H.; DiMucci, I. M.; Lancaster, K. M., Biological and Bioinspired Inorganic N–N Bond-Forming Reactions. *Chemical Reviews* **2020**.

17. Igarashi, N.; Moriyama, H.; Fujiwara, T.; Fukumori, Y.; Tanaka, N., The 2.8 Å structure of hydroxylamine oxidoreductase from a nitrifying chemoautotrophic bacterium, Nitrosomonas europaea. *Nature Structural Biology* **1997,** *4* (4), 276-284.

18. Bergmann, D. J.; Hooper, A. B., Cytochrome P460 of Nitrosomonas europaea. *European Journal of Biochemistry* **2003,** *270* (9), 1935-1941.

19. Ford, P. C.; Fernandez, B. O.; Lim, M. D., Mechanisms of Reductive Nitrosylation in Iron and Copper Models Relevant to Biological Systems. *Chemical Reviews* **2005,** *105* (6), 2439-2456.

20. Hoshino, M.; Maeda, M.; Konishi, R.; Seki, H.; Ford, P. C., Studies on the Reaction Mechanism for Reductive Nitrosylation of Ferrihemoproteins in Buffer Solutions. *Journal of the American Chemical Society* **1996,** *118* (24), 5702-5707.

21. Adams, H. R.; Krewson, C.; Vardanega, J. E.; Fujii, S.; Moreno, T.; Chicano; Sambongi, Y.; Svistunenko, D.; Paps, J.; Andrew, C. R.; Hough, M. A., One fold, two functions: cytochrome P460 and cytochrome c′-β from the methanotroph Methylococcus capsulatus (Bath). *Chemical Science* **2019**, 10, 3021-3041.

22. Andersen, J. F.; Ding, X. D.; Balfour, C.; Shokhireva, T. K.; Champagne, D. E.; Walker, F. A.; Montfort, W. R., Kinetics and Equilibria in Ligand Binding by Nitrophorins 1−4: Evidence for Stabilization of a Nitric Oxide−Ferriheme Complex through a Ligand-Induced Conformational Trap. *Biochemistry* **2000,** *39* (33), 10118-10131.

23. Ding, X. D.; Weichsel, A.; Andersen, J. F.; Shokhireva, T. K.; Balfour, C.; Pierik, A. J.; Averill, B. A.; Montfort, W. R.; Walker, F. A., Nitric Oxide Binding to the Ferri- and Ferroheme States of Nitrophorin 1, a Reversible NO-Binding Heme Protein from the Saliva of the Blood-Sucking Insect, Rhodnius prolixus. *Journal of the American Chemical Society* **1999,** *121* (1), 128-138.

24. Walker, F. A., Magnetic spectroscopic (EPR, ESEEM, Mössbauer, MCD and NMR) studies of low-spin ferriheme centers and their corresponding heme proteins. *Coordination Chemistry Reviews* **1999,** *185-186*, 471-534.

25. Walker, F., Nitric oxide interaction with insect nitrophorins and thoughts on the electron configuration of the FeNO complex. *Journal of Inorganic Biochemistry* **2005,** *99* (1), 216-236.

26. Shelnutt, J. A.; Song, X.-Z.; Ma, J.-G.; Jia, S.-L.; Jentzen, W.; Medforth, C. J.; Medforth, C. J., Nonplanar porphyrins and their significance in proteins. *Chemical Society Reviews* **1998,** *27* (1), 31-42.

27. Hunt, A. P.; Lehnert, N., Heme-Nitrosyls: Electronic Structure Implications for Function in Biology. *Accounts of Chemical Research* **2015,** *48* (7), 2117-2125.
28. Praneeth, V. K. K.; Paulat, F.; Berto, T. C.; George, S. D.; Näther, C.; Sulok, C. D.; Lehnert, N., Electronic Structure of Six-Coordinate Iron(III)−Porphyrin NO Adducts: The Elusive Iron(III)−NO(radical) State and Its Influence on the Properties of These Complexes. *Journal of the American Chemical Society* **2008,** *130* (46), 15288-15303.
29. Liptak, M. D.; Wen, X.; Bren, K. L., NMR and DFT Investigation of Heme Ruffling: Functional Implications for Cytochrome c. *Journal of the American Chemical Society* **2010,** *132* (28), 9753-9763.
30. Sun, Y.; Benabbas, A.; Zeng, W.; Kleingardner, J. G.; Bren, K. L.; Champion, P. M., Investigations of heme distortion, low-frequency vibrational excitations, and electron transfer in cytochrome c. *Proceedings of the National Academy of Sciences* **2014,** *111* (18), 6570-6575.
31. He, C.; Ogata, H.; Lubitz, W., Elucidation of the heme active site electronic structure affecting the unprecedented nitrite dismutase activity of the ferriheme b proteins, the nitrophorins. *Chemical Science* **2016,** *7* (8), 5332-5340.
32. Taylor, C. P. S., The EPR of low spin heme complexes Relation of the τ2g hole model to the directional properties of the g tensor, and a new method for calculating the ligand field parameters. *Biochimica et Biophysica Acta (BBA) - Protein Structure* **1977,** *491* (1), 137-148.
33. Can, M.; Zoppellaro, G.; Andersson, K. K.; Bren, K. L., Modulation of Ligand-Field Parameters by Heme Ruffling in Cytochromes c Revealed by EPR Spectroscopy. *Inorganic Chemistry* **2011,** *50* (23), 12018-12024.
34. Adams, H. R.; Krewson, C.; Vardanega, J. E.; Fujii, S.; Moreno, T.; Chicano; Sambongi, Y.; Svistunenko, D.; Paps, J.; Andrew, C. R.; Hough, M. A., One fold, two functions: cytochrome P460 and cytochrome c′-β from the methanotroph Methylococcus capsulatus (Bath). *Chemical Science* **2019,** *10* (10), 3031-3041.

35. Elmore, B. O.; Bergmann, D. J.; Klotz, M. G.; Hooper, A. B., Cytochromes P460 and c′-beta; A new family of high-spin cytochromes c. *FEBS Letters* **2007,** *581* (5), 911-916.

36. Savéant, J.-M., Concerted Proton-Electron Transfers: Fundamentals and Recent Developments. *Annual Review of Analytical Chemistry* **2014,** *7* (1), 537-560.

37. Markle, T. F.; Zhang, M.-T.; Santoni, M.-P.; Johannissen, L. O.; Hammarström, L., Proton-Coupled Electron Transfer in a Series of Ruthenium-Linked Tyrosines with Internal Bases: Evaluation of a Tunneling Model for Experimental Temperature-Dependent Kinetics. *The Journal of Physical Chemistry B* **2016,** *120* (35), 9308-9321.

38. Ma, J.-G.; Vanderkooi, J. M.; Zhang, J.; Jia, S.-L.; Shelnutt, J. A., Resonance Raman Investigation of Nickel Microperoxidase-11. *Biochemistry* **1999,** *38* (9), 2787-2795.

39. Shokhireva, T. K.; Berry, R. E.; Uno, E.; Balfour, C. A.; Zhang, H.; Walker, F. A., Electrochemical and NMR spectroscopic studies of distal pocket mutants of nitrophorin 2: Stability, structure, and dynamics of axial ligand complexes. *Proceedings of the National Academy of Sciences* **2003,** *100* (7), 3778-3783.

40. Ikezaki, A.; Ohgo, Y.; Nakamura, M., NMR studies on the electronic structure of one-electron oxidized complexes of iron(III) porphyrinates. *Coordination Chemistry Reviews* **2009,** *253* (15), 2056-2069.

41. Senge, M. O., Highly Substituted Porphyrins. In *The Porphyrin Handbook*, Kadish, K. M.; Smith, K. M.; Guilard, R., Eds. Academic Press: San Diego, CA, 2000; Vol. 1, p 241.

42. Jentzen, W.; Song, X.-Z.; Shelnutt, J. A., Structural Characterization of Synthetic and Protein-Bound Porphyrins in Terms of the Lowest-Frequency Normal Coordinates of the Macrocycle. *The Journal of Physical Chemistry B* **1997,** *101* (9), 1684-1699.

43. Graves, A. B.; Graves, M. T.; Liptak, M. D., Measurement of Heme Ruffling Changes in MhuD Using UV–vis Spectroscopy. *The Journal of Physical Chemistry B* **2016,** *120* (16), 3844-3853.

44. Caranto, J. D.; Weitz, A.; Hendrich, M. P.; Kurtz, D. M., The Nitric Oxide Reductase Mechanism of a Flavo-Diiron Protein: Identification of Active-Site Intermediates and Products. *Journal of the American Chemical Society* **2014,** *136* (22), 7981-7992.

45. Frear, D. S.; Burrell, R. C., Spectrophotometric Method for Determining Hydroxylamine Reductase Activity in Higher Plants. *Analytical Chemistry* **1955,** *27* (10), 1664-1665.

46. Williamson, G.; Engel, P. C., Butyryl-CoA dehydrogenase from Megasphaera elsdenii. Specificity of the catalytic reaction. *Biochemical Journal* **1984,** *218* (2), 521-529.

47. Zaugg, W. S., Spectroscopic Characteristics and Some Chemical Properties of N-Methylphenazinium Methyl Sulfate (Phenazine Methosulfate) and Pyocyanine at the Semiquinoid Oxidation Level. *The Journal of Biological Chemistry* **1964,** *293*, 3964-3970.

48. Golombek, A. P.; Hendrich, M. P., Quantitative analysis of dinuclear manganese(II) EPR spectra. *Journal of Magnetic Resonance* **2003,** *165* (1), 33-48.

49. Adams, P. D.; Afonine, P. V.; Bunkóczi, G.; Chen, V. B.; Davis, I. W.; Echols, N.; Headd, J. J.; Hung, L.-W.; Kapral, G. J.; Grosse-Kunstleve, R. W.; McCoy, A. J.; Moriarty, N. W.; Oeffner, R.; Read, R. J.; Richardson, D. C.; Richardson, J. S.; Terwilliger, T. C.; Zwart, P. H., PHENIX: a comprehensive Python-based system for macromolecular structure solution. *Acta Crystallographica Section D: Biological Crystallography* **2010,** *66* (2), 213-221.

50. Emsley, P.; Lohkamp, B.; Scott, W. G.; Cowtan, K., Features and development of Coot. *Acta Crystallographica Section D: Biological Crystallography* **2010,** *66* (Pt 4), 486-501.

51. Schrodinger, LLC, The PyMOL Molecular Graphics System, Version 1.8. 2015.

CHAPTER 3
FORMATION OF THE HEME-LYSINE CROSS-LINK IN CYTOCHROME P460

This work was conducted in collaboration with Sean H. Majer and my former undergraduate student Silas D. Ferrao. Data they collected will be reported in this chapter for narrative clarity. Data collected by anyone other than the author will be denoted in the figure caption, unless it was a joint effort, in which case individual contributions will be noted.

Introduction

Heme-based cofactors are ubiquitous across biological systems and serve a variety of functions inside the cell. These functions include gas transport, electron transfer, and catalysis. Nature has tuned heme cofactors for their respective functions by imposing different physical constraints on the active site to suit the protein's purpose.[1] For example, gas-carrying hemoproteins like myoglobin[2] or hemoglobin[3-4] induce a domed deformation to the cofactor, which promotes oxygen binding. In the case of the P460 cofactor found in the HAO and cyt P460 protein families, a protein-heme cross-link is essential for oxidative catalysis. In HAO, absence of the cross-link promotes reductive chemistry over oxidative.[5] With cyt P460 from AOB, however, the cross-link serves the purpose of positioning the cofactor close to a second-sphere proton-relaying Glu residue. In the absence of the cross-link, the protein is not active. Less importantly, the presence of the cross-link also changes the electronic structure of the protein in that it alters the UV-vis spectrum: cross-link-containing cyt P460 is green, whereas as CLD cyt P460 is red.

Protein-heme cross-links are not uncommon. In fact, the definition of a *c*-type heme is that the protein scaffold attaches to the macrocycle at the heme vinyl groups via thioether linkages in a highly conserved CXXCH domain,[6] leaving the terminal His residue in the sequence to coordinate the Fe center.[6] In these systems, the thioether cross-links form through a series of enzymatic reactions controlled by the cytochrome *c* maturation system.[6] In prokaryotes, there are two systems: System I and System II.[6]

Both of these systems will ultimately attach the cysteine S atoms to the heme vinyl groups under reducing conditions, thus allowing the protein to fold.[6]

In addition to the thioether linkages installed by enzymatic machinery, non-canonical cross-links have also been observed. These cross-links have been proposed to form under both oxidative and reducing conditions.[7] For example, human myeloperoxidase has three non-canonical cross-links:[7-8] Glu242 and Ap94 form ester cross-links using the carboxylates to attach to the heme methyl groups, in addition to a sulfonium cross-link from Met243 to the β-carbon of vinyl group in pyrrole A.[8] Metcalfe and co-workers[9] sought to establish a mechanistic understanding of the sulfonium linkage in myeloperoxidase by modeling it in recombinant pea ascorbate peroxidase. In this study, they performed site-directed mutagenesis to install a methionine residue near the heme vinyl group.[9] After reconstitution with heme, they treated the sample with H_2O_2 and verified cross-link formation through mass spectrometry and HPLC analysis.[9] Using stopped-flow UV-visible spectroscopy, they observed a compound I species, implicating radical rebound in the formation of the sulfonium linkage.[9] In addition, there are several other non-canonical heme-protein cross-links. This includes certain members of the cyt P450 protein family where an ester linkage is formed to the methyl groups[10] or a C–O bond that formed spontaneously between the phenolate oxygen and a heme-vinyl group in a Phe43Tyr mutant of myoglobin.[11] A more comprehensive review of known heme cross-links was contributed by Lin[7] in 2015. A summary of naturally occurring heme cross-links is shown in **Figure 3.1**.

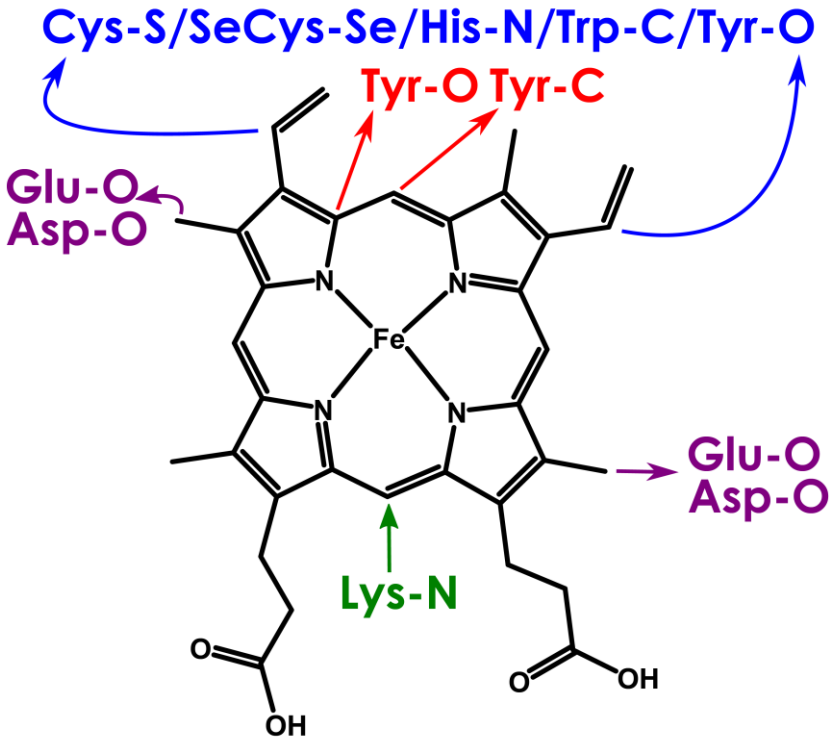

Figure 3.1. A summary of known, naturally occurring heme cross-links. Arrow and text colors correspond to bonds to the carbon atom at the origin of the arrow. Figure adapted from reference 7.

All of the previously mentioned post-translational modifications to heme proteins are formed between an amino acid residue and one of the heme substituents—specifically the heme vinyls or the heme methyls. Currently, the only known, naturally occurring heme systems containing a cross-link to the porphyrin ring directly share the P460 cofactor: HAO and cyt P460. In the case of cytochrome P460, the formation of the cross-link was previously speculated to form in an autocatalytic process, but was not investigated further.[12] In addition, a preliminary crystal structure of cyt P460 reported by Pearson and coworkers[13] found that the 5′ *meso* carbon was hydroxylated—opposite of the heme-lysine cross-link on the 13′ *meso* carbon. Given the fact that AOB are obligate aerobic microorganisms, we have hypothesized that the heme-Lys cross-link forms in an oxygen-dependent process—similar to other non-canonical cross-links—and does not require enzymatic machinery for formation. We[14-15] have not not yet been successful in generating a cross-link containing protein by

mutating the Lys to a different residue—nor has anyone else[12]. Regardless, we speculated that only a Lys will cross-link the heme and that the cyt P460 fold promotes this post-translational modification. Our hypothesis is that the γ *meso* carbon becomes hydroxylated which subsequently tautomerizes and allows for the nucleophilic attack of the amine N in the Lys sidechain.

Heme-lysine cross-link formation in cyt P460 is intrinsic to the protein fold

The Lys cross-link of cytochrome P460 is highly conserved across the protein family. A multiple sequence alignment of 236 annotated cytochrome P460 species showed that the predominant residue at the cross-link position is Lys (**Figure 3.2**). The next most frequent residue is Leu. One gene that is annotated as a cyt P460 but contains a Leu residue at the cross-link position is from the organism *Nitrosospira* sp. NpAV—Leu105 (**Figure 3.3**). Isolation of the WT *N.* sp. NpAV cyt P460 produces a red protein that has a Soret maximum at 412 nm, which is consistent with previously generated CLD cyt P460 species,[12, 14-15] cyt c′,[16] or cyt c'_{β}[17] (**Figure 3.4**). To test if cross-link formation was possible in a protein that does not natively have a cross-link, we generated the Leu105Lys variant of *N.* sp. NpAV cyt P460. This mutation resulted in a green protein with a Soret maximum at 439 nm and its UV-vis spectrum was similar in shape to WT *N. europaea* cyt P460 (**Figure 3.3**).[18] When reduced, the Soret maximum shifted to 460 nm, which is consistent with a cross-link containing protein species. The X-band EPR spectrum of this variant collected at 12K had a g_{max}, g_{mid}, and g_{min} of 6.63, 5.07, and 1.96 with an E/D of 0.02 (**Figure 3.3**), which is similar to the WT *N. europaea* parameters of 6.57, 5.09, and 1.97, respectively with an E/D of 0.03.[18] Generation of a cross-link containing heme species in a protein that does not natively contain a cross-link supported our hypothesis that something inherent to the protein fold promotes the formation of the heme-Lys cross-link.

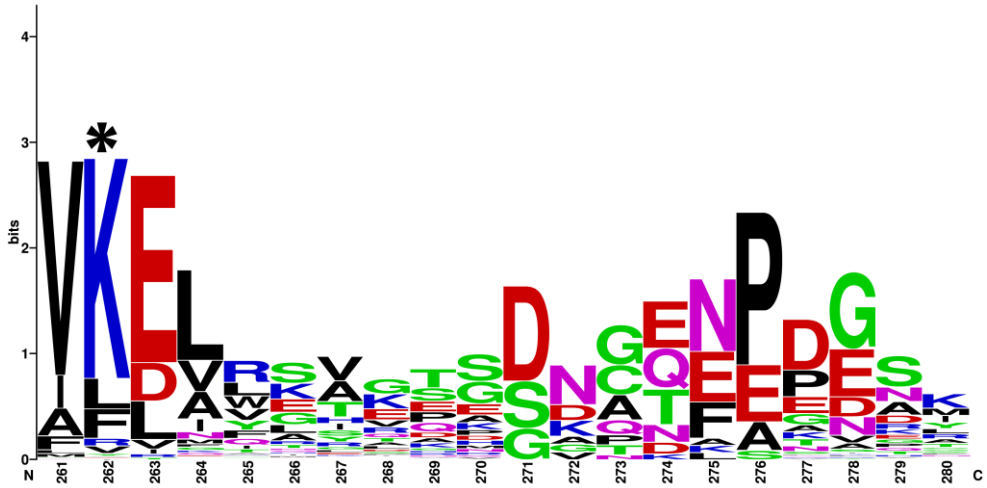

Figure 3.2. Sequence logo of cyt P460, showing a fragment with 20 amino acid residues. The position with the * denotes the cross-link position. The logo is based off a database of 236 entries curated by HMMER after using the *N. europaea* cyt P460 gene (NCBI Accession Number WP_011110663) as the query. The multiple sequence alignment was performed in MegaX using ClustalW. This multiple sequence alignment was uploaded into WebLogo to make the above figure. The relative size of the residue indicates the prevalence of a residue at that position.

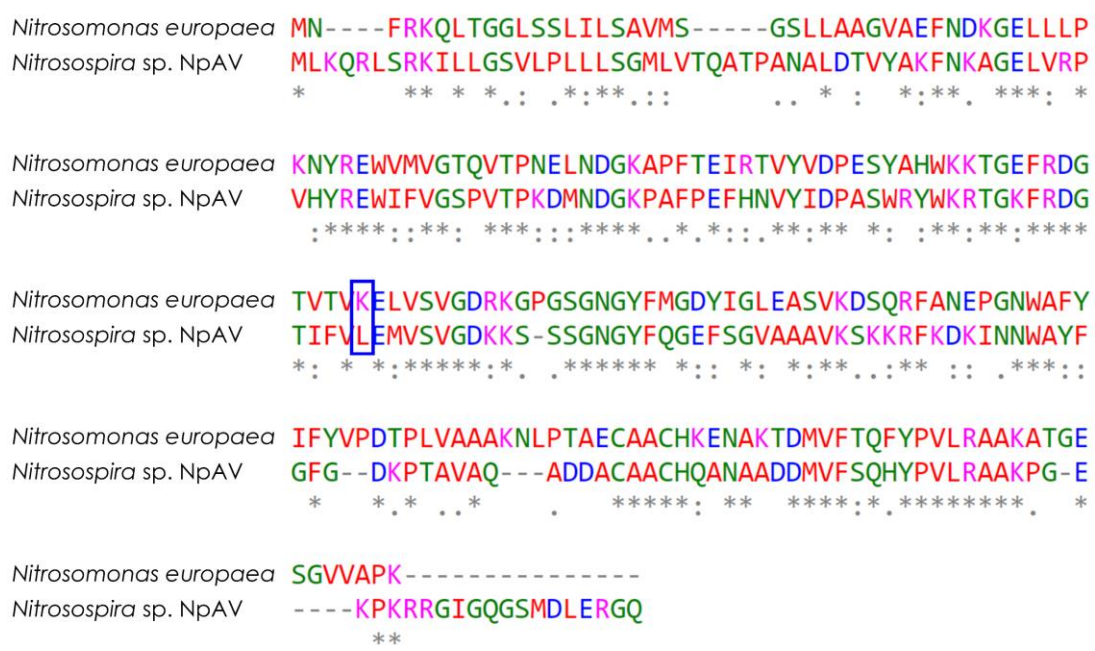

Figure 3.3. Sequence alignment generated in T-coffee using the ClustalW algorithm comparing *N. europaea* cyt P460 (NCBI Accession WP_011110663) and *Nitrosospira* sp. NpAV (NCBI Accession Number WP_052493891). The blue boxed residue indicates the cross-link position, noting the difference between *N. europaea* and *N.* sp. NpAV.

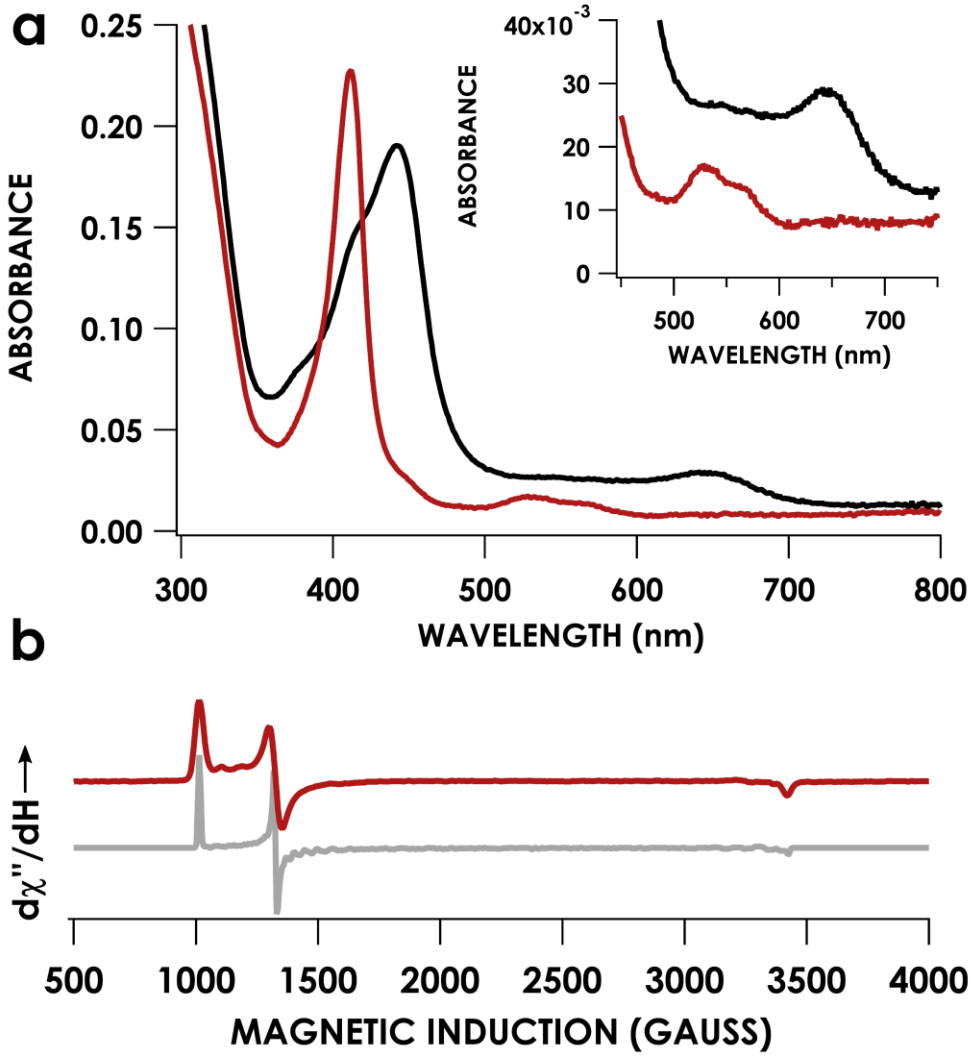

Figure 3.4. (a) UV-vis trace comparing WT *N.* sp. NpAV (red) and the mutant, *N.* sp. NpAV Leu105K (black). The inset shows the Q band region. (b) X-band EPR spectrum the Leu105Lys collected at 12K. The red trace shows the data and the gray trace shows the simulation. Data collected by SDF. Simulation performed by REC.

Exclusion of oxygen during protein expression produces a cross-link deficient cyt P460

Given our hypothesis that oxygen was also required for cross-link formation, this led us to develop a method to express the WT *N. europaea* enzyme under anaerobic conditions. The native AOB are obligate aerobic microorganisms, but we

express our protein recombinantly using *E. coli* cells, which are facultative anerobic microorganisms.[19] Expression of the protein under anaerobic conditions resulted in the isolation of a protein that was red and showed spectroscopic features characteristic of cross-link deficient cyt P460 species.[14-15] Produced this way, WT *N. europaea* cyt P460 can have a Soret maximum 403 nm (**Figure 3.5a**). With our setup, it is difficult to keep the protein completely anaerobic and depending on the prep, we can get a protein that is a mixture of both the reduced and oxidized species or a mixture of CL-containing and CLD protein. In the partially reduced isolations of cyt P460, the shoulder near 430 nm is indicative of the reduced species, and the Q-bands are consistent with this assignment; however, it is unclear what the reductant of this species is. If there is more exposure to oxygen during the growth and/or purification, the shoulder at 430 nm disappears and instead, a shoulder at 440 nm is observable, indicative of some CL-containing cyt P460. Both the second Soret at 440 nm and Q bands are indicative of a cross-link containing cyt P460 (**Figure 3.5b**). The anaerobic wild type (AWT) protein was inactive (*vide infra*).

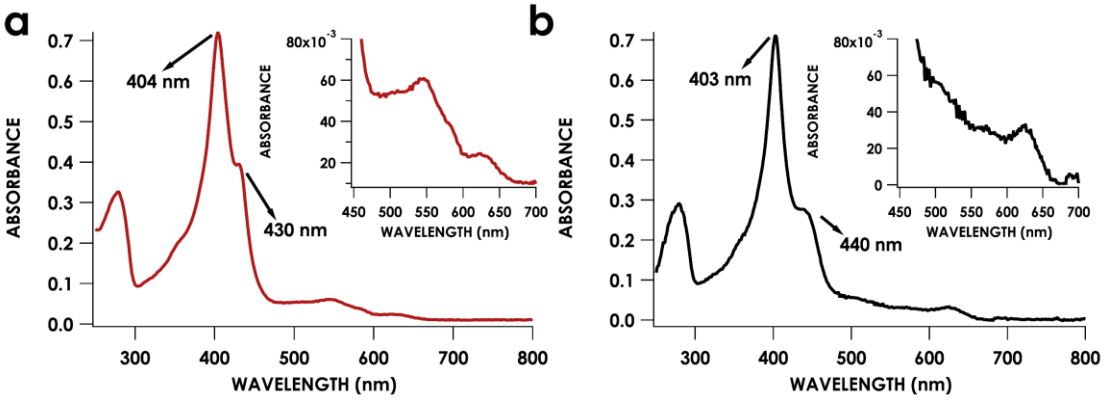

Figure 3.5. UV-vis spectra of as-isolated, anaerobically WT (AWT) *N. europaea* cyt P460 from two different preparations. A more anaerobic expression/purification is shown in (a) while an expression/purification that likely had more oxygen exposure is shown in (b).

Additional characterization of this protein in the EPR revealed a mixture of $S = {}^{5}/_{2}$ signals that were consistent with a cross-link containing and a CLD cyt P460 (**Figure 3.6**, **Table 3.1**). The CLD signal was the major component, making up 85%

of the species and the cross-link containing signal was the minor component. Regardless, knowing that majority of the protein isolated from this process was CLD allowed us to test how the cross-link of cyt P460 forms by exposing it to oxygen-containing species.

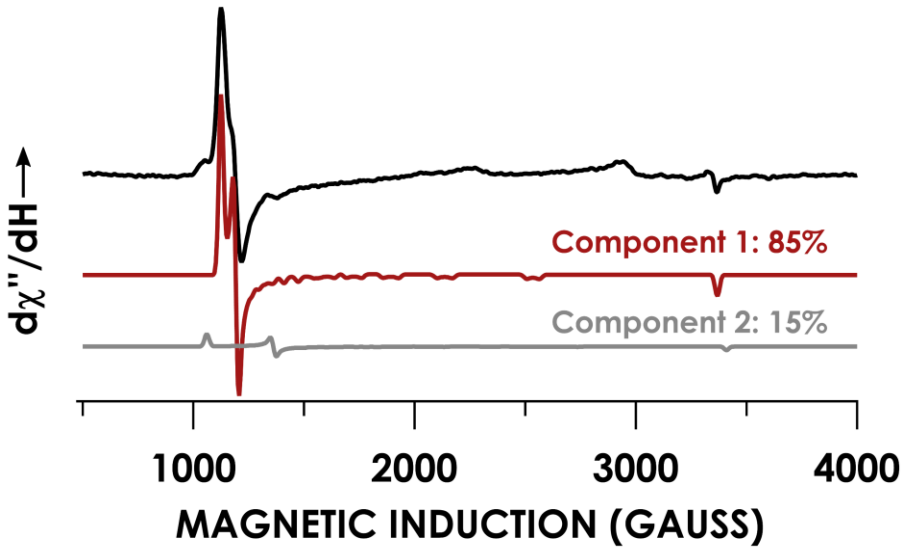

Figure 3.6. X-band EPR spectrum of AWT cyt P460 collected at 10 K. The black trace shows the raw data and the red and gray traces denote the simulations of the two components present in the data. Data collected by SDF. Simulation performed by REC.

Table 3.1 EPR parameters of various cyt P460 species, including anaerobically expressed WT cyt P460.

Cyt P460 Variant	**Resting Fe^{III} (S = 5/2)**		
	g_{eff} values	***E/D***	**Reference**
Aerobically expressed *Nitrosomonas europaea*	6.57, 5.09, 1.97	0.03	[18]
Nitrosomonas sp. AL212 Lys106Leu/Ala131Glu (cross-link deficient)	6.04, 5.65, 1.99	0.01	[15]
Anaerobically expressed *N. europaea* (major component)	5.97, 5.63, 1.99	0.01	This work
Anaerobically expressed *N. europaea* (minor component)	6.33, 4.93, 1.97	0.03	This work

Cyt P460 cross-link formation proceeds through a likely peroxide intermediate

Exclusion of oxygen during protein expression produces a protein without a cross-link, which strongly implicates some oxygen-containing species as a necessary

for cross-link formation. NH_2OH has been reported to protect hemes from reactive-oxygen species because it acts as a sacrificial reactant, and we included it in our initial reactions to form the cross-link.[17] We treated an 8 μM sample of the proenzyme with 10 mM NH_2OH inside an anaerobic cuvette and exposed it to O_2 in the headspace of the cuvette. In this experiment, we saw an immediate decay of the CLD Soret at 403 nm and a growth of the absorbance around 440 nm with rate constants of $1.62 \times 10^{-3} \pm 4.34 \times 10^{-5}$ s^{-1} and $1.29 \times 10^{-3} \pm 1.24 \times 10^{-5}$ s^{-1}, respectively (**Figure 3.7**). Closer inspection of this UV-vis traces showed the presence of a transient intermediate at 413 nm. Use of NH_2OH does not make physiological sense, however, because NH_2OH is cytotoxic to *E. coli*[20-21] and these cells are able to form the cross-link with no issue during recombinant expression. However, O_2 and NH_2OH have been reported to produce hydrogen peroxide (H_2O_2),[22] which led us to question if forming a hydroperoxo-adduct was necessary to form the heme-Lys cross-link.

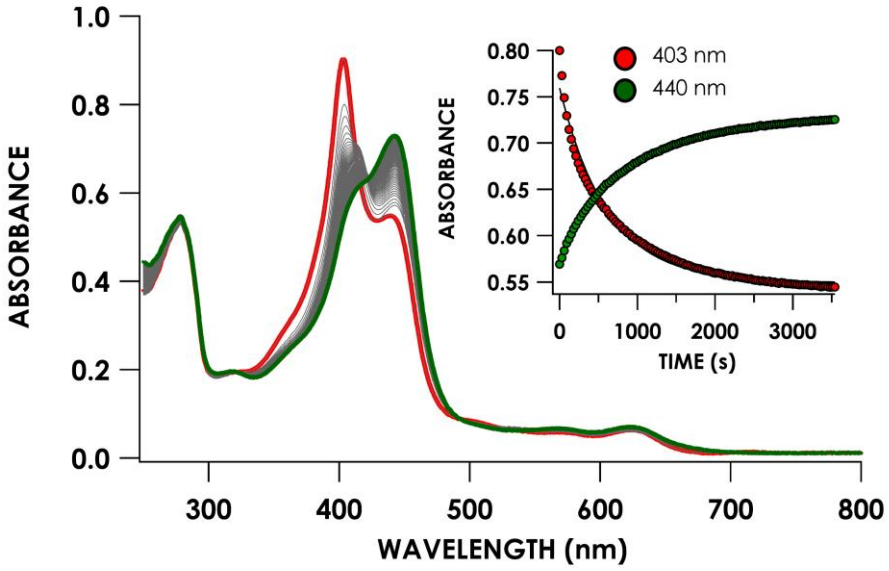

Figure 3.7. Reaction of 8 μM AWT cyt P460 treated with 10 mM NH_2OH and with O_2 bubbling in the headspace. The red trace shows the starting protein absorbance and the green trace shows the final. Gray lines in between are scans from every thirty seconds. The inset shows exponential fits for the decay at 403 nm and the growth at 440 nm, with rate constants of $-1.6 \times 10^{-3} \pm 4.3 \times 10^{-5}$ s^{-1} and $1.2 \times 10^{-3} \pm 1.2 \times 10^{-5}$ s^{-1}, respectively. Data collected by SDF. Exponential fits performed by REC.

To test if H_2O_2 was necessary for cross-link formation, the same reaction was conducted in the presence of catalase, which protects the cell from damage by converting H_2O_2 into O_2 and H_2O. In the presence of 1 μM catalase, both the rates decay of the CLD cyt P460 species and the in-growth of the cross-link containing cyt P460 were impeded (**Figure 3.8**, **Table 3.2**). The rate of decay of the 403 nm peak was 1.5x slower in the presence of catalase. Inhibition of these reactions by catalase strongly implies that hydrogen peroxide is mechanistically involved in the formation of the cross-link of cyt P460, at least *in vitro*. Potentially, the transient 413 nm intermediate observed in **Figure 3.7** could correspond to the hydroperoxo adduct. Being obligate aerobic microbes, *N. europaea* contain enzymes meant to neutralize reactive oxygen species like superoxide dismutase or catalase physiologically.[23] If the cell uses a similar mechanism as what we have observed *in vitro*, it would be interesting to study the regulation of these proteins and cyt P460 in response to various concentrations of NH_2OH. If the response was a down-regulation of catalase and an up-regulation of cyt P460 if cellular concentrations of NH_2OH were in the millimolar regime, it would support two hypotheses: that H_2O_2 is involved in cross-link formation and that cyt P460 serves a detoxifying role. Such a study is beyond the scope of this work and lab but could be an interesting avenue to study for those interested in AOB metabolism.

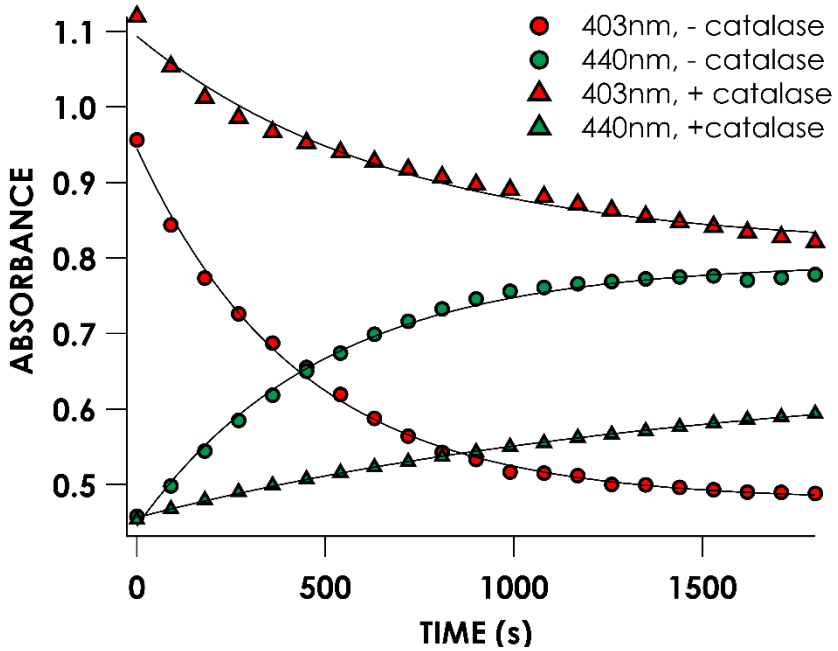

Figure 3.8. Single wavelength traces of the decay of the 403 nm peak (red) and formation of the 440 nm peak (green) in the presence (triangles) and absence (circles) of 1 μM catalase. 8 μM AWT cyt P460 was treated with 10 mM NH_2OH in an O_2 saturated buffer at 30°C. Data collected and fit by SHM.

Table 3.2. Rates of CLD decay and cross-link formation in the presence and absence of catalase.

	Decay of 403 nm (CLD cyt P460) (s^{-1})	Growth of 440 nm (cross-link containing) (s^{-1})
- catalase	$2.33 \times 10^{-3} \pm 7.00 \times 10^{-5}$	$2.03 \times 10^{-3} \pm 8.54 \times 10^{-5}$
+ catalase (1 μM)	$1.47 \times 10^{-3} \pm 1.54 \times 10^{-4}$	$6.58 \times 10^{-4} \pm 2.53 \times 10^{-5}$

Treatment of the pro-enzyme with H_2O_2 restores activity to the protein

Cyt P460 requires the heme-Lys cross-link for activity.[12, 14-15] To test if the treatment with H_2O_2 does restore activity to the protein, a sample of AWT cyt P460 was cross-linked by treatment with H_2O_2 and quenched by addition of sodium dithionite, which also reduces the heme center. This sample was then washed and an activity assay was performed. In this experiment, a cuvette containing 50 μM DCPIP and 6 μM PMS, were treated with 2 mM NH_2OH followed by 250 nM protein—either

WT cyt P460, as-isolated AWT cyt P460, or AWT cyt P460 post-cross-link formation. Compared to the control of WT cyt P460 with a specific activity of 8.4 ± 2.7 μM DCPIP μM cyt $P460^{-1}$ min^{-1}, the as-isolated protein was inactive—the specific activity was 1.9 ± 0.2 μM DCPIP μM cyt $P460^{-1}$ min^{-1}. After treatment of this species with H_2O_2, activity was restored to the protein, resulting in a specific activity of 13.0 ± 2.4 μM DCPIP μM cyt $P460^{-1}$ min^{-1} (**Figure 3.9**). The small amount of activity observed with the protein prior to treatment with H_2O_2 can be attributed to the small amount of cross-link character that is observable in the UV-vis and is likely a result of brief exposure to oxygen. This result strongly suggests that the cross-link of cyt P460 was formed because the cross-link is essential to position the heme relative to the second-sphere Glu residue.[15]

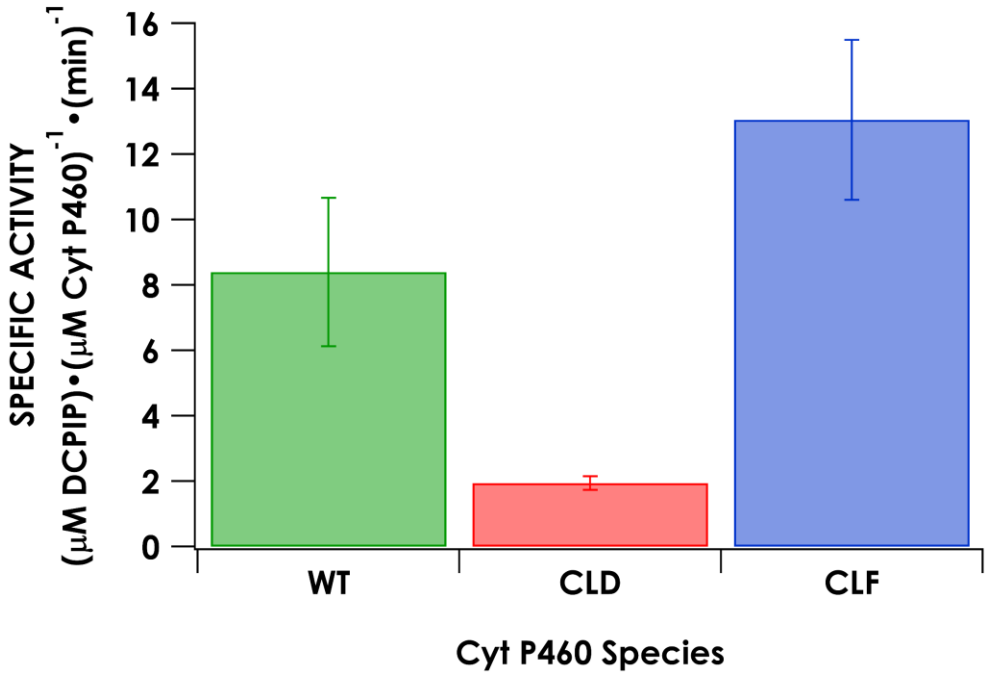

Figure 3.9. Specific activity of, from left to right, aerobically grown WT cyt P460, the as-isolated, CLD cyt P460, and that same protein after cross-link formation by treatment with H_2O_2.

Mechanism of cross-link formation in cyt P460

Knowing that H_2O_2 is involved in the cross-link formation reaction led us to hypothesize on the mechanism of cross-link formation in cyt P460. For the initial steps of the reaction, we have drawn inspiration from the enzyme heme oxygenase (HO), which is a protein that binds heme to degrade it into free Fe, carbon monoxide (CO) and biliverdin.[24] HO proceeds through three separate O_2 activation steps, the first of which results in the production of a *meso*-hydroxylated porphyrin ring in a regiospecific manner.[25] To do so, the protein will bind heme in its ferric state, reduce it such that it can bind O_2, which is followed by a second reduction that results in an Fe^{III}-OOH adduct, which is also necessary for cyt P450 enzymes prior to generation of compound I.[26] What happens after generation of the hydroperoxo adduct, however, is where these two enzymes differ: In cyt P450, the O–O bond is heterolytically cleaved to generate Compound I, whereas HO has been shown to use the hydroperoxo adduct directly to hydroxylate the *meso* carbon—not Compound I.[27-29]

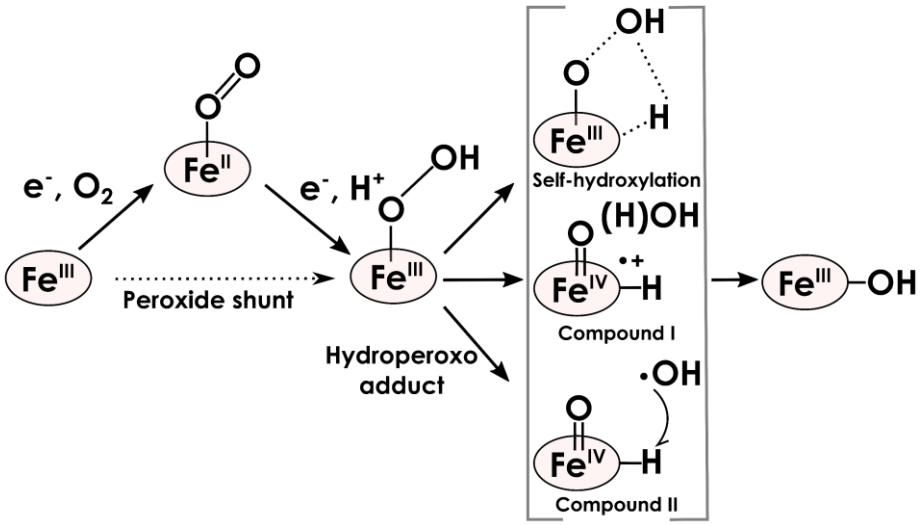

Figure 3.10. Mechanism of heme *meso* carbon hydroxylation in heme oxygenase (HO) adapted from reference [25]. HO binds the ferric heme and reduces the heme center and allows it to bind oxygen, then activates it by reducing the bound oxygen. Three potential mechanism have been proposed: a concerted self-hydroxylation, a compound I mechanism, and a compound II mechanism. In HO, compound I has been shown to not be operative. Adapted from reference 25.

In HO, compound I has been shown to be incompetent for *meso*-carbon hydroxylation[30] and instead either a concerted self-hydroxylation or formation of compound II and a transient hydroxyl radical (**Figure 3.10)**.[25] In the case of AWT, the protein seems incapable of forming compound I. In a stopped-flow UV-vis experiment, 20 μM AWT P460 were mixed with 40 μM *meta*-chloroperoxybenzoic acid (*m*-CPBA), which generates Compound I in heme systems,[31] at 22°C, but no reaction indicative of cross-link formation was observed in this experiment over the course of 5 minutes (**Figure 3.11**). Nothing resembling Compound I was observed, but that is not unusual. Matsui and co-workers[30] mixed their HO sample with guaiacol and observed formation of the oxidation product, tetraguiacol to test if Compound I was formed, and then if it was on-pathway for *meso* carbon hydroxylation. We could perform a similar experiment to test if AWT cyt P460 is even capable of Compound I formation by mixing it with *m*-CPBA and guaiacol. More experiments need to be carried out to establish which of the remaining two mechanisms form the cross-link of cyt P460, but regardless, once the *meso* carbon is hydroxylated, we believe that the porphyrin can undergo a tautomerization reaction, which would allow for the nucleophilic attack of the Lys70 residue (**Figure 3.12**), changing the proenzyme to an enzyme.

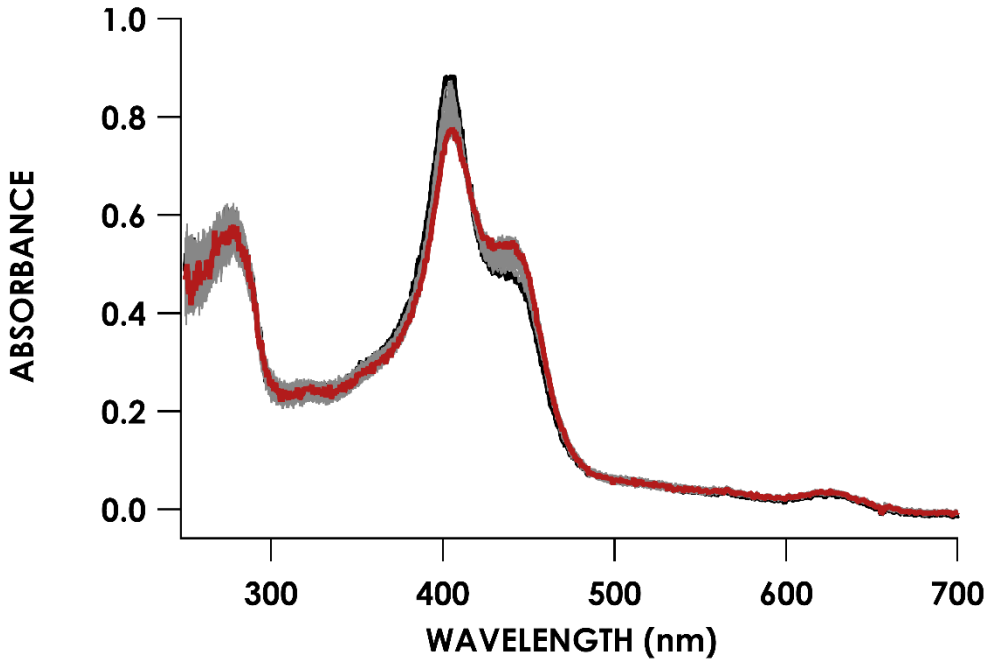

Figure 3.11. Stopped-flow UV-vis absorbance spectrum of 20 μM AWT cyt P460 mixed with 40 μM *meta*-chloroperoxybenzoic acid (*m*-CPBA) at 22°C over the course of five minutes. The black trace is the initial scan and the red trace is the final scan. Scans are every 296 ms. *m*-CPBA should generate Compound I in heme systems, but no reaction was observed, nor was any noticeable cross-link formation.

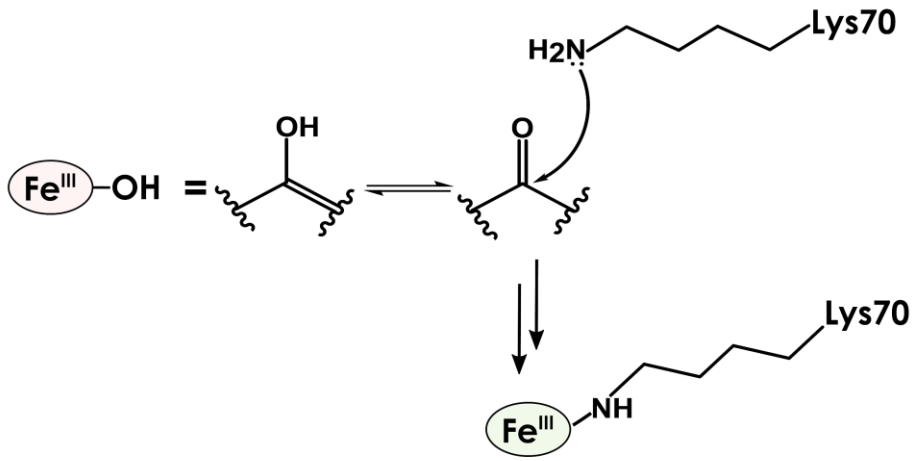

Figure 3.12. Hypothesis for the mechanism of cross-link formation *in vitro* for WT *N. europaea* cyt P460. We speculate that the *meso* hydroxylated carbon can tautomerize and allow for nucleophilic attack of the N atom of the lysine.

Additional experiments could be carried out to address if the remaining two HO mechanisms of heme *meso* carbon hydroxylation are operative in cross-link formation of cyt P460. To test for a self-hydroxylation mechanism, Wilks *et al*[32] used ethyl hydroperoxide instead of H_2O_2 to test the hydroxylation of the *meso* carbon. The product of this reaction was a *meso*-ethoxyheme species that had been added regiospecifically.[32] However, they also noted that this does not completely rule out a Compound II and hydroxyl radical mechanism.[32] A similar strategy could be used to further support that H_2O_2 is key feature of cross-link formation in cyt P460, and would further support that H_2O_2 is operative in cross-link formation.

In mammalian HO-1, a distal aspartate residue—Asp140—is required to hydroxylate the *meso* carbon because it is directly involved in hydrogen bonding interactions with a water molecule that has been shown to be the source of the proton necessary to form the hydroperoxyl adduct upon the second one-electron reduction.[33] However, containing a carboxylate moiety is not important. In various mutants of *Corynebacterium diptheriae* HO where the distal Asp residue was replaced with Phe, Ala, and Asn, only the Asn mutant was able to degrade heme with the same efficiency as that of the WT.[34] In fact, mutation of Asp140 to an alanine residue results in a

complete inability of HO-1 to form the *meso*-hydroxylated porphyrin species, but instead favored Compound I formation, which cannot hydroxylate the heme.[27, 33] Knowing HO's strategy to hydroxylate the *meso* carbon, we looked to the crystal structure of the CLD cyt P460: *N.* sp. AL212 Lys106Leu/Ala131 Glu (PDB ID 6W6N).[15] In this structure, there are four water molecules in and around the active site pocket that are involved in a hydrogen bonding network that is centered around a distal His residue (**Figure 3.13)**. The equivalent residue in *N. europaea* cyt P460 is an Arg; in fact, looking at this distal position in a sequence logo, the most common is His, then Arg, followed by Asp and Asn (**Figure 3.14)**, which are all residues capable of hydrogen bonding. The distal His residue hydrogen bonds with one of the heme propionate groups and helps orient in opposition to the heme plane. This propionate is capable of hydrogen bonding with a second water molecule that is interacting with a water molecule bound to the heme Fe as well as some additional water molecules around the heme site. Perhaps the distal His residue in the active site pocket serves a similar role to the Asp140 in HO—it stabilizes a water network, which, in turn, helps stabilize the reactive hydroperoxo adduct of HO.[25] Effects the second sphere residues on cross-link formation will be addressed in the following chapter.

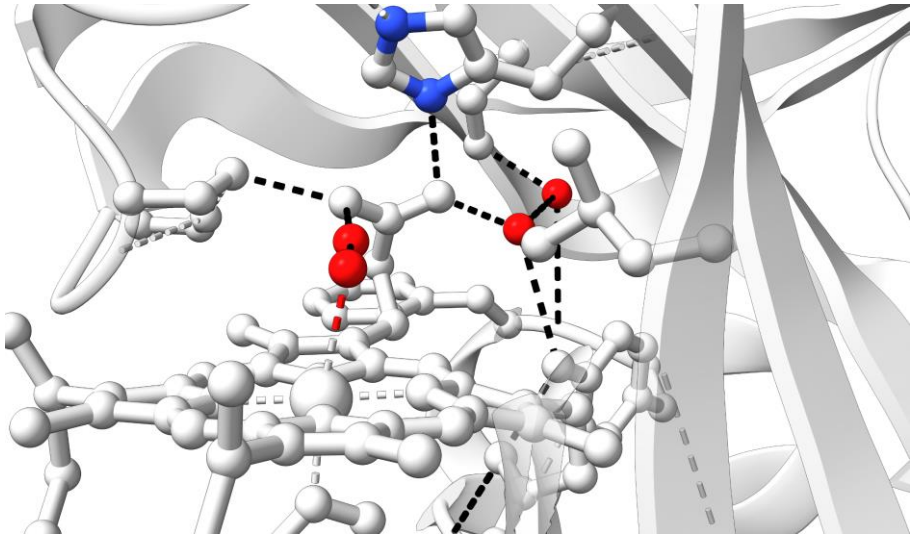

Figure 3.13. Water molecules (red) in the distal pocket of *N.* sp. AL212 Lys106Leu/Ala131Glu (PDB ID 6W6N) shown in conjunction with a distal His residue (N atoms are blue). The water network present in XLD variant of this protein could be similar to that of AWT *N. europaea* cyt P460 and assist in stabilizing the hydroperoxo adduct speculated to be involved in cross-link formation.

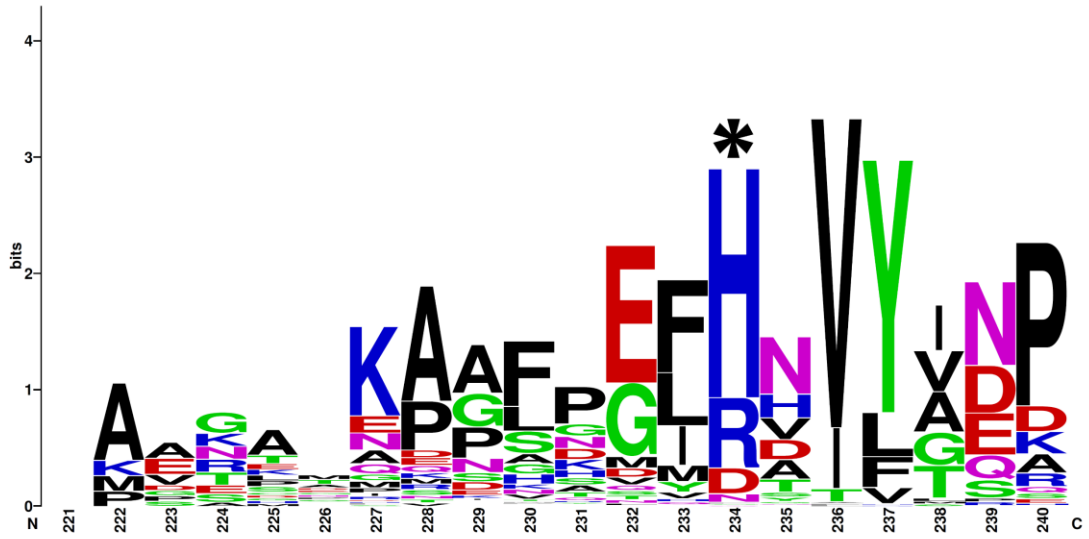

Figure 3.14. Sequence logo of cyt P460, showing a fragment with 20 amino acid residues. The position with the * denotes the residue in the distal pocket, noting a high conservation of residues capable of hydrogen bonding. The logo is based off a database of 236 entries curated by HMMER after using the *N. europaea* cyt P460 gene (NCBI Accession Number WP_011110663) as the query. The multiple sequence alignment was performed in MegaX using ClustalW. This multiple sequence alignment was uploaded into WebLogo to make the above figure.

Conclusion

The most unique feature of the heme P460 cofactor is that of the cross-link, which varies between a Tyr residue in HAO and a Lys in cyt P460.[13, 35-36] These two protein families are the only known, naturally occurring ones that have a direct modification onto the porphyrin macrocycle directly, as opposed to one of its substituents[7] and at least in the case of cyt P460, the cross-link was reported to form autocatalytically and not with specialized cellular machinery,[12] which is also supported by the ease of recombinant expression in phylogenetically distinct organisms.[12, 18] The fold of cyt P460 is relatively unique, only being found in the related protein family, cyt c′β[17, 37] and the fact that we can generate a cross-link in *N.* sp. NpAV cyt P460, which natively contains a Leu residue incapable of cross-link formation, by mutating a Lys in that position supports the fact that something inherent to the cyt P460 fold promotes cross-link formation. To test the hypothesis that cross-link formation is O_2 dependent, we expressed WT *N. europaea* cyt P460 in the

absence of O_2 and generated a cyt P460 that was spectroscopically identical to the previously generated, CLD cyt P460 species.[14-15] This strongly implicates some oxygen-containing species as a necessary component of cross-link formation. Compound I seems unlikely given that there is minimal reaction when the AWT cyt P460 is treated with *m*-CPBA, but H_2O_2 seems likely since it will produce an active cyt P460 species after treatment. Whether it self-hydroxylates or homolyticaly cleaves the O-O bond of H_2O_2 remains to be seen, but both of these mechanism are speculated to be how the first hydroxylation step of the enzyme HO works.[25] Regardless of how the hydroxylated *meso* carbon arises, we speculate that once formed, the heme cyt might undergo a tautomerization reaction, generating a carbonyl that is electrophilic enough to allow for the Lys residue to attack and form the cross-link. Subsequent studies of AWT cyt P460 will trap intermediates and provide more definitive evidence of this proposed mechanism. Additionally, aspects of the second-sphere that are necessary for cross-link formation are still largely unknown, but initial attempts to characterize them will be addressed in the following chapter.

Experimental

Plasmids and mutagenesis

Generation of *N.* sp. NpAV Leu105Lys cyt P460 was conducted using primers synthesized by Integrated DNA technologies. Primers are listed in the 5'→ 3' direction. The forward and reverse primers are as follows, with the underlined nucleotides representing the mutation:

FWD: GAC GGT ACC ATT TTT GTT <u>AAG</u> GAG ATG GTG AGC GTT GG

REV: <u>CTT</u> AAC AAA AAT GGT ACC GTC ACG GAA TTT GCC

Bioinformatics

A database of 236 cyt P460 sequences was curated by HMMER[38] using the WT *N. europaea* cyt P460 (NCBI Accession Number WP_011110663) as a search query, using the phmmer algorithm. These data were downloaded and MegaX[39] was used to generate a multiple sequence alignment of all 236 cyt P460 sequences using

the ClustalW[40] program. This multiple sequence alignment was uploaded to WebLogo[41] to generate the sequence logo of the cyt P460 protein family.

The alignment of *N. europaea* cyt P460 (NCBI Accession Number WP_011110663) and *N.* sp. NpAV cyt P460 (NCBI Accession Number WP_052493891) was performed in T-coffee[42] using the ClustalW program to perform the alignment.

Growth, expression, and purification of WT N. *sp. NpAV and* N. *sp. NpAV Lys105Leu*

Growth of *N.* sp. NpAV and its mutant were expressed as previously described,[18] but in brief, BL21(DE3) cells pre-transformed with the cyt *c* maturase system were transformed with the DNA by heat shock and plated. A single colony was picked and grown in LB until a suitable optical density had been reached. This starter culture was used to inoculate 2L of TB treated with 0.5% glycerol and grown at 37°C in the shaker at 200 rpm until an OD_{600} of 0.6 – 1.0 was reached. The cells were induced with 1 mM IPTG and allowed to expressed for 8 hours. The cells were harvested at 8000xg for 10 minutes. Cells were either stored in the -80°C freezer until ready for lysis or lysed directly by resuspending in buffer containing 20 mM MOPS pH 8.0, 150 mM NaCl, and 0.01% Triton X and by passaging through a French Press at 15,000 psi for 3-5 passages. The lysate was clarified by centrifugation at 18,000xg for 45 minutes and the lysate was applied to a Ni-resin. This lysate was washed with buffer containing 20 mM MOPS pH 8.0, 20 mM imidazole, and 150 mM NaCl. The protein was eluted by treatment with a buffer containing 20 mM MOPS pH 8.0, 330 mM imidazole, and 150 mM NaCl.

Growth, expression, and purification of N. europaea *anaerobic WT cyt P460*

This process has gone through two phases. The bulk of the protein that has been used in the above chapter was generated the way described below. Regardless of the method used, it is important that once the protein has been produced and purified, it should not be exposed to oxygen.

WT *N. europaea* cyt P460 was transformed into BL21(DE3) cells that were pre-transformed with the cyt *c* maturation system by heat shock and plated. The next day in the morning, a single colony was picked and used to inoculate 5 mL of an LB starter culture. Meanwhile, four 1L Schott bottles were filled with 750 mL of TB. A magnetic stir bar was added to the bottles. These bottles were septum sealed and partially closed with a lid containing a hole such that the septum seal covers it. The media was sterilized by autoclaving for 25 minutes.

Once the Schott bottles were cool, ampicillin and chloramphenicol, and 0.5% glycerol were added to them under sterile conditions. Before sealing, Teflon tape was wrapped around the threads of the bottle and around the septum. The bottle was then sealed by screwing the cap on. The media inside the bottles was degassed on a Schlenk line using a 22G needle by pulling vacuum on the headspace for 15 minutes and sparging with N_2 for 15 minutes, repeating this process two to three times, ending on N_2. To bring the bottles into the glovebox, electrical tape was used to cover the top of the bottles such that the bottles cannot leak through the top of the septum seal when inside the reduced pressure of the glovebox antechamber.

Once the starter cultures were grown, the cells were transferred into the Eppendorf tubes and pelleted. The Eppendorf was brought inside the glovebox and was resuspended in the Schott bottles, the Schott bottles were sealed and then brought outside of the glovebox. The bottles were placed inside an incubator at 37°C at 50 rpm for 12 to 18 hours—until an OD_{600} of about 0.6 – 1.0 was reached. The cells were brought back inside the glovebox using the same method as described above, along with a stock of 1 M IPTG. Both the Schott bottles and the IPTG were allowed to equilibrate with the box atmosphere for 30 minutes to 1 hour before inducing the cells with 1 mM IPTG inside the glovebox. These Schott bottles were brought back outside of the glovebox and allowed to express for 24 hours at 30°C and 50 rpm.

Overnight, centrifuge bottles were pumped inside the glovebox to allow any oxygen bound to the plastic to be pulled off. The cells were brought back inside the glovebox and poured into the centrifuge bottles. The cells were sealed inside 1 L centrifuge bottles inside the glovebox and spun down in a JLA 8.1 rotor for 25

minutes, using an additional three bottles filled with water as a counterbalance to the bottles filled with cells. The spun down cells were rapidly pumped back inside the box, where the used media was poured back into the Schott bottles. The cells were either scooped into a Falcon tube and stored in a dewar filled with liquid nitrogen or lysed right away. To lyse the cells, the pellet was resuspended in 5-10 mL of a buffer containing 20 mM MOPS pH 8.0, 300 mM NaCl, 0.1% Triton X-100, and 2 mM EDTA. The resuspended cells were put into a Dounce homogenizer and subjected to approximately 80 plunges of the Dounce homogenizer. Then, this mixture was added to a Hungate tube and 20 mg lysozyme, 10 mg DNase, and 10mg RNase were dissolved in this mixture. The Hungate tube was sealed with a septum and crimped with an aluminum cap and brought outside of the box and incubated at 37°C in a water bath for 45 minutes, inverting it once every 15 minutes. The Hungate tube was brought back inside the box and the lysate was distributed across multiple Eppendorf centrifuge tubes and spun down inside an Eppendorf centrifuge inside the glovebox at 14,000 rpm for 30 minutes. The lysate was gently pipetted off the cell debris and put into a beaker. IMAC wash buffer consisting of 20 mM MOPS pH 8.0, 20 mM imidazole, and 150 mM NaCl was added to lysate to dilute the EDTA to not strip the Ni column. This mixture was then applied to a Ni column and red protein was seen accumulating at the top of the column. This was washed with the same wash buffer for at least 5 column volumes and eluted with a buffer containing 20 mM MOPS pH 8.0, 330 mM imidazole, and 150 mM NaCl.

The eluted protein was pooled together and washed with 50 mM MOPS pH 8.0 using spin columns inside the glovebox until ready for experimentation.

The second method, developed more recently, uses the same purification process described above. The key difference is that the cells were still grown aerobically using 6L Erlenmeyer flasks filled with 2L of TB. The cells were grown up to an OD_{600} of 0.6 – 1.0, pelleted, and scooped inside Falcon tubes. The Falcon tubes were brought inside the glovebox and allowed to equilibrate with the box atmosphere for 30 minutes to an hour. Then the cells were resuspended in the Schott bottles and expression and purification proceeded as described above.

Cross-linking AWT cyt P460

The proenzyme was quantified by measuring the absorbance at the Soret at 403 or 404 nm, using an extinction coefficient of 110 mM^{-1} cm^{-1} from the *N. europaea* Lys70Tyr variant.[43] This uses the assumption that the proenzyme of WT cyt P460 has a similar extinction coefficient to this variant. H_2O_2 was quantified using an extinction coefficient of 43.6 M^{-1} cm^{-1}. Alternatively, lithium peroxide was also used as a peroxide donor and was quantified by weight.

To an 800 μL anaerobic cuvette, 5 μM AWT cyt P460 in 50 mM MOPS pH 8.0 was added and septum sealed. This reaction had no stir bar. The thermocouple was set to 25°C and the cuvette was allowed to equilibrate for at least five minutes before the reaction. To this solution, an equimolar amount of peroxide was added to the reaction and the final volume of the solution was 350 μL. The reaction was monitored for the disappearance of the Soret band at 404 nm—allowing for the observation of an intermediate at 413 nm—and the in-growth of a Soret around 440-450 nm. The reaction was quenched by adding sodium dithionite, shifting the Soret maximum to 463 nm, indicative of a cross-linked cyt P460. This solution was then washed with 50 mM MOPS pH 8.0 to remove residual dithionite. The UV-vis spectrum was checked to ensure that the ferric, as-isolated UV-vis spectrum was restored and the protein was quantified relative to the Soret band at 440 using an extinction coefficient of 52 mM^{-1} cm^{-1}.

Activity Assay

NH_2OH was quantified using the method reported by Frear.[44] DCPIP was quantified using an extinction coefficient of 20.6 mM^{-1} cm^{-1} at 605 nm[45-46] and PMS was quantified using an extinction coefficient of 26.6 mM^{-1} cm^{-1} at 388 nm.[47] To an 800 μL anaerobic cuvette and in 50 mM MOPS pH 8.0, 50 μM DCPIP and 6 μM PMS were added. Stock protein solutions and the stock NH_2OH solutions were brought out of the box in a septum-sealed vial. The cuvette was placed in the UV-vis in a water-jacketed cuvette holder held at 25°C. The cuvette was allowed to equilibrate for 5

minutes. Monitoring the disappearance of DCPIP at 605 nm, 2 mM NH_2OH was spiked into the cuvette using a Hamilton syringe to establish background consumption for 1.5 to 2 minutes. Then 250 nM protein was added to mixture. Rates of consumption were determined by the method of initial rates, using the first 10% of oxidant consumption after the addition of protein. Background consumption was subtracted from this value. All data reported were the average of three trials.

Electron paramagnetic resonance

X-band EPR were collected between 10-12K. Protein concentrations were anywhere between 100-160 μM protein. Samples were frozen in liquid nitrogen and stored in a nitrogen filled dewar until ready for data collection.

Stopped-flow UV-vis spectroscopy

The syringes of a KinTek SF-2004 were made anaerobic by treatment with sodium dithionite for one hours before washing with buffer. The 22°C temperature was maintained with a water jacket. All protein solutions were kept inside a N_2-filled glovebox and brought out inside capped syringes for use in the stopped-flow. *m*-CPBA was diluted in acetonitrile as per Rittle and Green.[31] 20 μM AWT cyt P460 were mixed with 40 μM *m*-CPBA, making the final concentrations 10 μM and 20 μM, respectively. Data were collected for 5 minutes.

REFERENCES

1. A. Shelnutt, J.; Song, X.-Z.; Ma, J.-G.; Jia, S.-L.; Jentzen, W.; J. Medforth, C.; J. Medforth, C., Nonplanar porphyrins and their significance in proteins. *Chemical Society Reviews* **1998,** *27* (1), 31-42.

2. Evans, S. V.; Brayer, G. D., High-resolution study of the three-dimensional structure of horse heart metmyoglobin. (0022-2836 (Print)).

3. Perutz, M. F., Regulation of oxygen affinity of hemoglobin: influence of structure of the globin on the heme iron. (0066-4154 (Print)).

4. Perutz, M. F.; Wilkinson Aj Fau - Paoli, M.; Paoli M Fau - Dodson, G. G.; Dodson, G. G., The stereochemical mechanism of the cooperative effects in hemoglobin revisited. (1056-8700 (Print)).

5. Ferousi, C.; Schmitz, R. A.; Maalcke, W. J.; Lindhoud, S.; Versantvoort, W.; Jetten, M. S. M.; Reimann, J.; Kartal, B., Characterization of a nitrite-reducing octaheme hydroxylamine oxidoreductase that lacks the tyrosine cross-link. *Journal of Biological Chemistry* **2021,** *296*.

6. Kranz, R. G.; Richard-Fogal, C.; Taylor, J.-S.; Frawley, E. R., Cytochrome *c* Biogenesis: Mechanisms for Covalent Modifications and Trafficking of Heme and for Heme-Iron Redox Control. *Microbiology and Molecular Biology Reviews* **2009,** *73* (3), 510-528.

7. Lin, Y.-W., The broad diversity of heme-protein cross-links: An overview. *Biochimica et Biophysica Acta (BBA) - Proteins and Proteomics* **2015,** *1854* (8), 844-859.

8. Fiedler, T. J.; Davey Ca Fau - Fenna, R. E.; Fenna, R. E., X-ray crystal structure and characterization of halide-binding sites of human myeloperoxidase at 1.8 A resolution. (0021-9258 (Print)).

9. Metcalfe, C. L.; Ott, M.; Patel, N.; Singh, K.; Mistry, S. C.; Goff, H. M.; Raven, E. L., Autocatalytic Formation of Green Heme: Evidence for H2O2-Dependent Formation of a Covalent Methionine−Heme Linkage in Ascorbate Peroxidase. *Journal of the American Chemical Society* **2004,** *126* (49), 16242-16248.

10. Hoch, U.; Ortiz de Montellano, P. R., Covalently Linked Heme in Cytochrome P4504A Fatty Acid Hydroxylases *. *Journal of Biological Chemistry* **2001,** *276* (14), 11339-11346.

11. Yan, D.-J.; Li, W.; Xiang, Y.; Wen, G.-B.; Lin, Y.-W.; Tan, X., A Novel Tyrosine–Heme C-O Covalent Linkage in F43Y Myoglobin: A New Post-translational Modification of Heme Proteins. *ChemBioChem* **2015,** *16* (1), 47-50.

12. Bergmann, D. J.; Hooper, A. B., Cytochrome P460 of Nitrosomonas europaea. Formation of the heme-lysine cross-link in a heterologous host and mutagenic conversion to a non-cross-linked cytochrome c'. *European Journal of Biochemistry* **2003,** *270* (9), 1935-1941.

13. Pearson, A. R.; Elmore, B. O.; Yang, C.; Ferrara, J. D.; Hooper, A. B.; Wilmot, C. M., The Crystal Structure of Cytochrome P460 of Nitrosomonas europaea Reveals a Novel Cytochrome Fold and Heme−Protein Cross-link. *Biochemistry* **2007,** *46* (28), 8340-8349.

14. Vilbert, A. C.; Caranto, J. D.; Lancaster, Kyle M., Influences of the heme-lysine crosslink in cytochrome P460 over redox catalysis and nitric oxide sensitivity. *Chemical Science* **2018,** *9* (2), 368-379.

15. Coleman, R. E.; Vilbert, A. C.; Lancaster, K. M., The Heme–Lys Cross-Link in Cytochrome P460 Promotes Catalysis by Enforcing Secondary Coordination Sphere Architecture. *Biochemistry* **2020,** *59* (24), 2289-2298.

16. Kruglik, S. G.; Lambry, J.-C.; Cianetti, S.; Martin, J.-L.; Eady, R. R.; Andrew, C. R.; Negrerie, M., Molecular Basis for Nitric Oxide Dynamics and Affinity with *Alcaligenes xylosoxidans* Cytochrome *c*. *Journal of Biological Chemistry* **2007,** *282* (7), 5053-5062.

17. Liew, F. N.; Brandys, M. A.; Biswas, S.; Nguyen, J. N.; Rahmawati, M.; Nevala, M.; Elmore, B. O.; Hendrich, M. P.; Kim, H. J., Cytochrome c′β-Met Is a Variant in the P460 Superfamily Lacking the Heme–Lysyl Cross-Link: A Peroxidase Mimic Generating a Ferryl Intermediate. *Biochemistry* **2020,** *59* (5), 704-716.

18. Caranto, J. D.; Vilbert, A. C.; Lancaster, K. M., *Nitrosomonas europaea* cytochrome P460 is a direct link between nitrification and nitrous oxide emission. *Proceedings of the National Academy of Sciences* **2016,** *113* (51), 14704-14709.
19. von Wulffen, J.; RecogNice, T.; Sawodny, O.; Feuer, R., Transition of an Anaerobic Escherichia coli Culture to Aerobiosis: Balancing mRNA and Protein Levels in a Demand-Directed Dynamic Flux Balance Analysis. *PLoS One* **2016,** *11* (7), e0158711-e0158711.
20. Kim, H.-E.; Nguyen, T. T. M.; Lee, H.; Lee, C., Enhanced Inactivation of Escherichia coli and MS2 Coliphage by Cupric Ion in the Presence of Hydroxylamine: Dual Microbicidal Effects. *Environmental Science & Technology* **2015,** *49* (24), 14416-14423.
21. Gross, P.; Smith, R. P., Biologic Activity of Hydroxylamine: A Review. *CRC Critical Reviews in Toxicology* **1985,** *14* (1), 87-99.
22. Song, W.; Li, J.; Liu, J.; Shen, W., Production of hydrogen peroxide by the reaction of hydroxylamine and molecular oxygen over activated carbons. *Catalysis Communications* **2008,** *9* (5), 831-836.
23. Chain, P.; Lamerdin, J.; Larimer, F.; Regala, W.; Lao, V.; Land, M.; Hauser, L.; Hooper, A.; Klotz, M.; Norton, J.; Sayavedra-Soto, L.; Arciero, D.; Hommes, N.; Whittaker, M.; Arp, D., Complete genome sequence of the ammonia-oxidizing bacterium and obligate chemolithoautotroph Nitrosomonas europaea. *J Bacteriol* **2003,** *185* (9), 2759-2773.
24. Maines, M. D., Heme oxygenase: function, multiplicity, regulatory mechanisms, and clinical applications. *The FASEB Journal* **1988,** *2* (10), 2557-2568.
25. Matsui, T.; Unno, M.; Ikeda-Saito, M., Heme Oxygenase Reveals Its Strategy for Catalyzing Three Successive Oxygenation Reactions. *Accounts of Chemical Research* **2010,** *43* (2), 240-247.
26. Meunier, B.; de Visser, S. P.; Shaik, S., Mechanism of Oxidation Reactions Catalyzed by Cytochrome P450 Enzymes. *Chemical Reviews* **2004,** *104* (9), 3947-3980.

27. Wilks, A.; Ortiz de Montellano, P. R., Rat liver heme oxygenase. High level expression of a truncated soluble form and nature of the meso-hydroxylating species. *Journal of Biological Chemistry* **1993,** *268* (30), 22357-22362.
28. Ishikawa, K.; Takeuchi N Fau - Takahashi, S.; Takahashi S Fau - Matera, K. M.; Matera Km Fau - Sato, M.; Sato M Fau - Shibahara, S.; Shibahara S Fau - Rousseau, D. L.; Rousseau Dl Fau - Ikeda-Saito, M.; Ikeda-Saito M Fau - Yoshida, T.; Yoshida, T., Heme oxygenase-2. Properties of the heme complex of the purified tryptic fragment of recombinant human heme oxygenase-2. *Journal of Biological Chemistry* **1995**
270 (11), 6345-6450.
29. Davydov, R.; Fleischhacker, A. S.; Bagai, I.; Hoffman, B. M.; Ragsdale, S. W., Comparison of the Mechanisms of Heme Hydroxylation by Heme Oxygenases-1 and -2: Kinetic and Cryoreduction Studies. *Biochemistry* **2016,** *55* (1), 62-68.
30. Matsui, T.; Kim, S. H.; Jin, H.; Hoffman, B. M.; Ikeda-Saito, M., Compound I of Heme Oxygenase Cannot Hydroxylate Its Heme meso-Carbon. *Journal of the American Chemical Society* **2006,** *128* (4), 1090-1091.
31. Rittle, J.; Green, M. T., Cytochrome P450 Compound I: Capture, Characterization, and C-H Bond Activation Kinetics. *Science* **2010,** *330* (6006), 933-937.
32. Wilks, A.; Torpey J Fau - Ortiz de Montellano, P. R.; Ortiz de Montellano, P. R., Heme oxygenase (HO-1). Evidence for electrophilic oxygen addition to the porphyrin ring in the formation of alpha-meso-hydroxyheme. (0021-9258 (Print)).
33. Davydov, R.; Kofman, V.; Fujii, H.; Yoshida, T.; Ikeda-Saito, M.; Hoffman, B. M., Catalytic Mechanism of Heme Oxygenase through EPR and ENDOR of Cryoreduced Oxy-Heme Oxygenase and Its Asp 140 Mutants. *Journal of the American Chemical Society* **2002,** *124* (8), 1798-1808.
34. Matsui, T.; Furukawa, M.; Unno, M.; Tomita, T.; Ikeda-Saito, M., Roles of Distal Asp in Heme Oxygenase from Corynebacterium diphtheriae, HmuO: A WATER-DRIVEN OXYGEN ACTIVATION MECHANISM*. *Journal of Biological Chemistry* **2005,** *280* (4), 2981-2989.

35. Cedervall, P. E.; Hooper, A. B.; Wilmot, C. M., Crystallization and preliminary X-ray crystallographic analysis of a new crystal form of hydroxylamine oxidoreductase from Nitrosomonas europaea. *Acta crystallographica. Section F, Structural biology and crystallization communications* **2009,** *65* (Pt 12), 1296-1298.
36. Zhu, X.; Burger, M.; Doane, T. A.; Horwath, W. R., Ammonia oxidation pathways and nitrifier denitrification are significant sources of N_2O and NO under low oxygen availability. *Proceedings of the National Academy of Sciences* **2013,** *110*, 6328-6333.
37. Elmore, B. O.; Bergmann, D. J.; Klotz, M. G.; Hooper, A. B., Cytochromes P460 and c′-beta; A new family of high-spin cytochromes c. *FEBS Letters* **2007,** *581* (5), 911-916.
38. Finn, R. D.; Clements, J.; Eddy, S. R., HMMER web server: interactive sequence similarity searching. *Nucleic Acids Research* **2011,** *39* (suppl_2), W29-W37.
39. Kumar, S.; Stecher, G.; Li, M.; Knyaz, C.; Tamura, K., MEGA X: Molecular Evolutionary Genetics Analysis across Computing Platforms. (1537-1719 (Electronic)).
40. Thompson, J. D.; Higgins, D. G.; Gibson, T. J., CLUSTAL W: improving the sensitivity of progressive multiple sequence alignment through sequence weighting, position-specific gap penalties and weight matrix choice. *Nucleic acids research* **1994,** *22* (22), 4673-4680.
41. Crooks, G. E.; Hon G Fau - Chandonia, J.-M.; Chandonia Jm Fau - Brenner, S. E.; Brenner, S. E., WebLogo: a sequence logo generator. (1088-9051 (Print)).
42. Notredame, C.; Higgins Dg Fau - Heringa, J.; Heringa, J., T-Coffee: A novel method for fast and accurate multiple sequence alignment. (0022-2836 (Print)).
43. Coleman, R. E.; Lancaster, K. M., Heme P460: A (Cross) Link to Nitric Oxide. *Accounts of Chemical Research* **2020,** *53* (12), 2925-2935.
44. Frear, D. S.; Burrell, R. C., Spectrophotometric Method for Determining Hydroxylamine Reductase Activity in Higher Plants. *Analytical Chemistry* **1955,** *27* (10), 1664-1665.

45. McD. Armstrong, J., The molar extinction coefficient of 2,6-dichlorophenol indophenol. *Biochimica et Biophysica Acta (BBA) - General Subjects* **1964,** *86* (1), 194-197.

46. Jahn, B.; Jonasson, N. S. W.; Hu, H.; Singer, H.; Pol, A.; Good, N. M.; den Camp, H. J. M. O.; Martinez-Gomez, N. C.; Daumann, L. J., Understanding the chemistry of the artificial electron acceptors PES, PMS, DCPIP and Wurster's Blue in methanol dehydrogenase assays. *JBIC Journal of Biological Inorganic Chemistry* **2020,** *25* (2), 199-212.

47. Halaka, F. G.; Babcock, G. T.; Dye, J. L., Properties of 5-methylphenazinium methyl sulfate. Reaction of the oxidized form with NADH and of the reduced form with oxygen. *Journal of Biological Chemistry* **1982,** *257* (3), 1458-1461.

CHAPTER 4
SECOND SPHERE EFFECTS ON CROSS-LINK FORMATION

Introduction

A defining feature of P460 cofactors are their non-canonical cross-links. In HAO, the cross-linker is a Tyr residue[1-2] but in cyt P460, the cross-linking residue is a Lys.[3] The cross-link is important for the catalytic function of both proteins. In HAO, the cross-link is essential for oxidative catalysis and in its absence, the protein instead catalyzes reductive chemistry.[4] In contrast, cyt P460's cross-link does not seem relevant for promoting oxidative chemistry and is instead necessary for positioning the heme P460 cofactor close enough to a second sphere Glu residue,[5] which is absolutely necessary to oxidize NH_2OH.[6] The cofactor is so named because the absorbance of the reduced cofactor is near 460 nm.[7] Additionally, the oxidized form of the protein also has a different UV-vis absorbance which is a direct result of how the cross-link interacts with the porphyrin a_{2u} and e_g orbitals.[8]

Previously cyt P460's cross-link was reported to form in an autocatalytic manner,[9] but was not investigated further. Chapter Three established that anaerobically expressed cyt P460 results in a protein that lacks the heme-Lys cross-link and is inactive. When the protein is treated with H_2O_2, the cross-link is restored to the protein and it regains its ability to oxidize NH_2OH. Chapter Three also demonstrated that cyt P460's ability to form its cross-link is intrinsic to the protein fold. *N.* sp. NpAV cyt P460 natively contains a Leu residue in the cross-link position, but mutation of the Leu to a Lys results in a protein that contains the cross-link and is spectroscopically consistent with the WT *N. europaea* cyt P460. This led us to question what specifically about the cyt P460 fold makes this post-translational modification possible, because understanding why the cross-link forms could be interesting for those who are interested in imbuing unique reactivity into hemoproteins. For example, the cross-link has been shown to prevent the NO-dependent loss of the axial His residue.[10] Alternatively, it could also position a heme towards specific residues which could alter reactivity.

An initial hypothesis for why the cyt P460 fold allows the cross-link to form was that the cofactor remains ruffled even in the absence of the cross-link.[5] In a study of MhuD, a noncanonical HO from *Mycobacterium tuberculosis* that degrades heme into nonheme iron and mycobilin,[11] Graves and coworkers[12] showed that increased ruffling increased both the spin-density and the electrophilicity on the heme meso carbons. If this trend holds for the P460 cofactor, this could help ensure that the putative Fe^{III}–OOH adduct proposed in the last chapter hydroxylates the *meso* carbon in a regiospecific manner. Looking at the *meso* carbon that participates in the cross-link, it becomes apparent that the most prominently distorted *meso* carbon is the γ *meso* carbon (**Figure 2.10**), which is influenced by two key amino acids in the active site pocket: A distal Arg44 and a proximal Tyr154, based off the numbering of the *N. europaea* cyt P460 (**Figure 4.1**). Based on a multiple sequence alignment, other prominent residues in the distal pocket are His, Asp, and Asn (**Figure 3.13**), which are all residues capable of hydrogen-bonding interactions with the heme. An alternative hypothesis proposed in the last chapter takes inspiration from canonical HO proteins. In HO, a distal Asp residue is involved in hydrogen bonding interactions with water molecules in the active site, which could assist in stabilizing the Fe^{III}-OOH adduct, provide protons, or stabilize a transient hydroxyl radical that then reacts with the heme *meso* carbon.[13] This chapter addresses the effects of the distal and proximal residues in the active site pocket and how they affect cross-link formation.

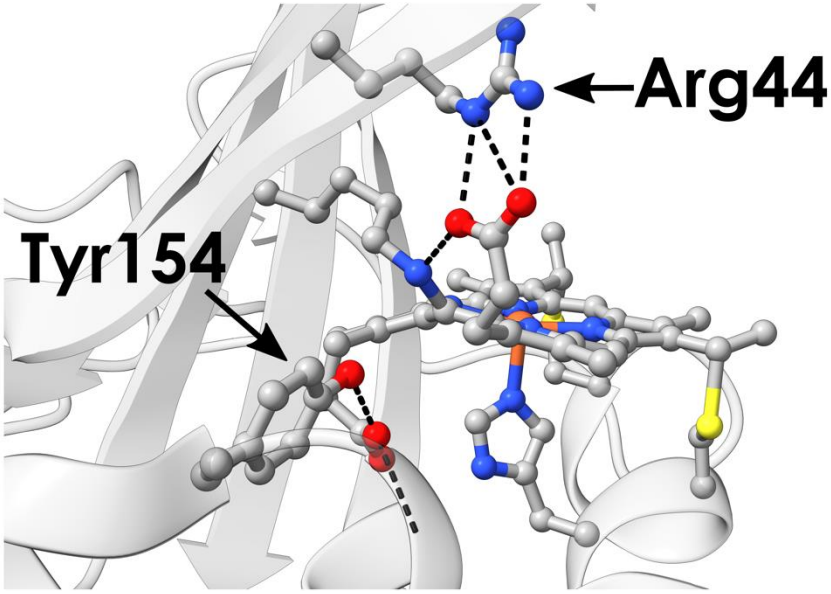

Figure 4.1. Crystal structure of *N. europaea* cyt P460 (PDB ID 2JE3) with the distal arginine and the proximal tyrosine residue shown. Hydrogen bonds are depicted as black, dashed lines.

Removal of the distal and proximal residues affects cross-link formation

Ala mutants of the distal Arg, the proximal Tyr, and the double mutation resulted in proteins that were spectroscopically identical to CLD cyt P460 species. The Soret maxima for the three variants are 402 nm, 403 nm, and 404 nm for Arg44Ala, Tyr154Ala, and Arg44Ala/Tyr154Ala, respectively (**Figure 4.2**). However, in the Tyr154Ala variant, there is also a shoulder at 443 nm, which typically corresponds to the as-isolated, WT protein of cyt P460. When these variant are reduced with sodium dithionite, both Arg44Ala and Arg44Ala/Tyr154Ala produce spectra that are consistent with the reduced spectra of CLD cyt P460 species; however, Tyr154Ala shows features that are consistent with CLD cyt P460 and the canonical, cross-link containing cyt P460 (**Figure 4.3**), confirming that Tyr154Ala variant is partially cross-linked by the time it is purified. Immediately, this strongly implies that the distal Arg residue is essential for cross-link formation. Why Tyr154Ala is isolated as a partially cross-linked protein is curious. It could imply that the proximal Tyr residue is

involved in stabilizing the heme to allow for cross-link formation, but perhaps is not directly involved in the mechanism. Looking at a multiple sequence alignment of the proximal residue, the Tyr observed in *N. europaea* is also highly conserved, with the next most common residue being an Arg, which could potentially be capable of H-bonding interactions if oriented correctly relative to the second heme propionate. It is possible the Tyr residue could also house a radical at some point during cross-link formation, but that would most likely necessitate a Compound I mechanism, which we have thus far not seen evidence of, but should be tested more thoroughly than it has been as of writing. Regardless, the high degree of conservation of this proximal Tyr residue implies that it is very important for something in cyt P460.

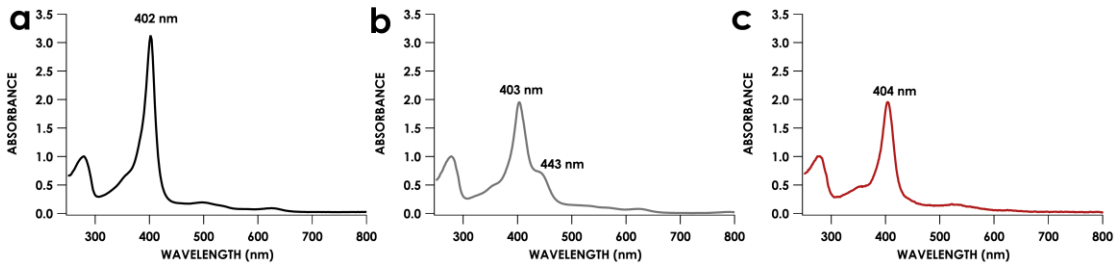

Figure 4.2. UV-vis comparison of the as-isolated, ferric spectra of (a) Arg44Ala, (b) Tyr154Ala, and (c) Arg44Ala/Tyr154Ala. All absorbances are normalized to the absorbance at 280 nm. The Soret maxima are noted on each of the figures.

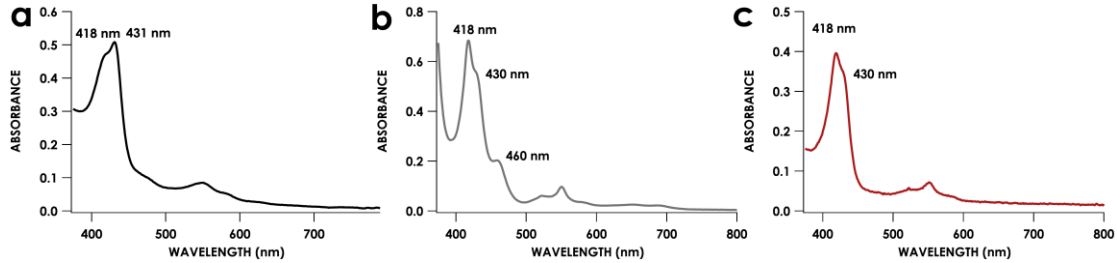

Figure 4.3. UV-vis comparison of the sodium dithionite-reduced spectra of (a) Arg44Ala, (b) Tyr154Ala, and (c) Arg44Ala/Tyr154Ala. Absorbances are not normalized to anything and the Soret features are noted on the figure.

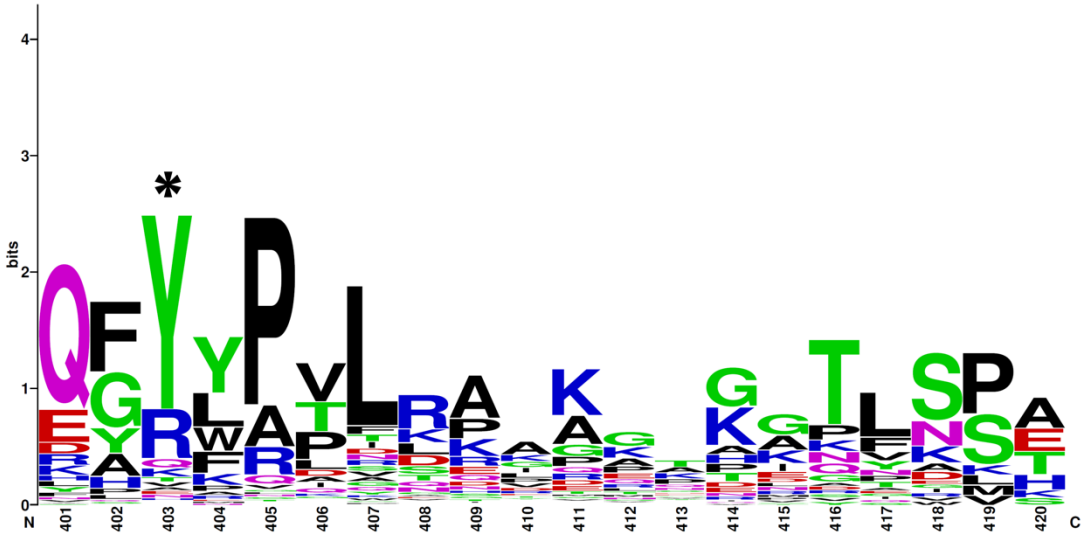

Figure 4.4. Sequence logo of cyt P460, showing a fragment with 20 amino acid residues. The position with the * denotes the proximal pocket. The logo is based off a database of 236 entries curated by HMMER after using the *N. europaea* cyt P460 gene (NCBI Accession Number WP_011110663) as the query. The multiple sequence alignment was performed in MegaX using ClustalW.

The protein is incapable of forming the cross-link in the absence of the distal and proximal residues

Activity assays need to be done with all three of mutants generated, but an activity assay was performed for the Tyr154Ala variant. In a cuvette containing 50 μM DCPIP and 6 μM PMS at 25°C and with stirring, 10 mM NH_2OH was added to establish background consumption of the oxidant, which was 4.8 ± 0.4 μM DCPIP • min^{-1}. After collecting the background for 1.5-2.0 minutes, 500 nM protein was added to the mixture, where the rate of DCPIP consumption was 5.6 ± 0.3 μM DCPIP • min^{-1} (**Figure 4.5**), and when the background consumption was subtracted and the amount of protein was taken into account, it resulted in an activity of 1.5 ± 0.2 μM DCPIP • μM protein • min^{-1}, which barely exceeds background and could likely be attributed to the minor presence of some cross-link cyt P460 character in the enzyme. Arg44Ala and Arg44Ala/Tyr154Ala are expected to be inert because lacking the cross-link

should mean they are not close enough to the second-sphere Glu residue. Further studies are required.

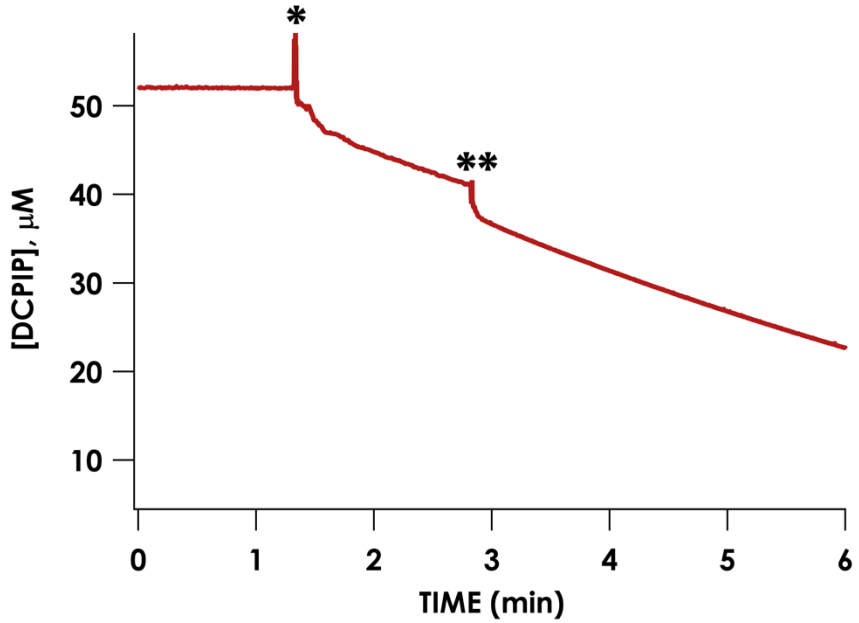

Figure 4.5. Representative example of a single-wavelength trace of the consumption of DCPIP, where the absorbance at 605 nm was converted to [DCPIP] using the extinction coefficient of 20.6 $mM^{-1}•cm^{-1}$. The cuvette initially contained 50 μM DCPIP and 6 μM PMS and at 25°C. The * corresponds to injection of 10 mM NH_2OH and the ** corresponds to injection of 500 nM Tyr154Ala.

Knowing that one of the variants is inactive and the remaining two are most likely inactive, it was worth testing if the cross-link of cyt P460 could be formed, especially in Tyr154Ala since that has some cross-link character. In an experiment similar to the one shown in **Figure 3.6**, approximately 5 μM Tyr154Ala was treated with 50 mM NH_2OH and O_2 gas was bubbled gently through the headspace. Unlike with AWT cyt, this protein exhibited a very slow decay of the heme center and no evidence of cross-link formation (**Figure 4.6**). Additionally, the absorbance at 280 nm increases, which suggests protein denaturation. This plausibly explains why the cross-link is unable to form since we know its formation is highly dependent on the protein scaffold.

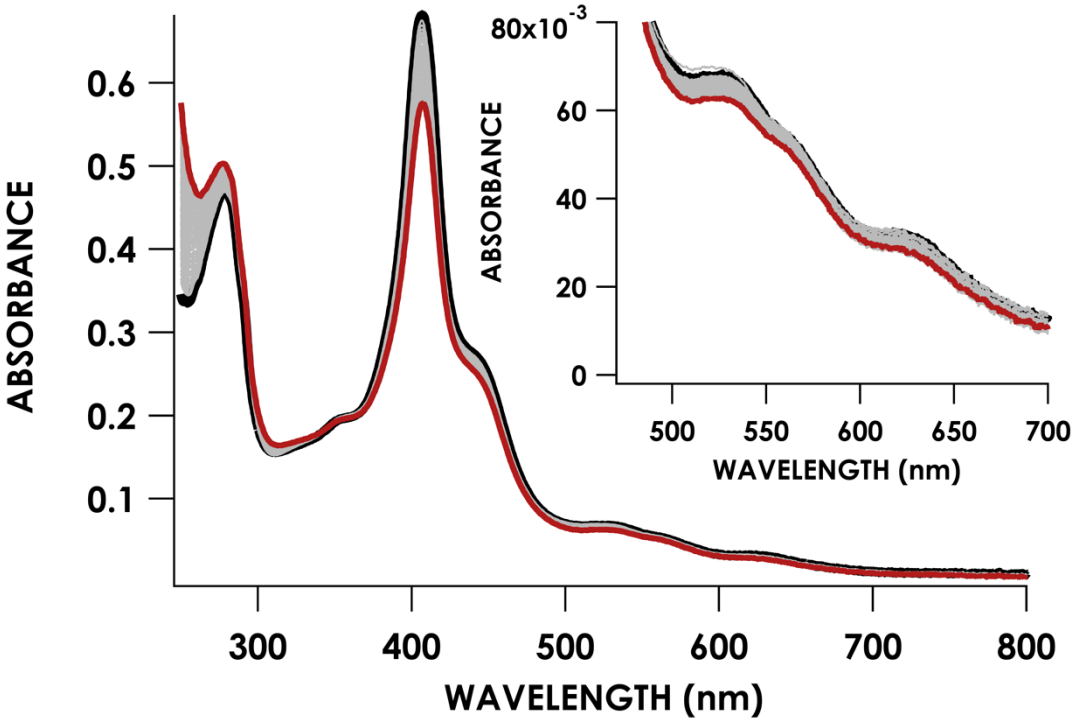

Figure 4.6. Approximately 5 μM *N. europaea* Tyr154Ala cyt P460 treated with 50 mM NH_2OH. The headspace was bubbled gently with O_2 for five minutes before removing the needle and letting collection for 40 minutes. Scans were collected 30 s. The initial scan is shown in black, intermediate scans shown in gray, and the final scan is shown in red.

Later, after we started using H_2O_2 to shunt to the putative Fe^{III}–OOH adduct, we tried a second experiment with 10 μM Arg44Ala where it was treated with 10 μM H_2O_2 and observed immediate degradation of the heme center (**Figure 4.7**). As was discussed in Chapter Three, this could be indicative of the fact that Arg44 plays a role similar to Asp140 in HO[13-14] in stabilizing the putative Fe^{III}-OOH adduct, whether through direct stabilization of the bound peroxide, a hydroxyl radical, or through a network of water molecules that stabilize either of the two species.[13] We hypothesize that Arg44 might play a role in determining if the Fe–OOH adduct or Compound I is formed: In the WT pro-enzyme, the distal Arg residue is present and able to stabilize the adduct, but in its absence, Compound I can form, which leads to heme bleaching. This is similar to what is seen with peroxidases, which are enzymes that break up

H_2O_2. However, peroxidases are inactivated by their substrate at high concentrations of H_2O_2. The degradation mechanism invokes Compound II reacting with excess H_2O_2 to form a porphyrinate Fe^{III}-peroxy radical known as Compound III, [15] which leads to enzyme bleaching,[16] which is what is observed in **Figure 4.7**.

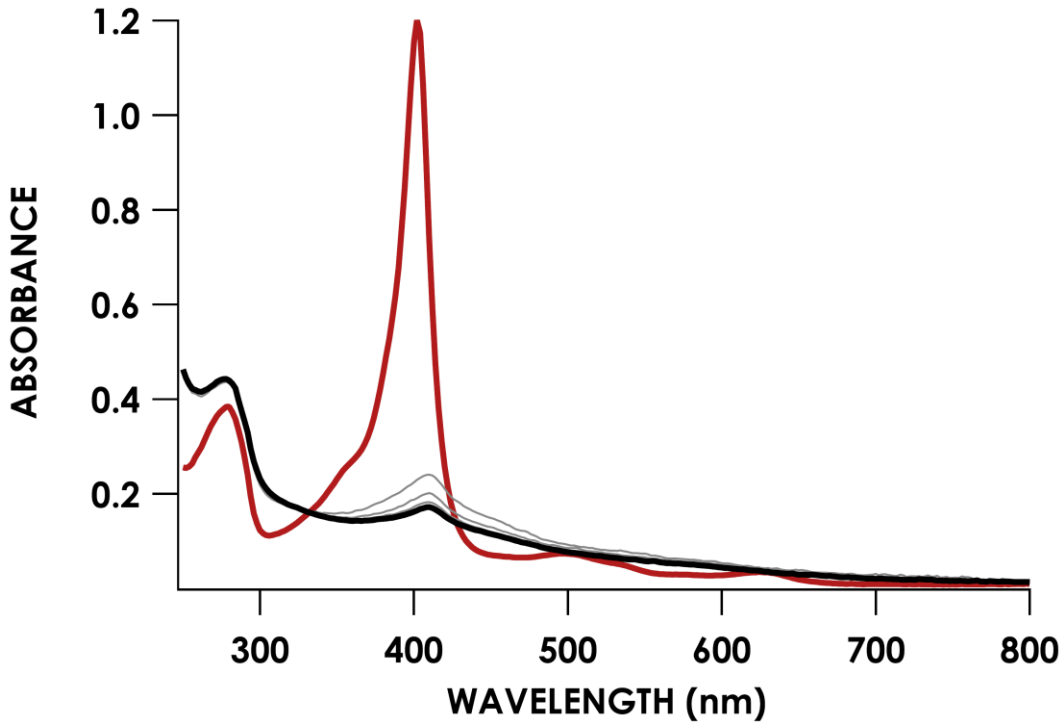

Figure 4.7. UV-vis spectrum of 10 μM Arg44Ala treated with 10 μM H_2O_2 at 25°C. The red spectrum is the initial time point and the black spectrum is the final. Scans were every thirty seconds.

This experiment has yet to be performed with the Arg44Ala/Tyr154Ala variant, but one would expect it to behave similarly to what is observed in Arg44Ala mutant of the protein.

To assess if heme ruffling was involved in cross-link formation, we treated both the Arg44Ala and Tyr154Ala variant with NO. Ruffled heme centers resist reductive nitrosylation and do not form an $\{FeNO\}^7$ through that mechanism.[17] This is because the d_{xy} orbital is destabilized because of the ruffling deformation. This prevents the NO radical from reducing the Fe center, stabilizing the Fe^{III}–NO adduct.[18] Initially we[5] speculated that the protein forms the cross-link because of heme-ruffling

and with the knowledge that the ruffling distortion in MhuD causes an increase in spin-density and electrophilicity on the heme *meso* carbon.[12] In doing this experiment, Arg44Ala showed no UV-vis features that were consistent with a $\{FeNO\}^6$ species of the protein and the Q bands were more consistent with that of a $\{FeNO\}^7$ (**Figure 4.8a**).[19] Interpretation of the Tyr154Ala result is a bit more complex because this protein has a mixture of cross-link containing and CLD character, but essentially, both the cross-link containing and the CLD components of the protein also showed no UV-vis features that were consistent with an $\{FeNO\}^6$ species and the protein underwent the known 6c-to-5c conversion (**Figure 4.8b**).[10] In fact, immediately after addition of NO to this sample, the Q bands show two features at 623 and 662 nm. We know that 662 nm corresponds to a transient Fe^{II} species that was previously observed in the stopped flow for the $\{FeNO\}^6$ of WT P460 treated with NH_2OH.[20] The species at 623 nm is likely the Fe^{II} variant of the CLD form, and is similar to one of the Q bands Fe^{II} observed the *N.* sp. AL212 Lys106Leu/Ala131Glu was electrochemically reduced.[5] This result strongly suggests that both the distal Arg and the proximal Tyr are directly involved in heme-ruffling in cyt P460 and could provide an explanation for why the cross-link is unable to form in this proteins in the correlation with ruffling and electrophilicity of the heme *meso* carbon observed in MhuD[12] is true in cyt P460. Why minor cross-link containing character is observed in the Tyr variant forms is curious. In the crystal structure Lys106Leu/Ala131Glu, one subunit was substantially more ruffled than the other and it was proposed that the cross-link serves the purpose of stabilizing the ruffled deformation.[5] Perhaps inside the cell or when the protein is folding, a subset of the population is sufficiently ruffled to allow for the Lys cross-link to form. Regardless, these experiments should be repeated and ideally, crystal structures of the *N. europaea* variants of these proteins would be grown. Additionally, reduction potentials of both of these variants should be obtained, because there is a correlation with heme ruffling and reduction potential.[21]

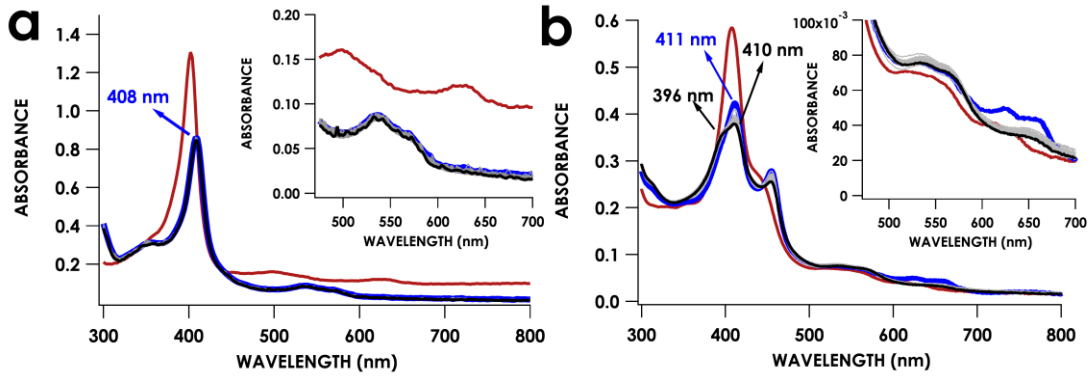

Figure 4.8. UV-vis spectra of 10 μM Arg44Ala (a) and 5 μM Tyr154Ala (b) treated with 100 uM NO from PROLINONOate. The red trace is the initial spectrum, the blue trace shows the injection of NO, and the black trace is the final spectrum. Scans were every thirty seconds. A transient Fe^{II} species can be observed in the inset of the Tyr154Ala variant right after addition of NO.

We were successful in purifying and crystallizing the *N.* sp. AL212 Ala131Glu/Tyr186Ala variant of cyt P460. Curiously, this protein was isolated as a green protein and featured UV-vis features consistent with a cross-link containing cyt P460 lacking CLD character. The crystal structure of the protein confirmed that this protein has an intact cross-link compared to its equivalent mutant in *N. europaea*. The heme propionate that points toward the proximal pocket is still oriented downwards and seems to be hydrogen bonding with the amide backbone of the Phe residue adjacent to the Tyr residue (**Figure 4.9**), which has also been seen in *N. europaea* crystal structures. This provides further support for the notion previously suggested that the Tyr residue is not be directly involved in cross-link formation. There are likely many other differences between cyt P460 across species that we are presently unaware of. It would be interesting to see if mutation of the axial His residue—His80 in *N.* sp. AL212—to an Ala would also result in CLD cyt P460 as with the Arg44Ala mutant. Future work should be done to address this question.

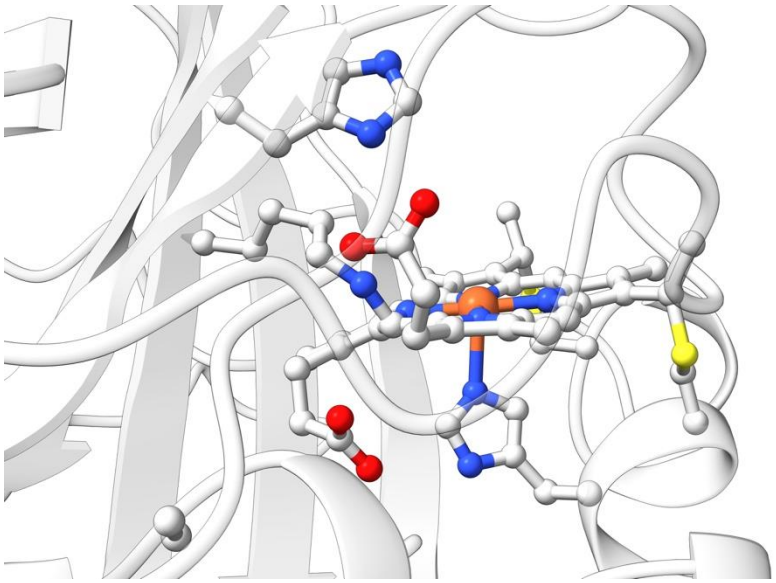

Figure 4.9. Crystal structure of *N.* sp. AL212 Ala131Glu/Tyr186Ala cyt P460. This protein, unlike its equivalent mutation in *N. europaea* resulted in a protein that was cross-link containing, suggesting yet unknown differences between *N. europaea* and *N.* sp. AL212 cyt P460.

Table 4.1 Crystallographic parameters of *N.* sp. AL212 Ala131Glu/Tyr186Ala cyt P460.

Wavelength (Å)	0.979
Temperature (K)	100
Space Group	P 2_1 2_1 2_1
a (Å)	45.422
b (Å)	75.004
c (Å)	109.885
α (deg)	90
β (deg)	90
γ (deg)	90
No. of reflections	150543 (3764)
No. of reflections in the R_{work} set	13858 (841)
No. of reflections in the R_{free} set	1386 (84)
Resolution (Å)	61.95 - 2.425 (2.511 - 2.425)
R_{merge} (%)	0.18 (0.7367)
$CC_{1/2}$	0.983 (0.659)
Completeness (%)	93.43 (57.76)
Redundancy	10.8 (4.4)
***I*/σ(*I*)**	12.06 (1.60)
R_{work}	0.2319 (0.4688)
R_{free}	0.2615 (0.5368)
Root-mean-square deviation from ideality	
Bonds (Å)	0.007
Angles (deg)	1.11
Average *B* factor (Å^2)	45.74
Ramachandran plot (%)	
Favored Regions	93.95
Allowed regions	4.78
Disallowed regions	1.27
PDBID	Unpublished

Conclusion

Second sphere interactions are indispensably to imbuding metalloenzymes with their functions.[22] In the case of cyt P460, we know that the second sphere Glu

residue is essential for NH_2OH oxidase capability[6] and that it is positioned towards this residue by support from the heme-Lys cross-link.[5] This cross-link is, as of writing, entirely unobserved anywhere else in nature.[23] Chapter Three addressed potential mechanisms of formation and this chapter addressed second-sphere effects of the protein, and this chapter addressed how the secondary coordination sphere affects cross-link formation. Mutants that remove a distal Arg and a proximal Tyr in the active site pocket of *N. europaea* cyt P460 show characteristics that are consistent with a CLD cyt P460. The current hypothesis is that Arg44 prevents formation of Compound I and favors formation of the Fe^{III}-OOH adduct, which reacts with the heme *meso* carbon to form the cross-link. The Arg44Ala mutant of cyt P460 bleached when exposed to H_2O_2. In contrast, the Tyr154Ala variant did not rapidly degrade when exposed to cross-link formation conditions and did not form the cross-link. However, the equivalent mutation in *N.* sp. AL212 cyt P460 was isolated in a fully cross-linked form, which is inconsistent with what has been observed in *N. europaea*. Both proteins were grown under the same conditions, but perhaps growing *N. europaea* Tyr154Ala cyt P460 slower might allow it to cross-link inside the cell. This could suggest in *N. europaea* cross-link formation is under kinetic control.

Additionally, both the distal and proximal residues of *N. europaea* cyt P460 rapidly undergo reductive nitrosylation when the Fe^{III} form is exposed to NO, which suggests that the heme site is not ruffled. This could further support the notion that cross-link formation is dependent on heme-ruffling because it increases the electrophilicity of the heme *meso* carbon.[12] A more complete analysis of these hypothesis should be done in the future.

Experimental

General Considerations

18.2 MΩ water was used to prepare all buffers and reagents. Protein samples were stored in 50 mM MOPS pH 8.0 unless otherwise noted. Protein was stored aerobically at 4°C in a cold room or anaerobically at room-temperature in an Mbraun N_2 filled glovebox. Anaerobic buffer solutions were degassed using a Schlenk line

using a 22G needle. Vacuum was pulled on the headspace for 15 minutes, followed by sparging with N_2 for 15 minutes using another 22G needle as a bleed. This cycle was repeated 2 additional times, ending on N_2 and brought inside the glovebox. Anaerobic protein solutions were brought into the glovebox and the cap was popped and allowed to equilibrate with the atmosphere overnight or buffer exchanged in air-free buffer using spin columns. A Cary 60 UV-vis spectrometer (Agilent) equipped with a water jacket was used to maintain temperature in all reactions. Data were fit in Igor Pro version 6.37 (WaveMetrics). NO was generated from disodium 1-(hydroxyl-NNO-azoxy)-L-proline (PROLI-NONOate) from Caymen Chemicals. NO delivered to an Fe center was quantified as described by Caranto *et al.*[24] NH_2OH was quantified using the method described by Frear *et al.*[25]

Plasmids and mutagenesis

The Arg44Ala mutant was generated using Q5 DNA Polymerase (NEB) per the kit instructions. Additionally, primers were designed using NEB's primer designer. Primers are as follows, with the lowercase letter denoting the mutation.
FWD: 5' TACCGAAATTgctACGGTTTATGTCGACC 3'
REV: 5'CTTACTACCATTTCGAGGCAA3'

The Tyr154Ala mutant was generated using Pfu Polymerase (Promega). Primers are as follows, with the lowercase letters denoting the mutation.:
FWD: 5'ACG CAA TTC gct CCG GTT CTG C 3'
REV: 5'agc GAA TTG CGT AAA CAC CAT GTC 3'

Protein Overexpression and Purification

Protein expression and purification occurred as previously described,[5, 8, 10, 26] but in specific differences and observations will be noted here:

Arg44Ala: Grown and purified as per the standard protocol.[26] Yield was not great, subsequent purifications should be tried with a 24 hour, 20°C induction.

Tyr154Ala: Cells were grown to an OD_{600} of 0.6 to 1.0 and induced for 24 hours at 20 °C. Cell lysis proceeded by French Press at 15,000 psi with three passes through the French press. After centrifugation—which proceeded as normal—the soluble fraction was a more brownish red color than observed with previously generated CLD variants.[5, 10] This was applied to Ni-resin and as the protein was accumulating on the column, it was a reddish color, but as the wash buffer was applied, it changed color to a more brownish color. Eluted protein was eluted per the standard protocol[26] and purified to homogeneity using a size-exclusion column per the standard protocol.[26]

Arg44Ala/Tyr154Ala: Grown and purified per the standard protocol.[26] Yield was not great, subsequent purifications should be tried with a 24 hour, 20°C induction.

Bioinformatics

A database of 236 cyt P460 sequences was curated by HMMER[27] using the WT *N. europaea* cyt P460 (NCBI Accession Number WP_011110663) as a search query, using the phmmer algorithm. These data were downloaded and MegaX[28] was used to generate a multiple sequence alignment of all 236 cyt P460 sequences using the ClustalW[29] program. This multiple sequence alignment was uploaded to WebLogo[30] to generate the sequence logo of the cyt P460 protein family.

The alignment of *N. europaea* cyt P460 (NCBI Accession Number WP_011110663) and *N.* sp. NpAV cyt P460 (NCBI Accession Number WP_052493891) was performed in T-coffee[31] using the ClustalW program to perform the alignment.

Steady-State Activity Assays

NH_2OH•HCl powder was brought into the glovebox and allowed to equilibrate overnight. NH_2OH was quantified using the method described by Frear *et al*[25] and brought outside the box using a crimpable GC vial (Wheaton)**.** Protein solutions were also brought out in a separate crimpable vial. Anaerobic Spectrosil quartz cuvettes were filled with 50 μM DCPIP and 6 μM PMS and allowed to equilibrate at 25°C for

five minutes. After this, 10 mM NH_2OH was added via a Hamilton syringe and background consumption was collected for 1.5-2 minutes, then the solution was spiked with an addition 500 nM protein sample, also using a Hamilton syringe. Final volumes were 2 mL. Data were fit by linear regression using the method of initial rates and using the first 10% of oxidant consumption. Rates reported are the average of three trials and the activity was determined by subtracting the background consumption.

{FeNO}^{6} Assessment of Ruffling

Inside the glovebox, protein was put inside an anaerobic cuvette and sealed. NO from PROLI-NONOate was quantified as previously described[24] and brought outside of the glovebox in a crimpable GC vial. A Hamilton was used to add 100 μM NO. Scans were collected every 30 s for one hour.

Cross-link formation Reaction

The cross-link formation experiment was performed using two different conditions because of massively different temporal differences of when the experiments were done. The first, for Tyr154Ala was done by treating a 5 μM sample in an anaerobic cuvette with 50 mM NH_2OH. Using a 22G needle, O_2 was gently put in the headspace of the cuvette for 5 minutes and removed, collecting scans while this was occurring.

The second reaction was done for the Arg44Ala variant. H_2O_2 was quantified using an extinction coefficient of $\varepsilon_{240} = 43.6\ mM^{-1}\bullet cm^{-1}$. 10 μM protein was placed inside an anaerobic cuvette and 10 μM H_2O_2 was added to the cuvette with continuous scanning.

Protein crystallography

Protein crystals were grown as previously described[5-6, 8] without modifications.

REFERENCES

1. Cedervall, P. E.; Hooper, A. B.; Wilmot, C. M., Crystallization and preliminary X-ray crystallographic analysis of a new crystal form of hydroxylamine oxidoreductase from Nitrosomonas europaea. *Acta crystallographica. Section F, Structural biology and crystallization communications* **2009,** *65* (Pt 12), 1296-1298.
2. Maalcke, W. J.; Dietl, A.; Marritt, S. J.; Butt, J. N.; Jetten, M. S. M.; Keltjens, J. T.; Barends, T. R. M.; Kartal, B., Structural Basis of Biological NO Generation by Octaheme Oxidoreductases. *Journal of Biological Chemistry* **2014,** *289* (3), 1228-1242.
3. Pearson, A. R.; Elmore, B. O.; Yang, C.; Ferrara, J. D.; Hooper, A. B.; Wilmot, C. M., The Crystal Structure of Cytochrome P460 of Nitrosomonas europaea Reveals a Novel Cytochrome Fold and Heme−Protein Cross-link. *Biochemistry* **2007,** *46* (28), 8340-8349.
4. Ferousi, C.; Schmitz, R. A.; Maalcke, W. J.; Lindhoud, S.; Versantvoort, W.; Jetten, M. S. M.; Reimann, J.; Kartal, B., Characterization of a nitrite-reducing octaheme hydroxylamine oxidoreductase that lacks the tyrosine cross-link. *Journal of Biological Chemistry* **2021,** *296*.
5. Coleman, R. E.; Vilbert, A. C.; Lancaster, K. M., The Heme–Lys Cross-Link in Cytochrome P460 Promotes Catalysis by Enforcing Secondary Coordination Sphere Architecture. *Biochemistry* **2020,** *59* (24), 2289-2298.
6. Smith, M. A.; Majer, S. H.; Vilbert, A. C.; Lancaster, Kyle M., Controlling a burn: outer-sphere gating of hydroxylamine oxidation by a distal base in cytochrome P460. *Chemical Science* **2019,** *10* (13), 3756-3764.
7. Andersson, K. K.; Kent, T. A.; Lipscomb, J. D.; Hooper, A. B.; Münck, E., Mössbauer, EPR, and optical studies of the P-460 center of hydroxylamine oxidoreductase from Nitrosomonas. A ferrous heme with an unusually large quadrupole splitting. *Journal of Biological Chemistry* **1984,** *259* (11), 6833-6840.

8. Smith, M. A.; Lancaster, K. M., The Eponymous Cofactors in Cytochrome P460s from Ammonia-Oxidizing Bacteria Are Iron Porphyrinoids Whose Macrocycles Are Dibasic. *Biochemistry* **2018,** *57* (3), 334-343.
9. Bergmann, D. J.; Hooper, A. B., Cytochrome P460 of Nitrosomonas europaea. Formation of the heme-lysine cross-link in a heterologous host and mutagenic conversion to a non-cross-linked cytochrome c'. *European Journal of Biochemistry* **2003,** *270* (9), 1935-1941.
10. Vilbert, A. C.; Caranto, J. D.; Lancaster, Kyle M., Influences of the heme-lysine crosslink in cytochrome P460 over redox catalysis and nitric oxide sensitivity. *Chemical Science* **2018,** *9* (2), 368-379.
11. Nambu, S.; Matsui, T.; Goulding, C. W.; Takahashi, S.; Ikeda-Saito, M., A new way to degrade heme: the Mycobacterium tuberculosis enzyme MhuD catalyzes heme degradation without generating CO. *J Biol Chem* **2013,** *288* (14), 10101-10109.
12. Graves, A. B.; Graves, M. T.; Liptak, M. D., Measurement of Heme Ruffling Changes in MhuD Using UV–vis Spectroscopy. *The Journal of Physical Chemistry B* **2016,** *120* (16), 3844-3853.
13. Matsui, T.; Unno, M.; Ikeda-Saito, M., Heme Oxygenase Reveals Its Strategy for Catalyzing Three Successive Oxygenation Reactions. *Accounts of Chemical Research* **2010,** *43* (2), 240-247.
14. Matsui, T.; Furukawa, M.; Unno, M.; Tomita, T.; Ikeda-Saito, M., Roles of Distal Asp in Heme Oxygenase from Corynebacterium diphtheriae, HmuO: A WATER-DRIVEN OXYGEN ACTIVATION MECHANISM*. *Journal of Biological Chemistry* **2005,** *280* (4), 2981-2989.
15. Valderrama, B.; Ayala M Fau - Vazquez-Duhalt, R.; Vazquez-Duhalt, R., Suicide inactivation of peroxidases and the challenge of engineering more robust enzymes. (1074-5521 (Print)).
16. Wariishi, H.; Gold, M. H., Lignin peroxidase compound III. Mechanism of formation and decomposition. *Journal of Biological Chemistry* **1990,** *265* (4), 2070-2077.

17. Ford, P. C.; Fernandez Bo Fau - Lim, M. D.; Lim, M. D., Mechanisms of reductive nitrosylation in iron and copper models relevant to biological systems. *Chemical Reviews* **2005,** *105* (0009-2665 (Print)), 2439-2456.
18. Walker, F. A., Nitric oxide interaction with insect nitrophorins and thoughts on the electron configuration of the {FeNO}6 complex. *Journal of Inorganic Biochemistry* **2005,** *99* (1), 216-236.
19. Coleman, R. E.; Lancaster, K. M., Heme P460: A (Cross) Link to Nitric Oxide. *Accounts of Chemical Research* **2020,** *53* (12), 2925-2935.
20. Caranto, J. D.; Lancaster, K. M., Nitric oxide is an obligate bacterial nitrification intermediate produced by hydroxylamine oxidoreductase. *Proceedings of the National Academy of Sciences* **2017,** *114* (31), 8217-8222.
21. Liptak, M. D.; Wen, X.; Bren, K. L., NMR and DFT Investigation of Heme Ruffling: Functional Implications for Cytochrome c. *Journal of the American Chemical Society* **2010,** *132* (28), 9753-9763.
22. Lancaster, K. M., Biological Outer-Sphere Coordination. In *Molecular Electronic Structures of Transition Metal Complexes I*, Mingos, D. M. P.; Day, P.; Dahl, J. P., Eds. Springer Berlin Heidelberg: Berlin, Heidelberg, 2012; pp 119-153.
23. Lin, Y.-W., The broad diversity of heme-protein cross-links: An overview. *Biochimica et Biophysica Acta (BBA) - Proteins and Proteomics* **2015,** *1854* (8), 844-859.
24. Caranto, J. D.; Weitz, A.; Hendrich, M. P.; Kurtz, D. M., The Nitric Oxide Reductase Mechanism of a Flavo-Diiron Protein: Identification of Active-Site Intermediates and Products. *Journal of the American Chemical Society* **2014,** *136* (22), 7981-7992.
25. Frear, D. S.; Burrell, R. C., Spectrophotometric Method for Determining Hydroxylamine Reductase Activity in Higher Plants. *Analytical Chemistry* **1955,** *27* (10), 1664-1665.
26. Caranto, J. D.; Vilbert, A. C.; Lancaster, K. M., *Nitrosomonas europaea* cytochrome P460 is a direct link between nitrification and nitrous oxide emission. *Proceedings of the National Academy of Sciences* **2016,** *113* (51), 14704-14709.

27. Finn, R. D.; Clements, J.; Eddy, S. R., HMMER web server: interactive sequence similarity searching. *Nucleic Acids Research* **2011,** *39* (suppl_2), W29-W37.
28. Kumar, S.; Stecher, G.; Li, M.; Knyaz, C.; Tamura, K., MEGA X: Molecular Evolutionary Genetics Analysis across Computing Platforms. (1537-1719 (Electronic)).
29. Thompson, J. D.; Higgins, D. G.; Gibson, T. J., CLUSTAL W: improving the sensitivity of progressive multiple sequence alignment through sequence weighting, position-specific gap penalties and weight matrix choice. *Nucleic acids research* **1994,** *22* (22), 4673-4680.
30. Crooks, G. E.; Hon G Fau - Chandonia, J.-M.; Chandonia Jm Fau - Brenner, S. E.; Brenner, S. E., WebLogo: a sequence logo generator. (1088-9051 (Print)).
31. Notredame, C.; Higgins Dg Fau - Heringa, J.; Heringa, J., T-Coffee: A novel method for fast and accurate multiple sequence alignment. (0022-2836 (Print)).

APPENDIX: MÖSSBAUER SPESCTROSCOPIC STUDIES OF CYT P460

Introduction

Early in my PhD, I was tasked with figuring out conditions to grow cyt P460 in minimal media so that we could do ^{57}Fe Mössbauer spectroscopy on the protein. ^{57}Fe Mössbauer spectroscopy is an iron-specific technique that provides electronic structure information about only the Fe center.[1] We wanted to see if there were substantial information differences between the electronic structure of a cross-link-containing cyt P460 species compared to the CLD variant. The short answer is there is nothing substantially different between them. All this being said, I wanted to make sure this data ended up somewhere so people can reference it.

Ferrous Mössbauer

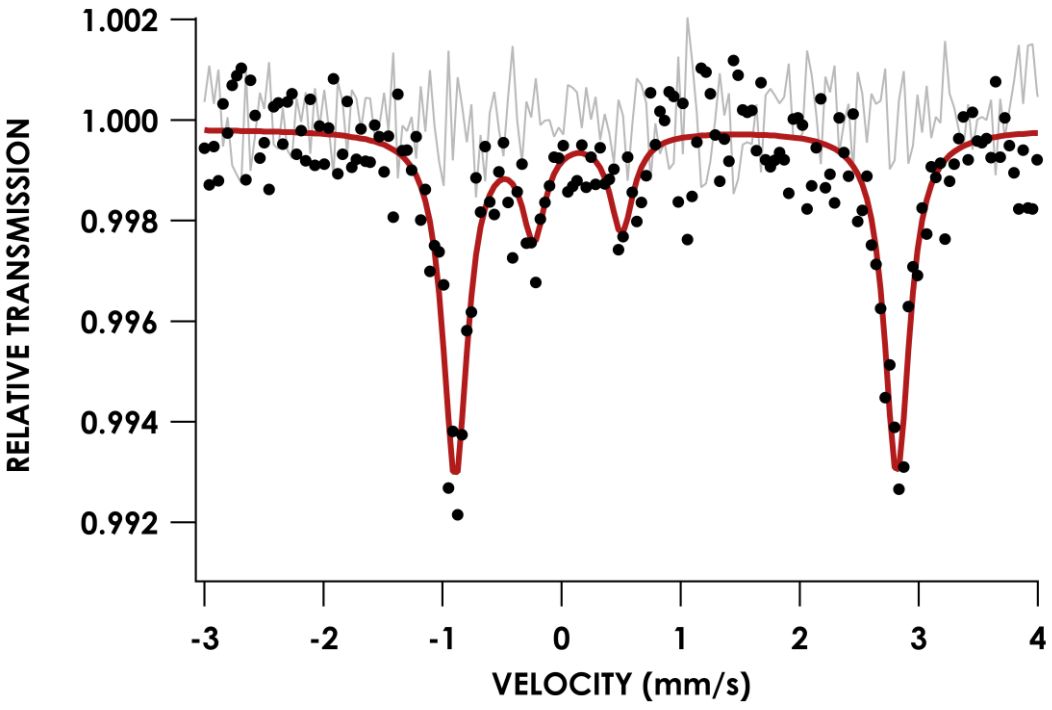

Figure A.1 Mössbauer spectrum of ferrous WT P460 at 4.2K and in zero magnetic field. The minor inner component is an unknown Fe component. The black dots are the raw data, the gray line is the residual, and the red line is the fit.

Table A.1 Mössbauer parameters of the ferrous WT cyt P460

	Fe_1	Fe_2
δ, mm/s	0.961 ± 0.006	0.135 ± 0.025
ΔE_Q, mm/s	3.710 ± 0.012	0.745 ± 0.056
Γ, mm/s	0.253 ± 0.020	0.245 ± 0.06
Relative Area, mm/s	0.531 ± 0.029	.148 ± 0.024
Reduced χ^2	0.999 ± 0.063	

The Fe_1 component is the heme P460 center and is consistent with the previously published ferrous Mössbauer spectrum of the ferrous WT cyt P460.[2] This is a diagnostic, HS Fe^{II} heme site and the quadrupole splitting is the largest observed one for heme systems.

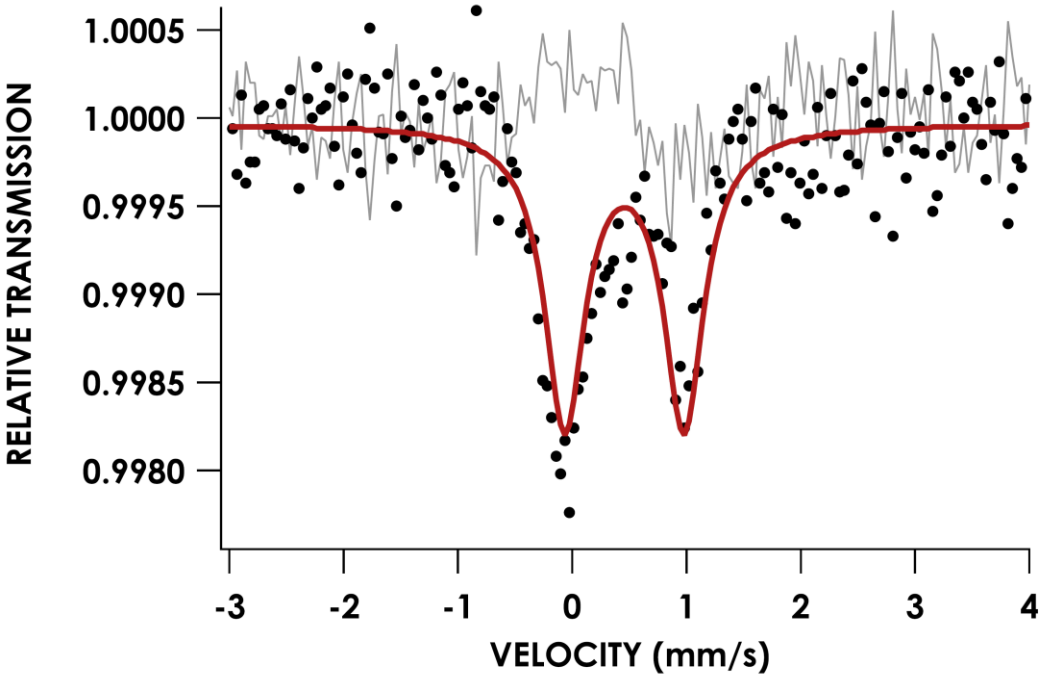

Figure A.2 Mössbauer spectrum of ferrous Lys70Tyr at 4.2K and in 0 magnetic field. The black dots are the raw data, the gray line is the residual, and the red line is the fit.

Table A.2 Mössbauer parameters of the ferrous Lys70Tyr cyt P460

	Fe
δ, mm/s	0.457 ± 0.011
ΔE_Q, mm/s	1.042 ± 0.023
Γ, mm/s	0.422 ± 0.031
Relative Area, mm/s	0.779 ± 0.037
Reduced χ^2	1.000 ± 0.071

These data are consistent with a LS Fe^{II} heme center.

Ferric

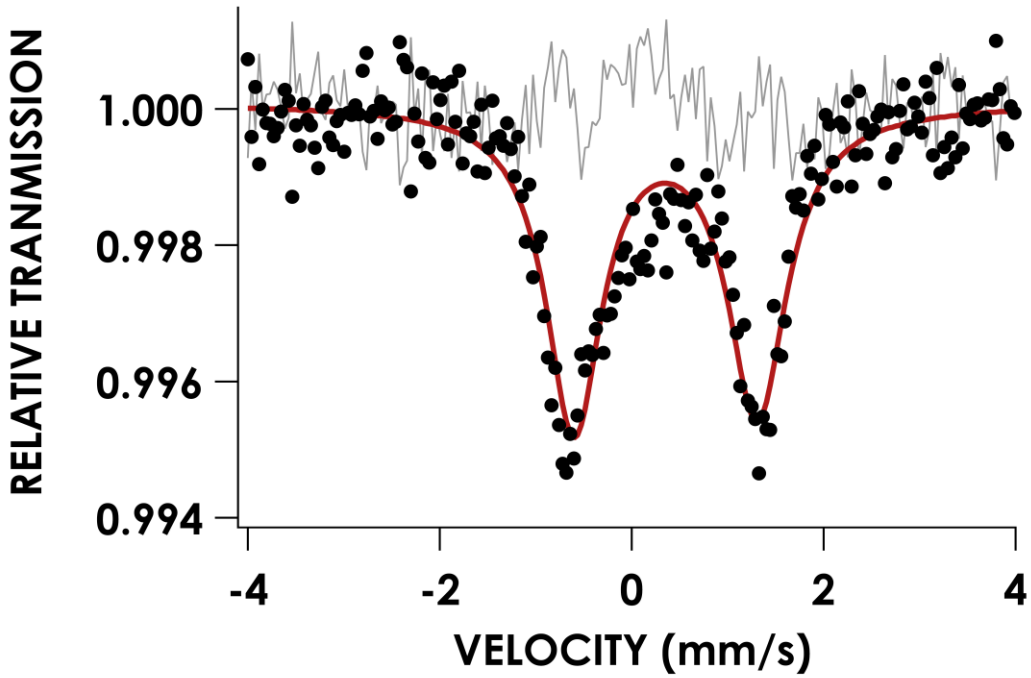

Figure A.3. Mössbauer spectrum ferric WT cyt P460 collected at 85K and zero magnetic field. The black dots are the raw data, the gray line is the residual, and the red line is the fit.

Table A.3. Mössbauer parameters of ferric WT cyt P460.

	Fe
δ, mm/s	0.357 ± 0.036
ΔE_Q, mm/s	1.908 ± 0.021
Γ, mm/s	0.722 ± 0.027
Relative Area, mm/s	1.183 ± 0.036
Reduced χ^2	0.995 ± 0.067

This data is a high spin Fe^{III} heme center.

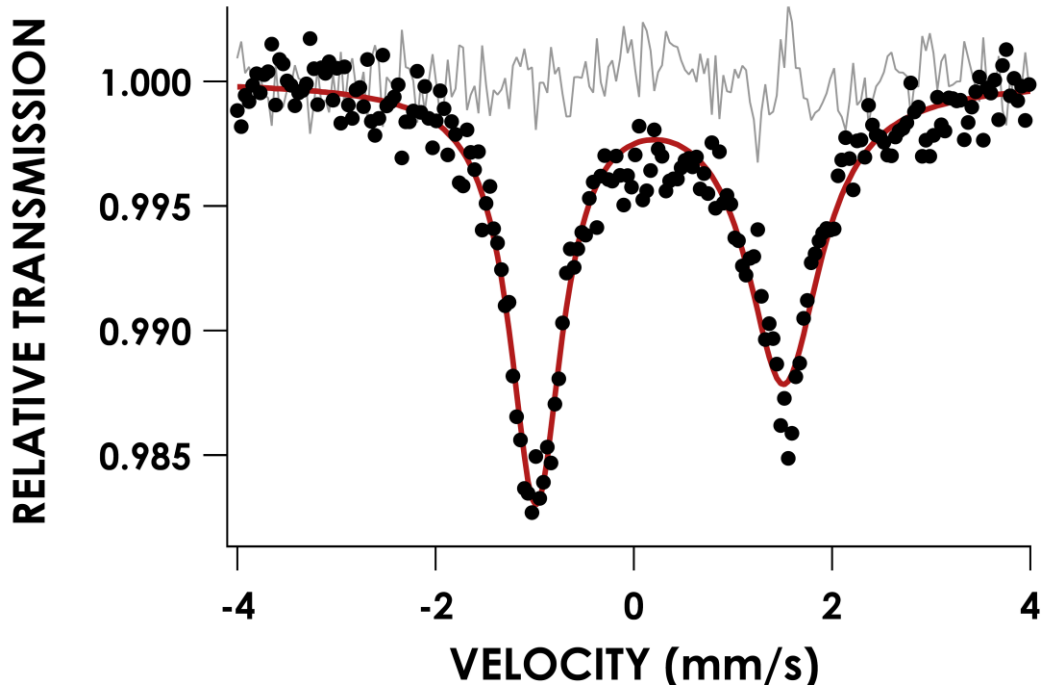

Figure A.4. Mössbauer spectrum of the ferric form of Lys70Tyr collected at 85K. The black dots are the raw data, the gray line is the residual, and the red line is the fit.

Table A.4 Mössbauer parameters of ferric Lys70Tyr cyt P460.

	Fe
δ, mm/s	0.261 ± 0.008
ΔE_Q, mm/s	2.500 ± 0.014
Γ left, mm/s	0.640 ± 0.019
Γ right, mm/s	0.899 ± 0.028
Relative Area, mm/s	1.032 ± 0.019
Reduced χ^2	0.992 ± 0.064

This spectrum is most probably a LS Fe^{III} center.

{FeNO}^{6}

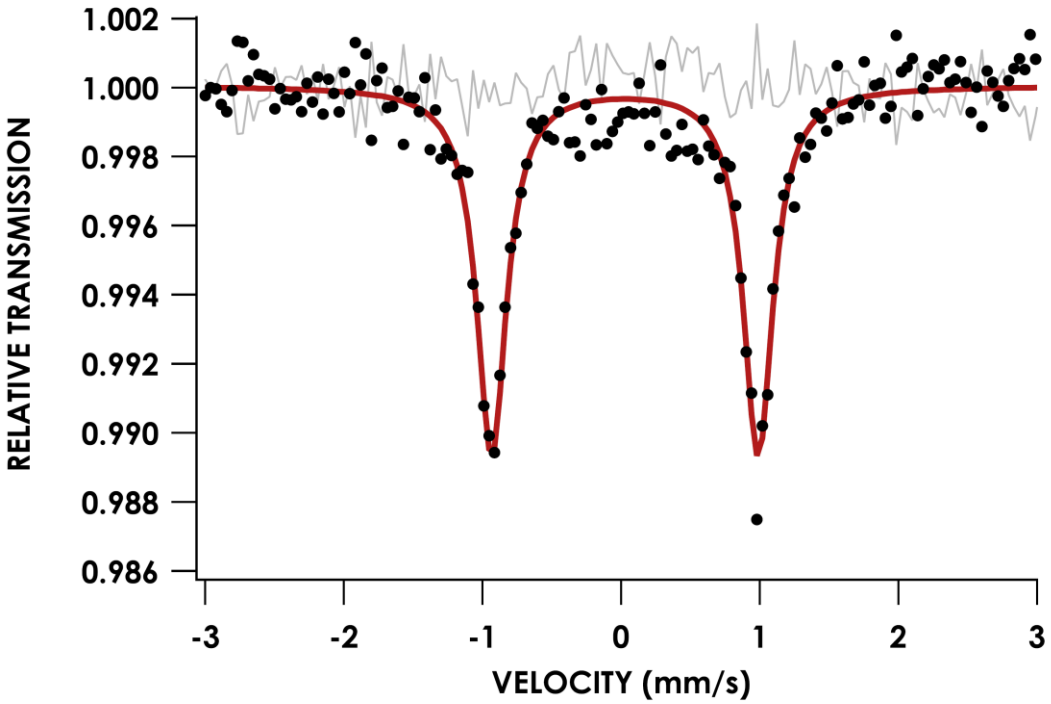

Figure A.5. WT cyt P460 treated with 10 mM NO collected at 4.2 K and 0 field. The black dots are the raw data, the gray line is the residual, and the red line is the fit.

Table A.5. Mössbauer spectrum of the {FeNO}^{6} of WT Cyt P460

	Fe
δ, mm/s	0.027 ± 0.004
ΔE_Q, mm/s	1.922 ± 0.008
Γ, mm/s	0.259 ± 0.010
Relative Area, mm/s	1.135 ± 0.032
Reduced χ^2	0.992 ± 0.063

This is consistent with other {FeNO}^{6} heme proteins, but Mössbauer is unable to differentiate between an Fe^{II}-NO^+ or an Fe^{III}-NO•.[3]

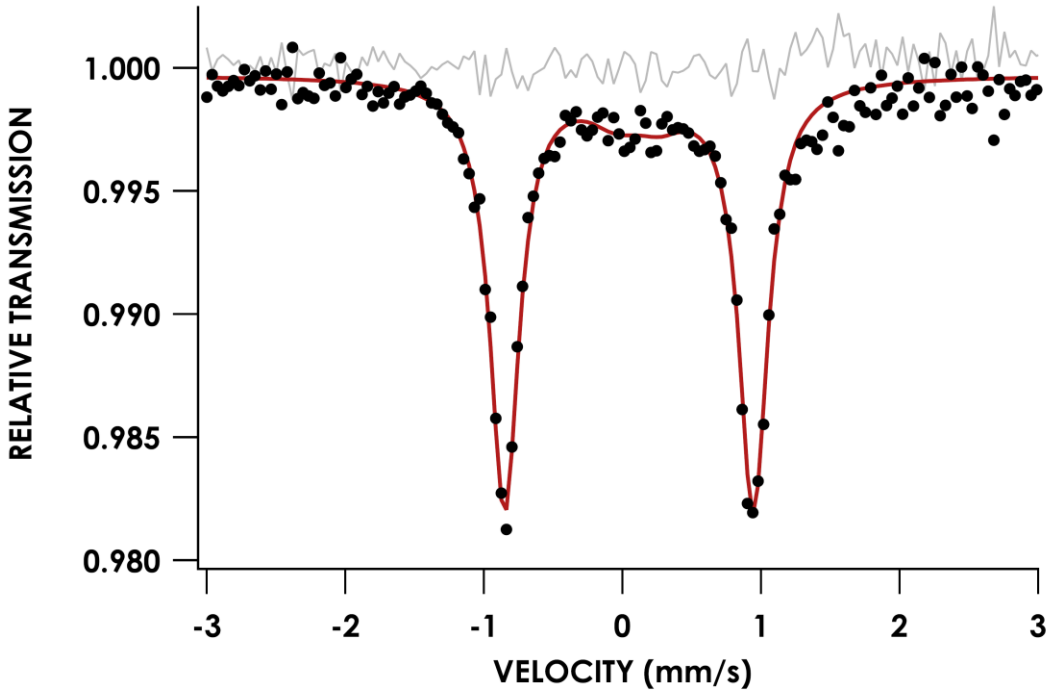

Figure A.6. Lys70Tyr cyt P460 treated with 10 mM NO collected at 4.2 K and 0 field. The black dots are the raw data, the gray line is the residual, and the red line is the fit.

Table A.6. **Mössbauer parameters of ferric WT cyt P460.**

	Fe_1	Fe_2
δ, mm/s	0.047 ± 0.005	0.167 ± 0.344
ΔE_Q, mm/s	1.794 ± 0.006	0.736 ± 0.941
Γ, mm/s	0.255 ± 0.014	0.426 ± 0.104
Relative Area, mm/s	0.634 ± 0.061	0.083 ± 0061
Reduced χ^2	1.011 ± 0.078	

Same analysis as for the WT. I would disregard the Fe2 center, it is not a real result and this was overfit. This does not, however, affect interpretation of Fe_1.

Experimental

General considerations

Enriched ^{57}Fe powder (ISOFLEX) was converted to $^{57}FeCl_2{\cdot}2H_2O$ per the previously established protocol. [4]

Overexpression of ^{57}Fe labeled protein

Starter cultures were picked from a plate of transformed BL21(DE3) *E. coli* cells and grown in LB. Once the cells were grown, the cells were spun down and resuspended in the minimal media consisting of:

Per 1L of media:

- 19.2 g $Na_2HPO_4{\bullet}7H_2O$
- 4.5 g KH_2PO_4
- 0.5 g NaCl
- 2 g NH_4Cl
- 100 mg each amino acid
- **Autoclave**
- 100 mg each antibiotic
- 10 mL 1 M $MgCl_2$ –filter sterilized
- 0.03725 g $^{57}FeCl_2$
- 10 mL Trace Metals—filter sterlized
- 10 mL vitamin cocktail—filter sterlized
- 65 mg δ-aminolevulinic acid—(need more from Crane lab, or I'll order some)
- 38 mg Thiamine•HCl
- 10 mL 50% glycerol

Trace Metals and Vitamin cocktail mixture were both from the recipe designated by Liptak *et al*.[5]

Cells were grown at 37°C until an OD_{600} of 0.6 to 1.0 was reached, at which time cells were induced by addition of 0.4 mM IPTG. Induction occurred for 24 hours at 20°C. Lysis and purification proceeded as normal,[6] except SEC chromatography was not performed.

Mössbauer Data Collection

Sample preparations are as designated below. All samples were placed in a Delrin Mössbauer cup and frozen in liquid nitrogen and stored in a LN_2 storage dewar until ready for use.

- Ferric WT P460: 400 μL of 586 μM—as isolated, nothing to prep.
- WT P460 $\{FeNO\}^6$: 300 μL of 586 μM cyt P460 were treated with 10 mM NO from PROLI-NONOate.
- Ferrous WT P460: 300 μL of 586 μM cyt P460 were treated with sodium dithionite and then frozen in liquid nitrogen to keep reduced.
- Ferric Lys70Tyr: 400 μL of 540 μM protein, as-isolated, nothing to prep.
- Lys70Tyr $\{FeNO\}^6$: used the above sample for the ferric Lys70Tyr sample and treated with 10 mM NO. Was freeze-thawed.
- Ferrous Lys70Tyr: 300 μL of 540 μM protein treated with sodium dithionite and then frozen immediately.

Mössbauer data were collected using a SEECo Resonant Gamma-Ray spectrometer (Model W304) at either 4.2K using liquid helium or 85K using liquid nitrogen. Room temperature Fe foil was used to calibrate the velocity scale. Data were fit using the WMOSS software package using Theoretical Model 3 to fit to quadrupole doublets. Uncertainties were derived from the standard deviations of 151-201 simulations for each spectrum.

REFERENCES

1. Münck, E., Aspects of ^{57}Fe Mössbauer Spectroscopy. In *Physical Methods in Bioinorganic Chemistry: Spectroscopy and Magnetism* 2nd ed.; Lawrence Que, J., Ed. University Science Books: Sausalito, CA, 2000; pp 287-319.

2. Andersson, K. K.; Kent, T. A.; Lipscomb, J. D.; Hooper, A. B.; Münck, E., Mössbauer, EPR, and optical studies of the P-460 center of hydroxylamine oxidoreductase from Nitrosomonas. A ferrous heme with an unusually large quadrupole splitting. *Journal of Biological Chemistry* **1984,** *259* (11), 6833-6840.

3. Wegner, P.; Benda, R.; Schünemann, V.; Trautwein, A. X.; Berry, R. E.; Balfour, C. A.; Wert, D.; Walker, F. A. In *How a blood sucking insect gets its meal: The ferriheme proteins Nitrophorin 2 and 4 studied by Mössbauer Spectroscopy*, Hyperfine Interactions (C), Dordrecht, 2002//; Thomas, M. F.; Williams, J. M.; Gibb, T. C., Eds. Springer Netherlands: Dordrecht, 2002; pp 253-256.

4. Muok, A. R.; Deng, Y.; Gumerov, V. M.; Chong, J. E.; DeRosa, J. R.; Kurniyati, K.; Coleman, R. E.; Lancaster, K. M.; Li, C.; Zhulin, I. B.; Crane, B. R., A di-iron protein recruited as an Fe[II] and oxygen sensor for bacterial chemotaxis functions by stabilizing an iron-peroxy species. *Proceedings of the National Academy of Sciences* **2019,** *116* (30), 14955.

5. Liptak, M. D.; Wen, X.; Bren, K. L., NMR and DFT Investigation of Heme Ruffling: Functional Implications for Cytochrome c. *Journal of the American Chemical Society* **2010,** *132* (28), 9753-9763.

6. Caranto, J. D.; Vilbert, A. C.; Lancaster, K. M., *Nitrosomonas europaea* cytochrome P460 is a direct link between nitrification and nitrous oxide emission. *Proceedings of the National Academy of Sciences* **2016,** *113* (51), 14704-14709.

Here, at the end of my thesis, I will put this quote from one of my favorite video games, EarthBound (1995), which somehow seems emblematic of the PhD experience:

I'm a little embarrassed to say it, but I'll tell you anyway... I thought "philosophy" was the study of stones. I now realize it's about studying all night.